Preferred citation: S. Östlund. Three-dimensional deformation and damage mechanisms in forming of advanced structures in paper. In **Advances in Pulp and Paper Research, Oxford 2017**, *Trans. of the XVIth Fund. Res. Symp. Oxford, 2017*, (W. Batchelor and D. Söderberg, eds), pp 489–594, FRC, Manchester, 2018. DOI: 10.15376/frc.2017.2.489.

THREE-DIMENSIONAL DEFORMATION AND DAMAGE MECHANISMS IN FORMING OF ADVANCED STRUCTURES IN PAPER

Sören Östlund

BiMaC Innovation, KTH Royal Institute of Technology, Department of Solid Mechanics, SE-100 44 Stockholm, Sweden

ABSTRACT

There is a large potential for wood-fibre based materials such as paper and board to contribute to lightweight structures in several applications, particularly packaging. Fibre-based packaging materials have important advantages in comparison to fossil-based plastics regarding biodegradability, recyclability and renewability. Individualisation has become a crucial criterion for the use of packaging solutions and forming of advanced paperboard structures is a key technology for manufacturing of such packaging shapes. New sustainable packaging concepts are creating a need for paper materials with considerably enhanced properties.

Paper and board are in manufacturing of geometrically advances structures in general subjected to complex and often little known multi-axial states of loading and deformation that are not necessarily quantified by conventional measures for paper performance. Today, commercial paperboard is optimised for folding and printing, and not for applications involving forming of advanced structures. It is likewise important to design the manufacturing processes to meet the particular properties of paperboard. Manufacturing methods that are suitable for metals and plastics are inevitably not suitable for paper and board since the deformation and damage mechanisms of fibre network materials are different from metals and plastics.

In this paper recent findings in the literature on 3D forming of paper and paperboard structures are reviewed. In particular, deformation and damage mechanisms involved in pertinent forming operations and how they are related to paper and board properties in order to enhance the development of new advanced paper materials and structures are analysed.

In the last decade, there have been major advancements in the development of geometrically advanced 3D paperboard structures including technological advances of various forming processes, enriched understanding of the importance and influence of process parameters, and new paperboard materials with significantly improved forming properties. However, there is still a lack of knowledge regarding the deformation mechanisms of these complex systems, and particularly regarding the influence of friction. One remedy would be the enhancement of numerical simulation tools. Optimisation of existing forming processes and development of new ones as well as tailored paper and board materials with properties customised to the demands of existing and new 3D forming processes will also play important roles. This development is only in its beginning and major progress is expected in the near future.

Keywords: 3D paperboard structures, deformation and damage mechanisms, deep-drawing, press-forming, hydro-forming, material properties, modelling and simulations.

1 INTRODUCTION

Motivated by sustainability arguments, not the least, but also by cost arguments, there is a large potential for wood-fibre based materials such as paper and board to contribute to lightweight structures in several different applications such as vehicle components, building materials and packaging, among others. Fibre-based packaging materials have important benefits in comparison to fossil-based plastics regarding biodegradability, recyclability and renewability. However, for ultimate success, paper exhibits several drawbacks that today seriously limit this potential, three of them being moisture sensitivity, barrier properties and limited formability [1].

Individualisation and branding have become crucial criteria for the use of packaging solutions and forming of geometrically advanced paperboard structures is a key technology for manufacturing of such packaging shapes [2]. Thus, the demands for new sustainable packaging concepts are creating a need for paperboard with

considerably enhanced properties. Obviously, reduced moisture sensitivity and improved extensibility are two of these, but the complex deformation and damage mechanisms that paperboard is subjected to in prospective processes for manufacturing of advanced packaging structures put increasing demands also on various other mechanical and frictional properties. The complex nature of fibre network materials and the large number of process parameters decrease the reliability of the manufacturing process and limit the possible shapes, [2].

Three-dimensional (3D) forming of paper products paves the way for replacement of plastic components with paper products, and opens up for packaging solutions that have never been possible for conventional paper products. The 3D forming technology imposes greater demands on the stretchability of paper materials than all the current end-use processes. Overcoming the problem with the poor ability to form paperboard structures of advanced geometrical forms is one of the keys to novel paperboard packaging solutions [3].

Paper and board in 3D forming processes are in general subjected to complex and often scarcely understood multi-axial states of loading and deformation that are not necessarily quantified by conventional measures for paper performance. The estimated tensile strains experienced by paperboard in 3D forming processes are, for example, commonly higher than what is measured in standard tensile tests. Today, commercial paperboard is optimised for folding and printing, and not for applications involving 3D forming. It is likewise important to design the manufacturing processes to meet the particular properties of paperboard. The manufacturing methods that are suitable for metals and plastics are inevitably not suitable for paper and paperboard since the deformation and damage mechanisms of fibre network materials are different from metals and plastics. Thus, successful progress in the development of advanced paper and board structures requires both enhancements of the operational window of the physical properties of paper and board and developments of the manufacturing processes.

The objective of this paper is to review the recent findings in 3D forming of paper and paperboard structures. In particular, to analyse the deformation and damage mechanisms involved in the relevant forming operations and how they are related to paper and paperboard properties in order to enhance the development of new advanced paper materials and structures.

Before proceeding to forming operations particularly considered for advanced paperboard structures, we need to define what is here meant by an advanced structure. There are numerous paper structures that definitely can be termed advanced, although they will be excluded from the review in this paper. This category includes, for example, novel packaging structures from folding of pre-creased paperboard blanks, advanced origami structures and crumpled structures as illustrated in Figure 1. Mechanics of advanced origami structures and crumpled structures are extensively researched, e.g. [4] and [5], but are not further considered here.

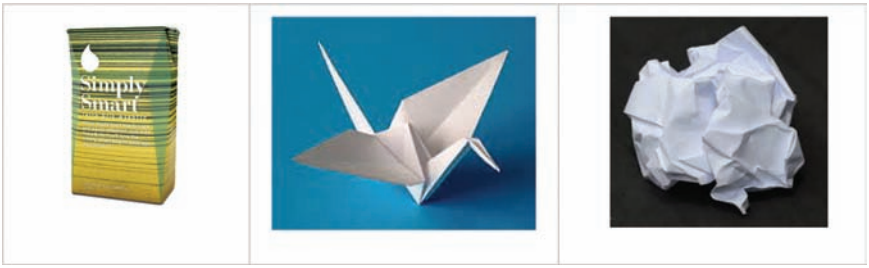

Figure 1. Illustration of advanced paper structures made by folding or crumpling. From Tetra Pak (*left*), Andreas Bauer Origami-Kunst [6] (*middle*) and [7] (*right*).

There are a number of materials with excellent barrier properties that can be combined with paperboard. Such barrier layers are often brittle and are easily damaged during manufacturing processes. However, specific barrier properties and the mechanical properties of barrier materials are not covered in this review. Three-dimensional forming is one way of producing packages from coated paperboard for barrier applications and there are several recent papers illustrating that 3D paperboard structures formed with the methods discussed here are applicable also for packaging using paperboard coated with both fossil-based and bio-based polymers coatings [8–11], although there are still both scientific and practical problems in this area that remain to be solved.

Furthermore, this review does not consider brim-forming of paperboard cups, as exemplified by [12], and pulp-moulding despite the recent interest for this method in forming of e.g. paper bottles [13]. Prospects for moulded pulp manufacturing process technology are discussed in a recent paper [14].

2 FORMING CONCEPTS

Of particular interest in this paper are structures that contain double-curved smooth surface elements. This does not exclude creasing and folding operations, but the overall objective is to create smooth structures and not folded corners. The presentation will focus on structures for packaging since this is an area of large application potential, but it should be emphasized that there are other possible applications, for example in furniture, automotive and construction businesses [15], [16]. Figure 2 shows examples of the type of paperboard structures and the related manufacturing techniques that are of particular interest in this paper.

There is no established way to quantitatively define an advanced structure, but there are, at least, two apparent ways to assign a measure of the difficulty to form

a certain structure. One is the stretch, defined as the change in length of a line element from the flat reference state to the deformed state. This could be exemplified by estimating the stretch,

$$\lambda = \frac{\pi r}{2r} \approx 1.57, \tag{1}$$

required to form a flat circular surface of radius r into a semi-spherical surface with the same radius. Another example is the stretch of the left structure in Figure 2 being approximately 1.21. The strain defined in this way is not equivalent to the maximum strain in the formed structure, since the strain distribution is, in general, not homogeneous. Furthermore, it is typically affected by material anisotropy, non-linear material behaviour, climate conditions, etc. and a function of location in the formed structure as exemplified by [17] for hydroforming using a pear shaped forming cavity.

Another way is to use the forming ratio, here defined as the ratio of the height of the formed structure divided by a characteristic dimension of the bottom surface. This is not necessarily the definition used in deep-drawing of metals. For a structure with a circular base shape, this definition would degenerate to the height of the formed structure h divided by the diameter of the circular base d as illustrated in Figure 3.

This definition is particularly useful for forming of close to cylindrical structures with flat bottom regions and local regions of high strain, such as the last two types of structures in Figure 2, while, possibly, the definition according to Equation (1) is more appropriate for the first type of structure in Figure 2.

Forming of advanced paper and board structures are in general related to converting processes where the fibre network experiences large in-plane and out-of-plane strains, as well as local deformation and damage mechanisms such

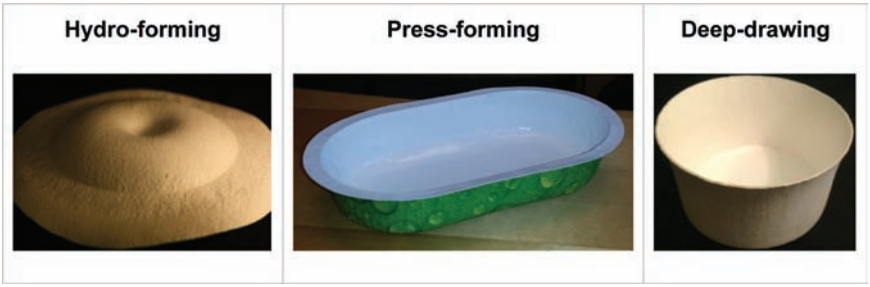

Figure 2. Double-curved paperboard structures, from KTH Royal Institute of Technology (*left*), Lappeenranta University of Technology (*middle*) and TU Dresden (*right*).

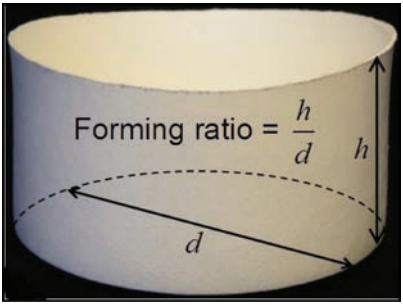

Figure 3. Definition of the forming ratio for a cylindrical structure with a circular base.

as, e.g. wrinkling and delamination. There are few conventional paperboard converting and end-use operations, where such deformations and damage mechanism play a critical role, although general improvements of the mechanical properties of paper and paperboard is continuously ongoing for all paper and board makers. Wrinkling during sheet forming is of course not limited to paper and board structures and is an important deformation mechanism both for metals and anisotropic composite sheets as exemplified by e.g. [18].

Manufacturing of rigid paperboard packaging is almost exclusively dominated by converting operations based on creasing and folding. Consequently, design of paperboard materials has for a long time been driven by the requirements of these operations, where high bending stiffness and delamination resistance being two of the most important ones. This leads to multi-layered paperboard designs where different types of fibres and network structures in an efficient way contribute to the bending stiffness. To achieve high bending stiffness, designs with dense, stiff and strong outer layers and bulky inner layers are typically used, while delamination properties can be tailored by, e.g. chemical treatment of the interfaces between layers. While, these particular properties are of importance in conventional converting and end-use operations, this is not necessarily the case for forming of advanced three-dimensional paperboard structures. There has, however, in recent years been an increasing interest in this topic, exemplified by e.g. the development of commercial paperboards with considerably enhanced extensibility [19], [20].

One well-known example for which improved extensibility, at comparable strength, will increase the ductility as characterised by the tensile energy absorption (TEA) is converting of sack and bag paper grades. This has been shown to contribute positively to the end-use performance of sack paper products [21]–[23]. Creasing and folding of paperboard in packaging is an application where local delaminations are essential. The quality of creases and folds is of

utmost importance for the performance of paperboard in both filling machines and for the stacking strength of boxes.

The history of forming of advanced paper and board structures and the development of materials adapted for such processes are with only few exceptions not very long. Below we will describe the fundamentals of the methods of current interest for converting of paperboard into 3D structures containing double curved surface elements will be described. As a general rule, forming of cylindrical surfaces by bending will not be considered, since this is in general straightforward for paper and board. For corrugated board this is, however, not the case and the recent development of bendable corrugated board should be accredited, although not further elaborated upon here [24].

2.1 Sliding blank and fixed blank principles

Manufacturing processes for forming of advanced paperboard structures are traditionally characterised by being either sliding blank or fixed blank processes (Figure 4).

Sliding blank methods are characterised by movement of the paperboard blank into the forming cavity. The lateral contraction, which is enforced by compatibility with the forming cavity, is taken care of by compressive strains and local wrinkling of the blank, either at pre-manufactured creases or at more or less

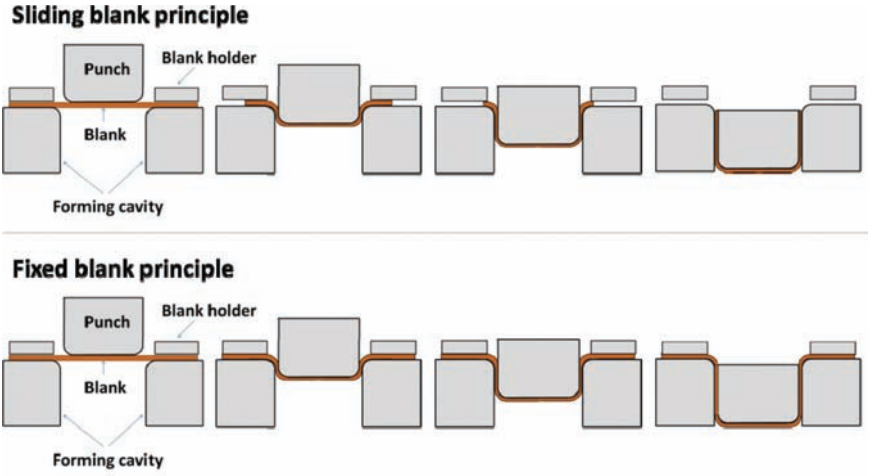

Figure 4. Two-dimensional schematic illustrations of the sliding blank and fixed blank principles.

random locations. In both cases, the heterogeneous structure of the fibre network material plays an important role since characteristic lengths (such as the wave length) of the formed wrinkles typically are very short and in general of the same order as the microscopic structure of the fibre network.

Fixed blank methods are characterised by restraining the edge of the paperboard blank at the mould and then stretching and pushing the blank into the forming cavity by different means of mechanical loading. These methods typically subject the material to large in-plane tensile plastic strains and properties such as sheet extensibility and strength are important for successful forming. It should be noted that extensibility and strength are important also in sliding blank processes when forming for example concave shape elements [25], or forming of structures with large punch edge radius [26].

In methods of practical interest, the movement of the blank is in general, to different degrees, a combination of sliding and fixed, and these notations are capturing the dominating character of the methods rather than being precise definitions. Figure 5 schematically illustrates three methods of current interest, and paperboard structures formed with these methods are shown in Figure 2.

From a materials point of view, the requirements for the sliding and fixed blank processes are different [28]. The loading and geometrical constraints that the paperboard experiences in the respective processes activate different local deformation and damage mechanisms, and this needs to be taken into consideration in the design of both the paperboard and the manufacturing process.

2.2 Deep-drawing

A sliding blank method that has found industrial applicability is deep-drawing of paperboard, Figure 6. ❶: Initially, the paperboard blank is clamped between the top of the forming cavity and the blank holder. Both the punch and the forming cavity are heated and the blank holder applies a pressure on the flange area of the

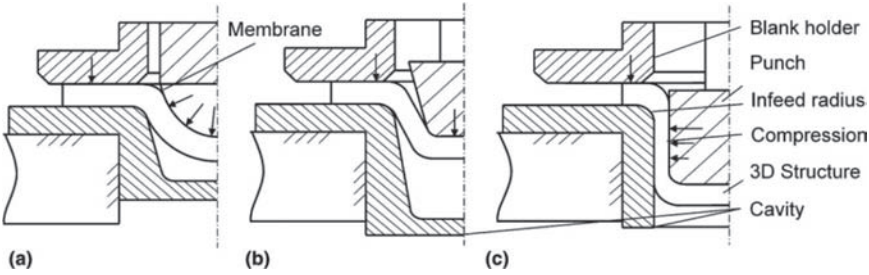

Figure 5. Sheet material forming techniques of current interest for forming of advanced paperboard structures: (a) hydro-forming, (b) press-forming and (c) deep-drawing, [27].

blank. ❷: The movement of the punch then pushes the blank into the forming cavity with a certain velocity. The first part is known as the infeed. ❸: After leaving the infeed, the paperboard blank is immediately compressed, and ❹ flattened between the punch and the forming cavity. ❺: After reaching the final position, the structure is dried for a certain dwell-time and ❻ finally spring-back of the material occurs when the punch leaves the forming cavity.

Early developments in deep-drawing of paperboard are dated back to the 1930s [29]. The development thereafter, available in the open literature, is limited to only a few publications as reviewed by [2]. Improvement in quality of the formed paperboard structures was then restricted because of the few possibilities to affect the process in a meticulous way. Formed structures showed distinctive wrinkles, abrasion at wrinkles, wavy edges and decolouration as illustrated in Figure 7. These defects are caused by large wrinkles. Thus, the quality of the formed parts even at a low forming ratio was not, in general, accepted for higher value or premium packaging [2].

In deep-drawing with rigid tools the paperboard blank experiences immediate through-thickness compression after having passed the infeed as illustrated in Figure 6, STEP ❸. This will have a profound effect on the outcome of the forming operation, as discussed below, and, despite sharing the name, deep-drawing of

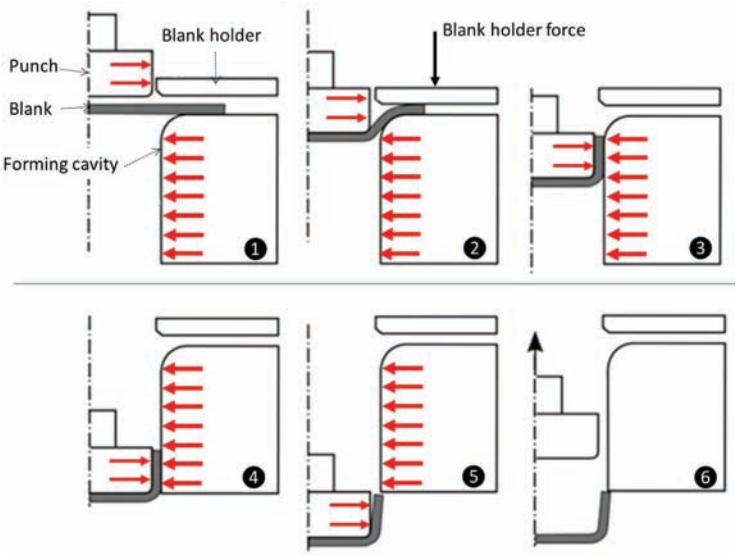

Figure 6. Schematic illustration of the deep-drawing process, adapted from [30]. The red arrows indicate heat applied during the entire process.

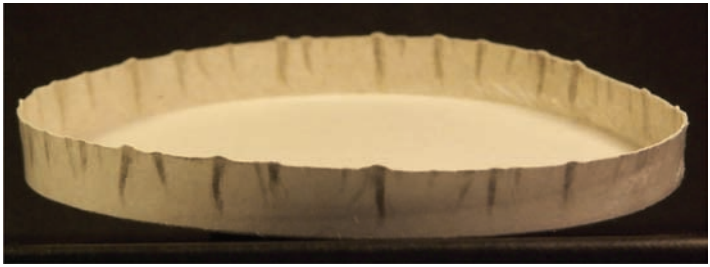

Figure 7. Distinctive wrinkles, earing, abrasion, wavy edges and discolouration of deep-drawn paperboard structure. Picture reproduced with kind permission of Dr. M. Hauptmann, TU Dresden.

paperboard exhibits only a few features similar to deep-drawing of sheet metal due to the particular properties and deformation mechanisms of fibre network materials, [31]. Beginning with the pioneering work of [32], major advancements in the knowledge and technology of paperboard deep-drawing have been made recently. Leading in this work is Technische Universität Dresden, Germany (TU Dresden), but important contributions are given also elsewhere.

Two-dimensional illustrations of the geometrical conditions in the deep-drawing tool are presented in Figure 8, and details of the stresses at different positions in the process are illustrated in Figure 9.

During the infeed (defined as the sum of the die radius and the punch edge radius), it can be assumed that the punch presses only against the part of the paperboard blank that will form the bottom of the 3D structure. The paperboard blank will then be loaded by the drawing stress σ_d the compressive circumferential stress σ_x the blank holder pressure p_{bh} and frictional shear stresses between blank holder and forming cavity, below the punch τ_{bh} and at the radius of the forming cavity τ_{infeed} as illustrated schematically in Figure 9.

After the punch has moved this distance, the paperboard is clamped between the punch and forming cavity and experiences full out of plane compression as long as the drawing gap (here defined as the difference between forming cavity radius and punch radius) is smaller than the effective material thickness, i.e. the thickness of the cross-section loaded in tension, Figure 10. The effective material thickness will be dependent on the in-plane compressive behaviour, the thickness of the material and the formation of wrinkles. The loading of the paperboard blank when located in the drawing gap is illustrated schematically by the two bottom subfigures in Figure 9.

When the paperboard is being clamped between the punch and the forming cavity, two frictional shear stresses are acting on the material at this point, one

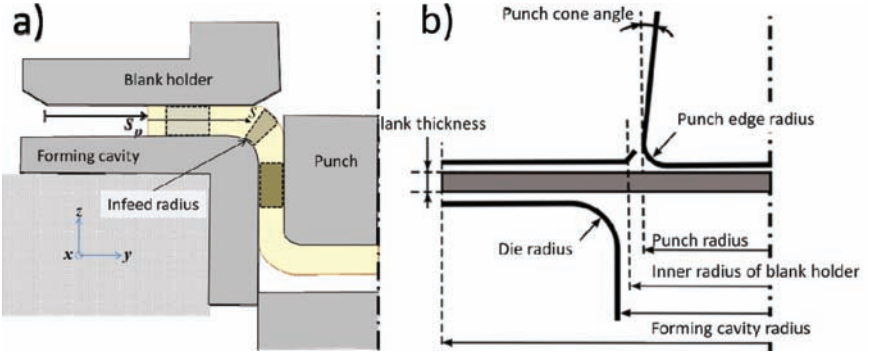

Figure 8. Schematic illustration of deep-drawing tool and geometrical parameters of importance, adapted from (a) [31] and (b) [30]. The dashed elements refer to the material elements in Figure 9.

between the punch and paperboard τ^1_{dg} and one between forming cavity and paperboard τ^2_{dg} (Figure 9). As long as τ^1_{dg} is higher than τ^2_{dg} the bottom can theoretically not break at this point and the loaded cross section of the material is relocated to a position above this point, (Figure 11b). During drawing of the material into the cavity the restraining forces below the blank holder are reduced due to the reduction in the frictional forces due to τ^1_{bh} and τ^2_{bh} that are balancing the drawing stress in the loaded cross section and also an increase in the cross section loaded in tension (Figure 10) since paperboard has a limited capacity to compensate for material excess by fibre-to-fibre movement, [27]. At this point the reduction in the restraining forces below the blank holder makes it possible to increase the blank holder force to a value that could be higher than the initial value. The benefits of this will be discussed further in section 4.4.

When approaching the position when the blank is leaving the blank holder, the blank holder force should typically be reduced to the lowest possible value in order not to damage the edge of the formed structure. In [31] different approaches for the blank holder force trajectory, between the possible rise in force when the blank enters the drawing clearance and the final decrease, are investigated as discussed further below.

2.3 Press-forming

Press-forming is a relatively established industrial method, based on the sliding blank principle, for manufacturing of paperboard plates and shallow trays, that largely resembles paperboard deep-drawing. There are in the literature several patents describing different press-forming related methods, cf. [33]; [34].

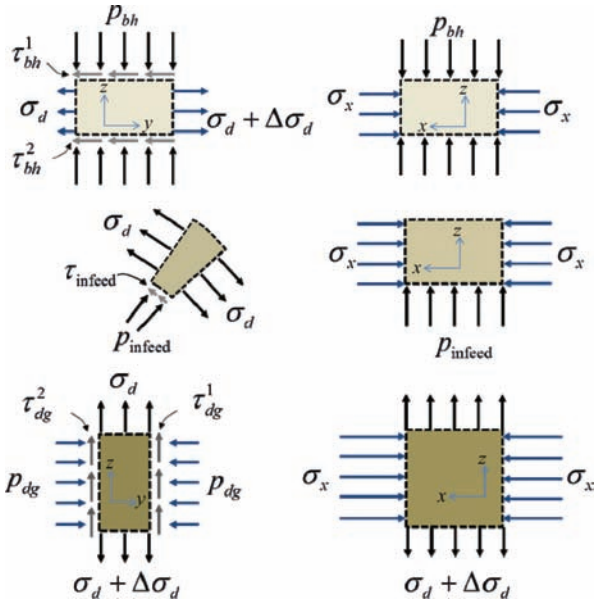

Figure 9. Schematic illustration of the stresses of the paperboard in the deep-drawing tool. The elements refer to two views of a material element at different positions in the drawing tool. All stress components are functions of the coordinate *s*, according to Figure 8. Note, that these figures do not illustrate gradients that are affecting the stress-state, for example, close to the edges and corners of the forming tools.

The basic steps in press-forming of paperboard are illustrated schematically in Figure 12. ❶: The paperboard blank is positioned between the blank holder and the forming cavity. The blank is in general pre-creased to adsorb circumferential compressive strains in convex corners as discussed further below. In general the forming cavity is heated, while the possibility to heat the punch is limited by polymeric coatings on the top side of the paperboard. ❷: The blank is clamped at the rim of the forming cavity using a blank holder force. ❸: The punch is pressed into the forming cavity. In contrast to deep-drawing, the paperboard blank is not subjected to immediate through-thickness compression. ❹: Flattening of the formed structured is instead accomplished by the final pressing of the punch into the forming cavity during a certain dwell time, and ❺ flattening of the compressed flange by a rim tool. ❻: Spring-back occurs when the tray is removed from the forming cavity. Final rigidity of the tray is achieved after cooling to room temperature. A more rigid tray is obtained if the paperboard blank is oriented such that the long side of a rectangular tray is in MD, [35].

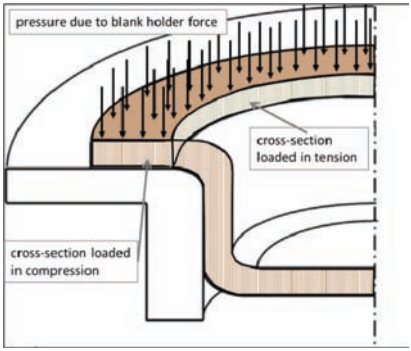

Figure 10. Illustration of the pressure due to the blank holder force when the paperboard blank is drawn into the forming cavity.

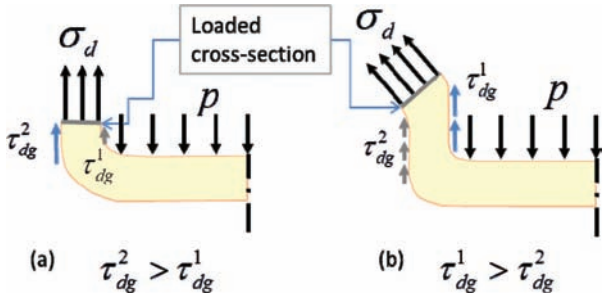

Figure 11. Illustration the stresses contributing to the tensile load in the paperboard blank when the paperboard is compressed between forming cavity and punch. The loaded cross-section in case (b) is relocated to a position further away from the base.

Commercially available press-formed paperboard products are in general limited to moderately shallow structures. Here, focus will be on the recent developments towards packaging applications, with leading contributions from primarily Lappeenranta University of Technology (LUT), Finland, but also elsewhere. The possibility to manufacture deep tray structures will make it a strong candidate for replacing fossil-based plastics, for example, in modified atmosphere packaging (MAP), [36]. Here, the most important findings will be reviewed, particularly, with respect to deformation and damage mechanisms, but also with respect to issues related to MAP.

The details of the geometrical conditions in the press-forming tool are illustrated in Figure 13, and details of the stresses at different positions in the process are illustrated in Figure 14.

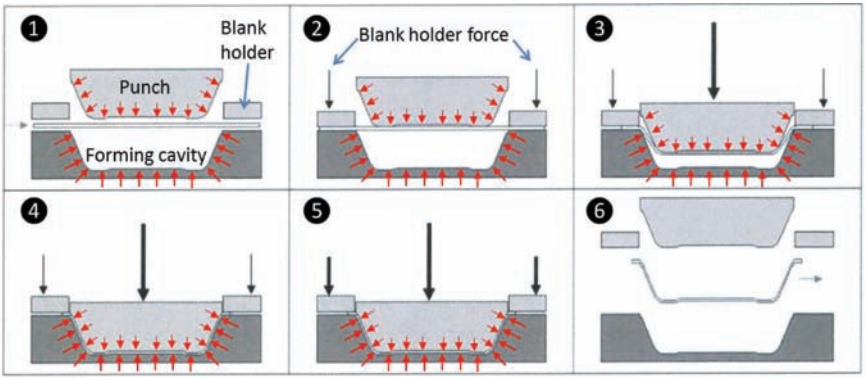

Figure 12. Major steps in press-forming of paperboard, redrawn from [37]. The red arrows indicate heat applied during the entire process.

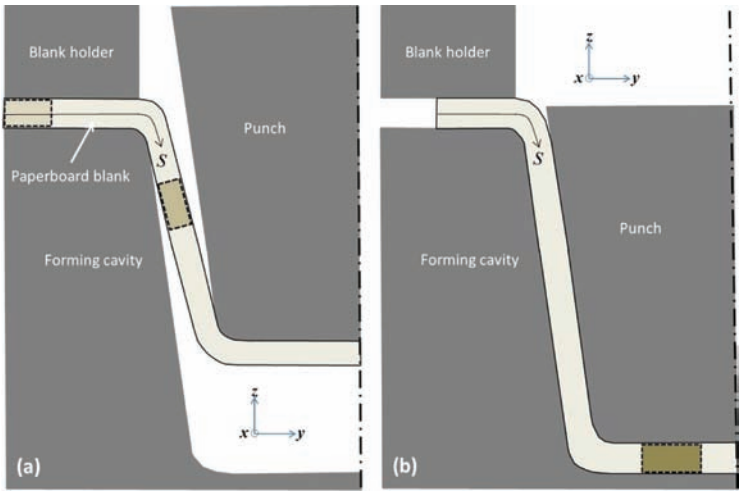

Figure 13. Details of (a) the infeed of the paperboard blank into the forming cavity and (b) the paperboard blank filling the forming cavity. The dashed elements refer to the material elements in Figure 14.

It is noticed that in the infeed, the paperboard blank will be subjected to a tensile loading from the punch and a compressive loading due to the material excess when being pushed into the forming cavity. The compressive loading will lead to wrinkling of the creases. To seal the creases, the paperboard blank is typically coated with a polymer layer. In order to soften the polymer layer and seal adjacent creases, the punch is typically held at the bottom of the female mould for

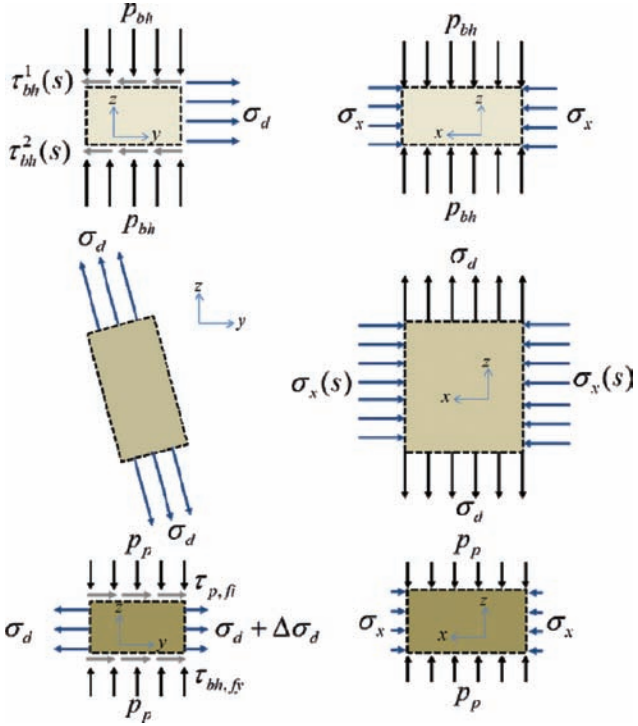

Figure 14. Schematic illustration of the stresses of the paperboard in the press-forming tool. The elements refer to two views of a material element at different positions in the forming tool. All stress components are functions of the coordinate *s*, according to Figure 13. Note, that these figures do not illustrate gradients that are affecting the stress-state, for example, close to the edges and corners of the forming tools.

a pre-set dwell time; see Steps 4 and 5 in Figure 12. Examples of tight and leaking seals are illustrated in Figure 15. Different deformation mechanisms of creases will be further discussed in section 4.3.

2.4 Hydro-forming

Hydroforming of paperboard is a fixed blank method schematically illustrated in Figure 16, and therefore, the notation stretch forming is also used for this and similar methods. ❶: The paperboard blank is clamped between the forming cavity and the blank holder. ❷: The paperboard structure is formed by applying pressure on a rubber membrane to inflate the membrane and the blank. Restraint is enforced on the edge of the paper blank by pressure from the blank holder outside the

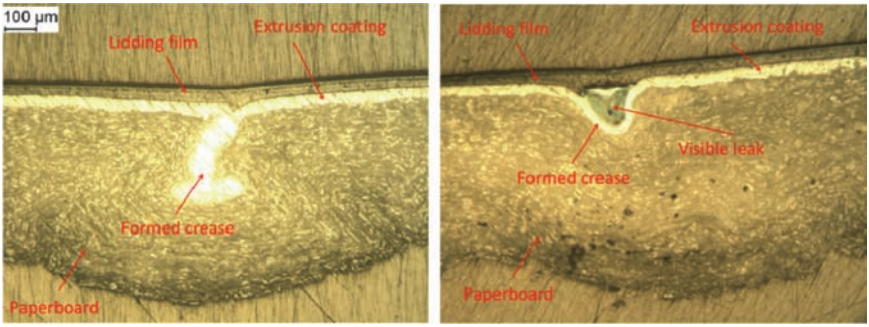

Figure 15. Optical light microscopy images of tight (*left*) and leaking (*right*) seal, [38].

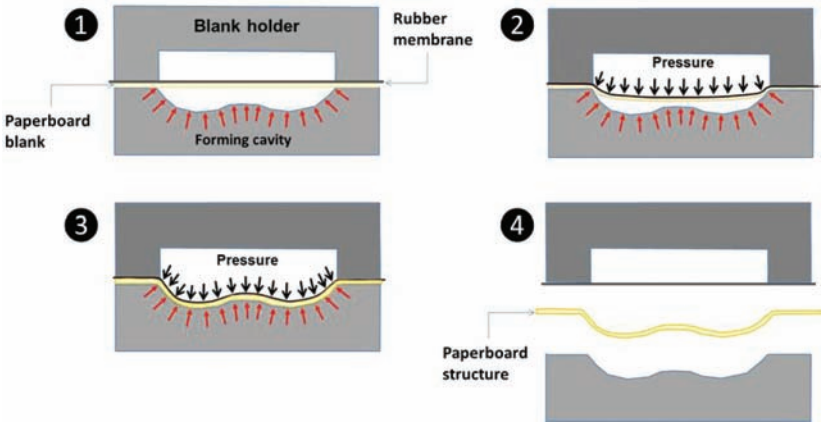

Figure 16. Schematic illustration of hydroforming of paperboard. The red arrows indicate heat applied during the entire process.

balloon against the forming cavity.❸: Below the blank is a heated forming cavity against which the paper specimen is pressed by the balloon for a certain dwell time. In contrast to deep-drawing and press-forming, the influence of mould clearance in relation to blank thickness is not an issue for hydroforming, and, in general, only a limited amount of sliding occurs below the blank holder. ❹: Spring-back occurs when the formed structure is removed from the forming cavity. Final rigidity of the tray is achieved after cooling to room temperature.

Hydroforming for paper materials was recently brought to attention by two separate research groups at KTH Royal Institute of Technology, Sweden and Technische Universität Darmstadt, Germany. The experimental study by [39] and

the combined experimental and numerical study by [15] identify many of the important process parameters for paperboard hydro-forming such as forming pressure, blank-holder force, forming cavity temperature, moisture content, friction and material properties. However, neither of these studies quantifies in detail the extent to which these factors affect the hydro-forming result. Hydro-forming is still in the laboratory scale, but recent success in development of materials particularly suitable for forming of 3D-structures [19] makes it an interesting option also for applications both in packaging and elsewhere.

The details of the geometrical conditions in the press-forming tool are illustrated in Figure 17, and details of the stresses at different positions in the process are illustrated in Figure 18. It is noticed that below the rubber membrane, the paperboard blank will, in general, be subjected to a biaxial loading producing an enhanced biaxial tensile behaviour in both MD and CD, in contrast, partly, to deep-drawing and press-forming. Despite being a fixed-blank method, hydro-forming of paperboard still could lead to wrinkles. One reason is geometric nonlinearity. At large deformation bending of paper, the paper tries to take on one of two cylindrical shapes. Forcing the paper to be double-curved leads to buckling; this may cause wrinkles [40]. The other obvious reason for wrinkling is that some material is still being drawn towards the centre of the mould, which decreases the circumference of the material circle, and avoiding these wrinkles, by restraining the edge of the blank, increases the risk of fracture.

At the infeed, the paperboard blank will be subjected to a tensile loading σ_d from the pressure on the rubber membrane. It is more difficult to speculate about the value of σ_x. If the paperboard blank is perfectly clamped at the edge of the forming cavity a uniaxial loading would lead to compressive stresses, but, on the

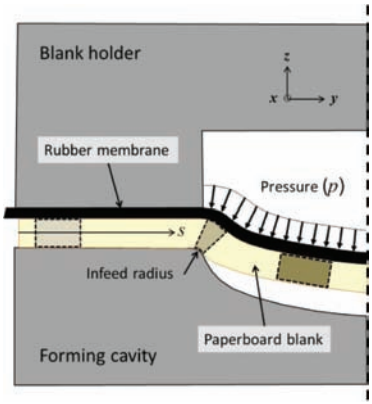

Figure 17. Schematic illustration of the details of the infeed of the paperboard blank into the forming cavity. The dashed elements refer to the material elements in Figure 18.

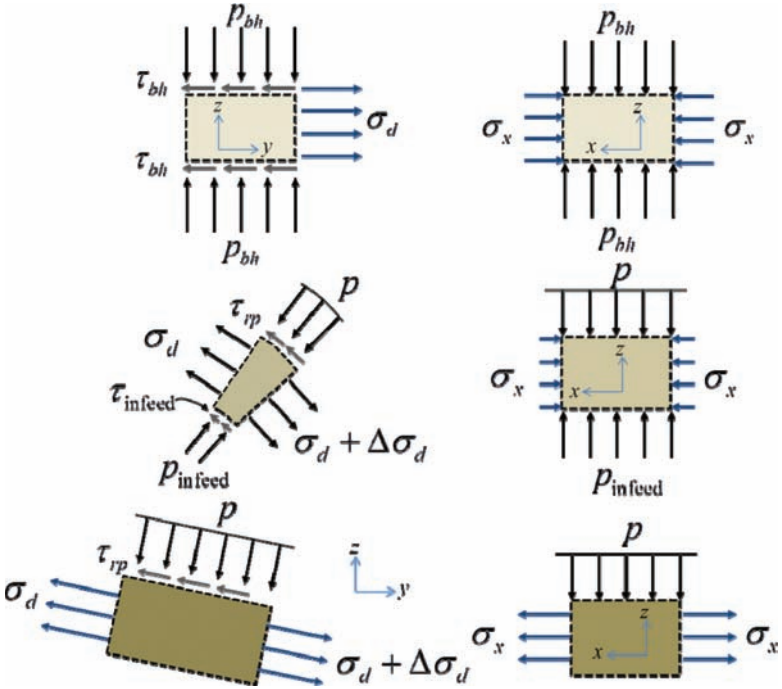

Figure 18. Schematic illustration of the stresses of the paperboard in the hydro-forming tool. The elements refer to two views of a material element at different positions in the forming tool. All stress components are functions of the coordinate *s*, according to Figure 17. Note, that these figures do not illustrate gradients that are affecting the stress-state, for example, close to the edges and corners of the forming tools.

other hand, the biaxially loaded blank would also generate a tensile contribution parallel to the edge of the forming cavity further away from the edge.

2.5 Other forming methods

Geometrically advanced cellulose-fibre based structures are also produced by other methods. There are in general similarities between these methods and the three methods described above.

One example is hot-pressing. This method exhibits large similarities with press-forming, but in contrast to press-forming, the structure in hot-pressing is formed into the desired shape, typically in a wet state, before being pressed and dried at increased temperature rather than being formed and dried in the same

step, [41]. In this way the amount of defects, such as wrinkles, can be avoided or at least limited.

Another example is thermoforming that exhibits large similarities with both press-forming and hydro-forming. This method is commonly not applicable to paper and paperboard due to the porous structure of such materials, but packaging materials are in general laminated with plastic coating layers that enable the material to be formed also in industrial equipment for thermoforming although being somewhat limited by the temperature sensitivity of polymer films.

3 QUALITY MEASURES

The need for a strategy to quantitatively evaluate the quality of formed paperboard structures was identified by [2]. Evaluation of *rupture* and *structural damage* are obviously two such parameters, but more refined measures are needed since there are large variations in quality also for structures that do not fail. Obviously, the potential success for advanced 3D paperboard structures is strongly dependent on the quality of the formed structure, and not only if it does not fail. To meet this demand they define and investigate three such measures: *shape accuracy*, *shape stability* and *visual quality*.

3.1 Rupture

In processes for forming of advanced 3D paperboard structures, the material will be subjected to complex states of loading close to the limits of the operational window of the material. While damage occasionally could be beneficial for the formability of paperboard, rupture of the material is never acceptable. Rupture in deep-drawing, press-forming or hydro-forming of paperboard is not one single phenomenon. There are in general several potential sources for defects, and their visual appearance depends on both process and material parameters.

Four important modes of rupture for deep-drawing of paperboard are identified by [42] as illustrated in Figure 19. Obviously, these different modes are activated by different less effective combinations of tool, material and process properties (Table 1).

In press-forming, failure is typically initiated at the corners close to the bottom of the structure. Similarly to deep-drawing, particular combinations of tool, material and process properties will trigger the different types of rupture. Different types of failures can be identified by more detailed analysis of the pressing forces as described in section 4.5. In press-forming, the polymer coating layer is of utmost importance for sealing the wrinkles of the pre-creased paperboard blank, and a damaged polymer layer will jeopardise the gas tightness of a MAP. This

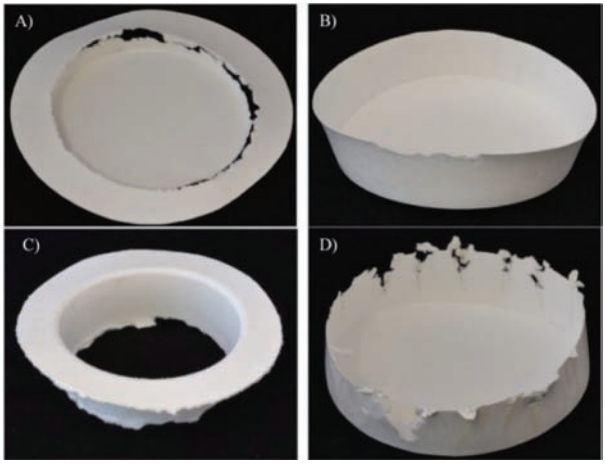

Figure 19. Examples of rupture modes in paperboard deep-drawing according to Table 1, [42].

Table 1. Important modes of rupture in 3D deep-drawing of paperboard [42]

Mode	*Rupture*	*Damage mechanism*
A	Rupture occurs at the radius of the punch	Initial blank holder force is too high and/or the drawing clearance is too small.
B	Rupture at the edge of the cup	Blank holder force is not reduced sufficiently and the local pressure at the flange is too high.
C	Rupture during the in-feed process	Coefficient of friction between the punch and the paperboard is lower than between the die/cavity and the paperboard.
D	Material destruction at the edge of the flange	Conical angle of the punch and the blank holder force is too low. This leads to large wrinkles entering a too tight drawing gap creating very high local compressions and multiple rupture due to friction in combination with high local compression occurs.

damage mechanism is particularly critical in the creased regions, and examples of cracking of the polymer coating layer are shown in Figure 20.

Different modes of rupture are also encountered in hydro-forming of paper materials. A typical mode of fracture is illustrated in Figure 21 where the paperboard fails perpendicular to the weakest material direction. More complex modes of failure are presented in Figure 22. When attempting to hydro-form pear-shaped

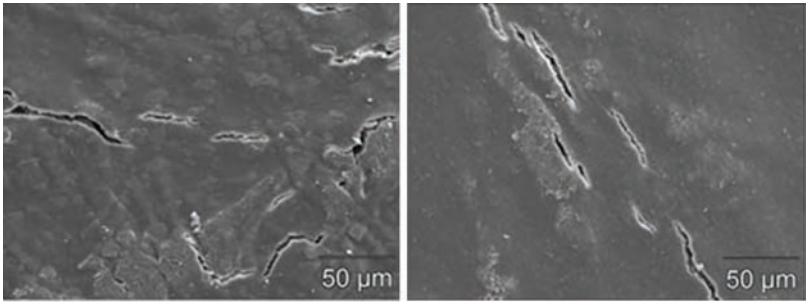

Figure 20. Cracking in the polymer layer of the creased regions of paperboard press-formed tray structure, [11].

Figure 21. Typical mode of rupture in paperboard hydroforming. Fracture occur perpendicular to the weakest material direction, [39].

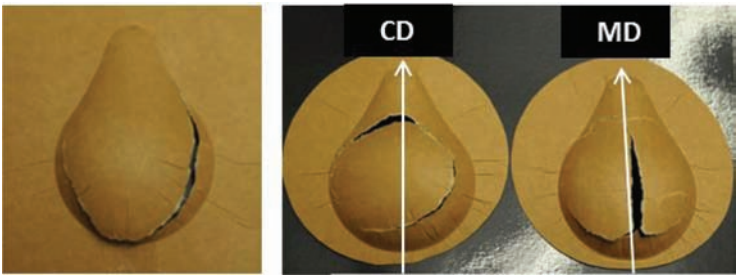

Figure 22. (*Left*) Experimental MD forming using 3 bars pressure and fixed boundaries, (*right*) experimental forming with different sheet orientation using 5 bars pressure and free boundaries, [17].

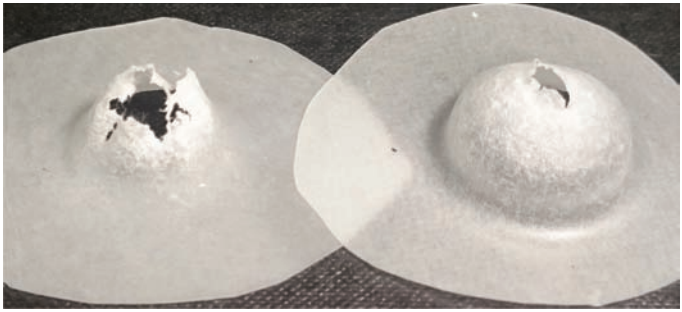

Figure 23. Two modes of failure for hydroforming of a sheets made of modified cellulose fibres. (*Left*) Forming pressure 2.0 bars, relative humidity (RH) 90%, forming cavity temperature 23 °C. (*Right*) Forming pressure 5.0 bars, RH 50%, forming cavity temperature 100 °C, [43].

paperboard structures, at least three different modes of rupture can be triggered by the material orientation and the clamping boundary conditions.

The moisture content and the forming temperature could also influence the failure mechanisms (Figure 23). Here, hydro-forming of highly strainable isotropic sheets made of modified cellulose fibres results in two seemingly different modes of failure by varying forming pressure, forming cavity temperature and relative humidity (RH).

3.2 Shape distortions

Shape accuracy is perhaps the most important criterion, since failure to meet shape accuracy in general renders other criteria irrelevant. In [2], two parameters to describe shape distortions, *spring-back* and *deflection*, as illustrated in Figure 24, are introduced. Spring-back is described by the angle between the base and the wall, and deflection is described by the horizontal distance between the border and the angular line of spring-back measurement. Shape accuracy is also affected by changes of the base shape due to the material anisotropy, but this change will also affect the spring-back angle, and was not considered separately by [2]. Shape distortions are, undeniably, consequences of the stress and strain fields in the formed parts, but to measure those in the formed part is not straight-forward since they are the result of a complex, non-linear, history-dependent thermo-mechanical process, and similar results can be achieved with different loading histories (including temperature and moisture) and different materials.

Deflection and spring-back angle are both related to the outer dimensions of the formed tray which are important for sealing of MAP as well as for packaging logistics in the supply chain [44] and further discussed in section 4.5. The outer

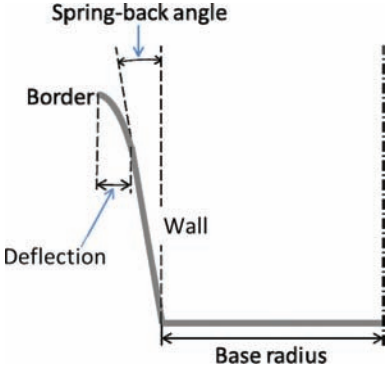

Figure 24. Definition of spring-back angle and deflection for analysis of shape accuracy, adapted from [2].

dimensions are typically affected by parameters that influence the elastic-plastic deformation of the paperboard blank during the forming operation and by parameters that influence the spring-back behaviour of the tray after being removed from the forming cavity. In general, the outcome of deflection and spring-back are structural dimensions larger than the values used in the tool design, and this has to be considered in design irrespective of the forming method chosen.

The walls of successfully formed three-dimensional paperboard structures will, irrespective of the visual appearance and shape distortions, have different, in most cases reduced, stiffness and strength properties compared to the unformed material due to irreversible deformation and damage mechanisms. This is illustrated in Figure 25 which shows reduced stiffness, strength and strain at break for a paperboard material after hydro-forming.

In the case of deep-drawing an important contribution is obviously due to the formation of wrinkles [45], and, similarly, in press-forming wrinkling of the creases subjects the material to high local stresses and strains, and in hydro-forming high tensile strains will influence stiffness and strength properties.

The final formed structure should resist any loading that occurs during end-use, and it should be sufficiently stiff and strong. To meet this requirement, [2] introduce the concept of shape stability. Ideally, it should be possible to measure the stiffness and strength properties of the formed structure in-situ. This is not, in general, possible, and perceiving that the most compliant in-plane direction in deep-drawn structures is perpendicular to the wrinkles formed in the wall, they find that the tensile work to failure W_{tens} of test pieces cut from the wrinkled wall varies significantly with process parameter variations and yields a relevant measure on the irreversible processes during the deep-drawing operation. This test and the related measure, being analogous to the tensile energy absorption

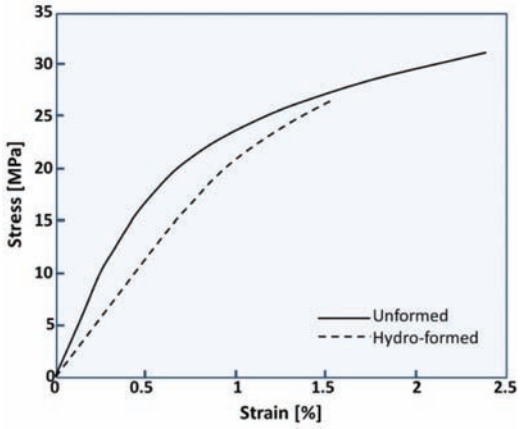

Figure 25. Typical tensile stress-strain curves for a paperboard material before and after being hydro-formed, [39].

(TEA) previously discussed for sack and bag paper grades, is illustrated in Figure 26.

One difficulty with 3D forming of paperboard structures, such as deep-drawn cups and, particularly, press-formed trays, is that the formed parts cannot be sealed gastight for modified atmosphere packaging (MAP) due to wrinkles formed in the manufacturing process. While the geometrical material overflow in metals and plastics are compensated by plastic deformation, this is in general not the case for paperboard, [8]. The wrinkles in parts formed from pre-creased board represent capillary tubes (Figure 27) that are not closed by heat or ultrasonic sealing since the melting of the plastic coating cannot fill the capillary tubes. However, if the forming

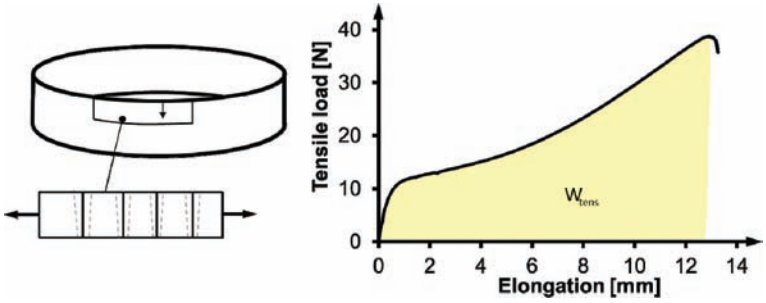

Figure 26. Shape stability testing for deep-drawn cup with wrinkles and illustrations of the force-elongation characteristics. Picture used with kind permission of Dr. M. Hauptmann, TU Dresden.

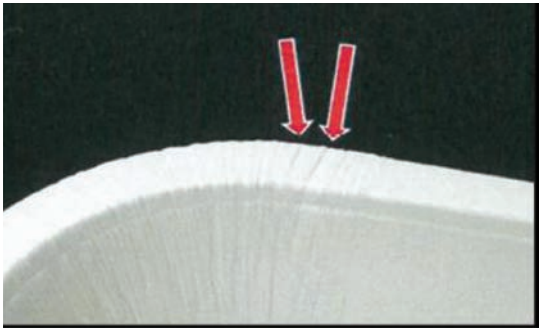

Figure 27. Examples of creases that have been formed inadequately leaving gaps between flat areas surrounding the crease, [46].

of the wrinkles and the distance between wrinkles is carefully designed, the relative uniformity of the wrinkled sections would allow for gastight sealing of MAPs. Thus, an important step in achieving geometrically advanced packaging from coated paperboard is to understand influence of process and material properties on the deformation and damage mechanisms of forming of wrinkles.

3.3 Subjective measures

The visual appearance of formed structures is an important criterion in packaging design being strongly related to the brand value. Typical defects in deep-drawing of paperboard are abrasion and ears at the rim. It is found by [2] that such defects and the visual quality are closely related to the number of wrinkles in the wall of the formed structure, since they cannot be completely avoided due to the material excess when the blank is drawn into the forming cavity (Figure 28). More wrinkles in general lead to a reduction in abrasion and ears. The visual appearance related to the number of wrinkles can be described by the average distance between wrinkles and the standard deviation of the measured distances between wrinkles. Thus, a large number of small, shallow wrinkles will lead to a short distance between the wrinkles [28], and the standard deviation is related to the uniformness of the wrinkle distribution. Improved visual quality is in general obtained for a more uniform wrinkle distribution.

To the knowledge of the author, there is no objective, quantitative, measure for the visual quality of press-formed structures. Examples of acceptable and poor quality trays are shown in Figure 29, and although the differences at the corner are clear, the quality analysis still relies on subjective measures.

In [37], the quality of the press-formed tray wall and the surface smoothness is analysed using a subjective grading system based on the visual appearance of the surface of the trays. The grades used in this system are defined in Table 2 and typical appearances including also rupture are illustrated in Figure 30.

Figure 28. Formed shape with wrinkles and microscope image of the wrinkles.

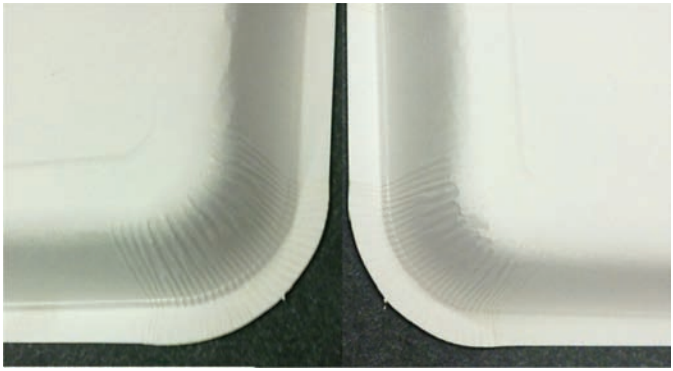

Figure 29. Examples of acceptable (left) and poor (right) quality for press-formed paperboard trays. Picture reproduced with kind permission of Dr. P. Tanninen, Lappeenranta University of Technology.

Table 2. Subjective grading scale for analysis of tray wall quality [37]

Grade	*Description*
–2	Mould clearance too large, creases fold irregularly
–1	Mould clearance a bit too large, unaccomplished crease smoothening
0	Mould clearance ideal, crease perfectly smoothed
+1	Mould clearance a bit too small, tray wall starts to polish too much
+2	Mould clearance too small, compaction of material causes fracture

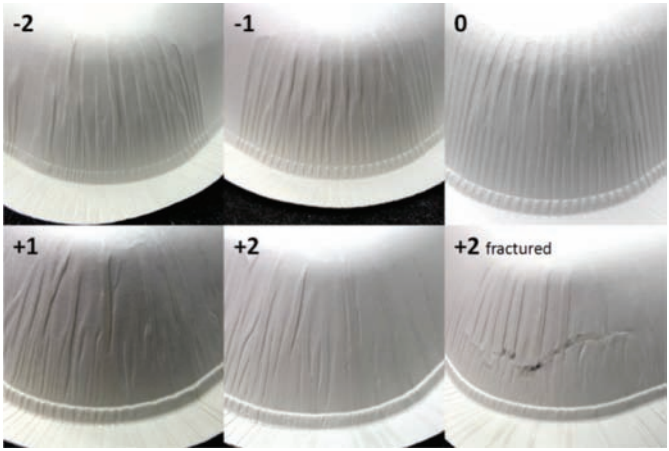

Figure 30. Example of the different quality grades according to Table 2 at observation point D (see Figure 65), [37].

4 PROCESS PARAMETERS

Advances in forming of three-dimensional paperboard structures require a thorough knowledge of the deformation and damage mechanisms that the material is subjected to during the different forming operations and how these are affected by tool properties, process parameters and material properties. Forming of advanced 3D paperboard structures are complex processes including a large number of more or less important parameters and properties. The task is to identify which factors have the largest influence, and how to tune those in order to achieve structures of desired quality. In the last decade, the number of scientific papers on different aspects of 3D forming has increased. The driving force behind this is to a large extent the demand for sustainable packaging, but also new paperboard materials with considerably improved properties underwrite this interest.

A more open investigation of the impact of traditional paperboard properties on the performance in different forming processes is reported by [28]. They investigate the formability of seven different commercial paperboards formed in three different types of laboratory forming devices; 2D formability tester, 3D spherical forming device and 3D deep-drawing equipment. Schematic illustrations and examples of structure formed in these pieces of equipment are shown in Figure 31.

The formability is evaluated using the depth of the formed parts and their visual appearance. Variables describing these properties are defined for each

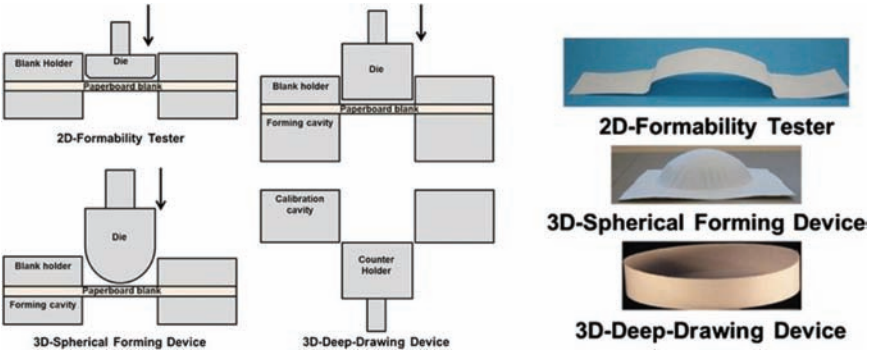

Figure 31. Principal modes of operation for the 2D formability tester, 3D spherical forming device and 3D deep-drawing device, and examples of shapes formed, [28].

forming device as formability strain (2D formability tester), maximum drawing limit (3D spherical device) and the number of compression wrinkles on the wall of the cylindrical shape (3D deep-drawing device). The formability strain is defined from the elongation of the material at failure due to the downward movement of the die, and the maximum drawing limit was estimated from the die position at failure, the dimensions of the forming tools and the thickness of the paper.

The paperboard properties included are tensile strain, compressive strain and strength, paper-to-metal friction, sheet thickness and mass density as well as the influence of elevated moisture and temperature. Here, it should be noted that with the exception of the tensile properties, the other properties are not necessarily straight-forward to measure. In [28] the compressive properties were measured using the ring crush test, the z-directional stiffness was measured using a 1 mm diameter steel ball on a pile of four sheets, and the friction was measure using a sliding device. Although straight-forward to imagine, these measures are by no means accepted without criticism in conventional testing of paperboard. Particularly, issues related to the frictional properties in forming operations are of great concern as further discussed in section 4.2.

4.1 Temperature and moisture content

The mechanical and frictional properties of paper and board are strongly influenced by changes in temperature and moisture content, and, therefore, these parameters are of utmost importance for the formability. The influence of the temperature and moisture content on paper properties is covered in the excellent review by [1] and optimal temperature and moisture content in different

3D-forming processes are presented by [47]. Here, only the knowledge of importance for the present purposes will be summarised.

Increasing the temperature and the moisture content will promote softening of the material leading to reduced stiffness and increased failure strain. Changes in temperature also will contribute to the drying of the material, and it is important to understand how the interaction between temperature and moisture content affects the material behaviour, see e.g. [48] and [49]. To the knowledge of the author, there are only a few investigations on the interaction between temperature changes and moisture transport in 3D paperboard forming processes. The influence of the coupling between temperature and moisture content on constitutive parameters describing the mechanical properties of paper is important, and this is investigated by [50]. They find that the coupling to the constitutive properties of paper is limited to the strength of the material, only. Thus, in the analysis of the deformation mechanisms in different forming operations, the influence of temperature and moisture content can, to a good approximation, be considered as uncoupled, and they apply this observation in their analysis of paperboard hydro-forming in order to capture the influence of drying on the shape accuracy of the formed structures [51].

Applying moisture to the blank prior to forming is one way of improving the formability and increasing the forming ratio. However, it is important to note that high moisture content decreases the strength of the paper, increases the paper-to-metal friction, and, therefore, may lead to fracture and breaks, [28] and [39]. The temperature of the forming cavity has a significant effect on the tray dimensions, because an increase in temperature has a strong effect on the spring-back of cellulose based materials as is noted by [2] for deep-drawing, [41] for hot-pressing and [39] for hydro-forming, among others.

It is shown by [28] that elevated temperature has a positive influence on the formability of paperboard, but the different forming devices behaves differently. In the 2D formability tester, the paper is heated by continuous contact with the heated punch. Paper with a grammage of 80–250 g/m^2 can be preheated to the die temperature within 0.5–0.7 s. This means that the temperature at forming is close to the temperature of the die, [28]. Since the 2D formability tester is not sealed from the surrounding atmosphere, moisture can escape from the board, and the optimal temperature is limited to temperatures well below 100 °C since the softening effect at higher temperatures is reduced by the reduction of the moisture content of the material, [52]. In the 3D spherical forming device, the paperboard is heated by convective heat transfer and direct contact with the forming device. In this case, the entire paperboard is not in direct contact with the forming device, and the temperature of the material is considerably lower than the temperature of the forming cavity. Furthermore, drying of the paperboard is restricted by the closed atmosphere, allowing for a softening of the material.

In forming using 3D deep-drawing, formability was evaluated using the wrinkle distribution. It is proposed by [28] that this parameter may not be directly affected by softening of the material. They also find that forming below 100 °C is not possible. They argue that the reason for this might be the influence of temperature on paper-to-metal friction, which decreases with increasing temperature as illustrated in Figure 32 for both static and dynamic friction. This argument is by no means obvious, since, intuitively, formation of wrinkles should be affected by the stiffness properties, but the state of loading is complex and further analysis is needed.

The approach for choosing the forming temperature should be based on achieving sufficient softening while at the same time avoiding excessive drying during the forming phase, [28]. Drying after forming is completed will reduce springback. This means that phenomena such as heat-transfer within the paper-board, moisture evaporation, softening of the paper and the effect of temperature on friction all need to be considered both in the design of forming operation, [28] and in development of simulation models.

A high forming cavity temperature also increases the number of wrinkles, and enhances the shape accuracy. The temperature of the forming cavity influences both the material properties and the gap between the punch and the die. Since the strength of the material is reduced by the increasing temperature, the blank holder force must be reduced. Thus, the blank holder force and forming cavity temperature need to be varied simultaneously, and there is a combination that optimises the number of wrinkles. The punch temperature has no effect on the number of wrinkles, but a high punch temperature has a significant and positive effect on the shape accuracy [53]. A possible explanation for this lack of effect on the number of wrinkles is that increasing the temperature of the punch diminishes the drawing gap and increases the through-thickness compression in the area between the punch and the forming cavity. This reduces the depth of wrinkles and perhaps also their visibility in the surface scan analysis tool used to determine the wrinkle distribution.

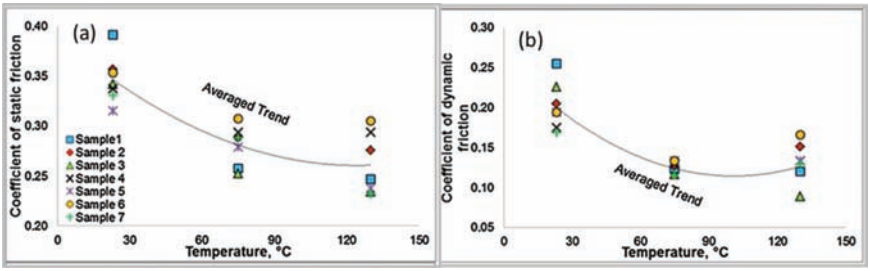

Figure 32. Influence of temperature on the static (a) and dynamic (b) paper-to-metal friction coefficient for different commercial samples, [28].

4.2 Friction

A decrease in the coefficient of friction is in general advantageous for the formability of paperboard. Sliding between paperboard and tool surface under through-thickness compression is a deformation mechanism of utmost importance in all three-dimensional forming operations. The frictional properties of paper based materials in general have both structural and chemical causes. As described by [1] there are many parameters affecting the frictional properties of paper materials, and for three-dimensional forming operations, parameters such as moisture content, temperature and sliding velocity are of importance, both for formability and runnability issues. Of particular importance is the influence of through-thickness compression since an increase in pressure will, in general, increase the contact area which is found to increase the friction. The frictional behaviour is also influenced by chemicals originating both from inside the material as well as from handling of the material, and this could have a significant effect on the runnability of the forming operation.

The significance of the frictional properties in different forming operations is shown in Figure 33(a) for the 2D formability tester and 3D spherical forming device, and in Figure 33(b) for the 3D deep-drawing device.

The technique developed by [35] to control the forming forces, based on a set of force sensors rather than one sensor only, is also used to estimate the coefficient of friction for different coated paperboard blanks. They find that the coefficient of friction obtained with standardised laboratory test methods (ASTM D 1894–63) does not differ substantially from the values estimated from force measurements in press-forming at 23 °C. For higher temperatures, the coefficient of friction can increase substantially compared to the room temperature values. It is also noted

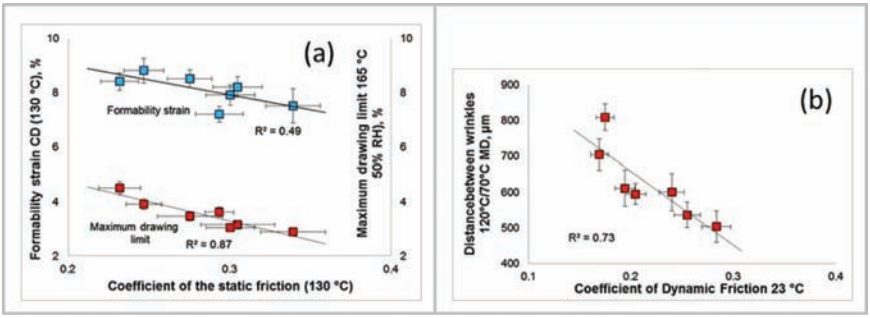

Figure 33. (a) The correlations between the formability strain (70 °C), the maximum drawing limit (165 °C) and the coefficient of friction (130 °C), and (b) the relationship between the coefficient of dynamic friction measured at 23 °C and the distance between wrinkles 120/70 °C, for different commercial samples, [28].

by [35] that the pressing force decreased substantially with increasing temperature of the forming cavity. This indicates that the softening properties of the fibre network are important for successful forming and that the plastic deformation of the blank must be large, as expected.

As illustrated above, the paper-to-metal frictional properties play important roles in all processes for forming of advanced paperboard structures. In general they are related to both deformation and damage mechanisms that the blank experiences during the forming. This is clearly illustrated in deep-drawing where too high friction between forming cavity and blank immediately would lead to fracture of the paperboard, [42]. Thus, devices for reliable and representative characterisation of the paperboard-to-metal frictional properties are of utmost importance for 3D-forming of paperboard.

With few exceptions, standards and measurement devices are designed for contact forces applicable to printing process, such as transportation of the web or sheet through a printer, [54]. This means contact pressures that are order of magnitude smaller than what is experienced by the paperboard in forming operations. Furthermore, it should be possible to measure the frictional properties also for the relatively high temperatures that prevail in forming operations.

To meet these demands, a new device is developed by [54]. This device has an amplifier for heating of the material, a pneumatic unit that enables control of the normal force, and the translation of the test piece is realised by a servo-drive. Furthermore, different measurement concepts are possible due to a stiff design. In order to generate plane tool contact a ball scraper is also used. In [54], the contact pressure and distribution is measured with pressure sensitive sheets, and the performance of the device is simulated using the finite element method. Results for two-sided paper-to-metal friction coefficients at two different material orientations are shown in Figure 34. It is noticed that while contact force definitely influences the coefficient of friction, at least compared to a very low contact force, material orientation and sliding velocity, to a lesser degree, are also affecting the results. In this context, it is important to bear in mind the fact that the frictional properties of paper are of both structural and chemical origin and, particularly, the effect of different chemicals, such as e.g. wood extractives, fatty acid and waxes could be significant and very difficult to control. Therefore, great care is needed when handling the material both in testing and in forming operations.

4.3 Deformation of creases and wrinkles in folding and 3D-forming

In 3D forming methods, pre-creasing of the paperboard blank is often used [26, 38]. Creasing is an essential part of the die-cutting process in paper and board converting [55]. The creasing tool scores the paperboard blank to define folding or wrinkling lines in the material, as illustrated in Figure 35. In printing and

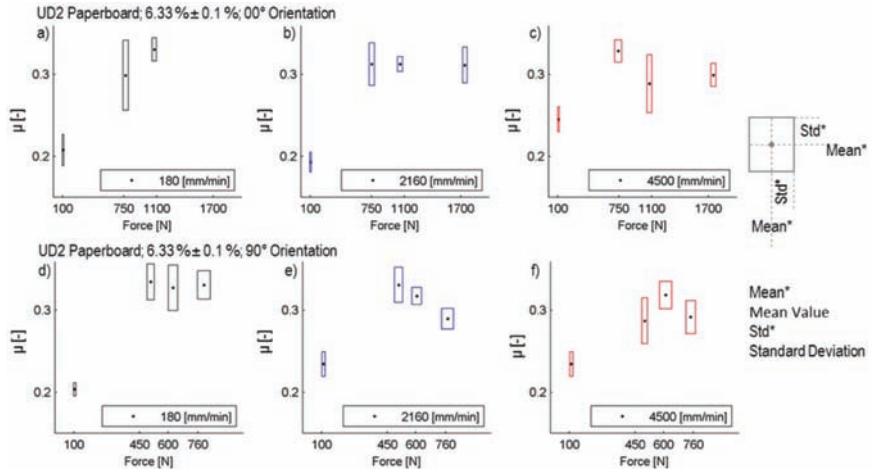

Figure 34. Experimentally determined friction coefficients for two-sided paper-to- metal as function of contact force for two material orientations at different sliding velocities, [54].

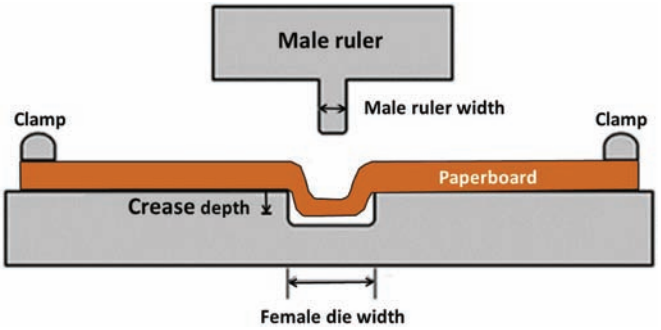

Figure 35. Schematic illustration of paperboard creasing and geometrical parameters affecting the creasing operation.

packaging applications, scores are used to enable trouble free folding of coated paper and paperboard along these score lines. Correctly designed creases will contribute to crack free folding that will improve the aesthetics appearance of printed products, and uniform creases will improve the packaging performance. In 3D forming, creases are used to control the blank forming process. In regions of high compression the strains are handled by wrinkling of the sheet material.

There are in general no noteworthy differences in the deformation and damage mechanisms of the creasing operation for folding and forming applications,

respectively. The creasing operation itself involves parameters related to the geometrical shape of the creasing groove and material properties. It is, however, noticed by [11] that the geometry has minor effects only on the cracking tendency of coated paperboard and not on the formability, but that details in the tool geometry could be of importance for more demanding applications.

Analysis of the deformation and damage mechanisms in creasing of paperboard has been a topic of considerable interest in recent years, and today it is possible to investigate the relations between fundamental paperboard properties and the creasing performance using novel experimental techniques and state-of-art numerical simulations based on the finite element method [56]–[60].

The subsequent deformation mechanisms in folding and wrinkling of paperboard are different. This is illustrated in Figure 36. In folding, the surfaces of the creased region are not loaded in the thickness direction, and part of the material is expected to bulge at delaminations created by the creasing operation. Ideally, the performance of the crease should be the same along the entire fold. A typical appearance of the cross-section after folding along a score line is shown in Figure 37. In forming processes score lines are used to control the deformation. The creased region is typically subjected to a compressive through-thickness loading that restricts the thickening of the sheet. Referring to Figure 36, this results in a deformation mechanism that absorbs the in-plane compressive strain

$$\varepsilon = \frac{l'}{l} \tag{2}$$

by shortening the width of the score line.

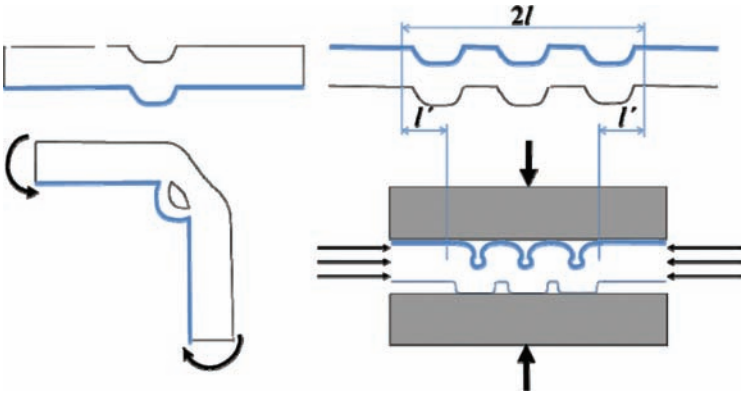

Figure 36. Illustration of different local deformation mechanisms of folding and press-forming, adapted from [46].

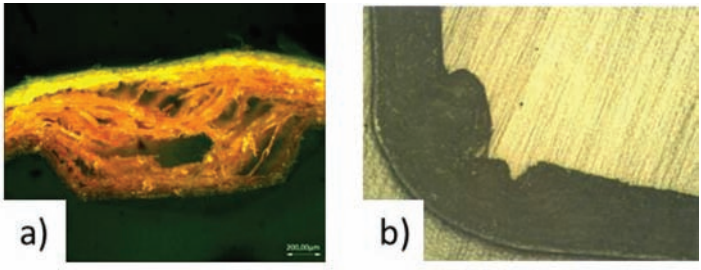

Figure 37. Microscopic image of folding of a creased paperboard, (a) [61] and (b) [37].

Although not formed in a completely similar way, it is interesting to notice the similarities between the deformation mechanism for wrinkling of creased and uncreased paperboard in a fixed blank process (press forming) (Figure 38) and sliding blank process (deep-drawing) (Figure 39). Ideally, the strain between

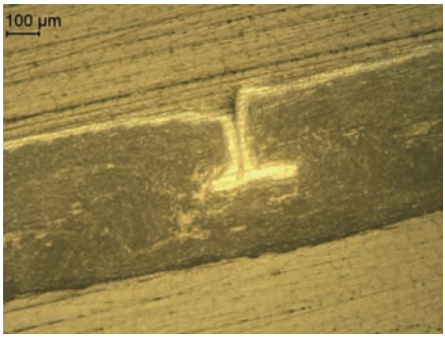

Figure 38. Micrograph of the deformation of a single crease of a press-formed tray of PET-coated paperboard, [37].

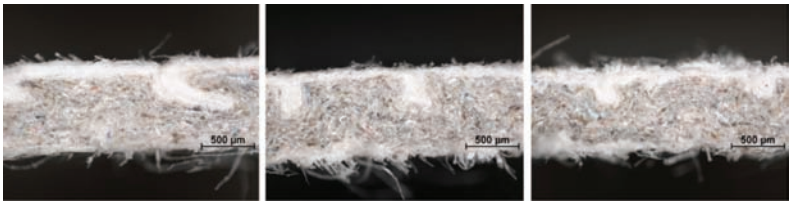

Figure 39. Cross-sectional cut of walls made by deep-drawing at different blank holder forces in microscopic scale. Picture reproduced with kind permission of Dr. M. Hauptmann, TU Dresden.

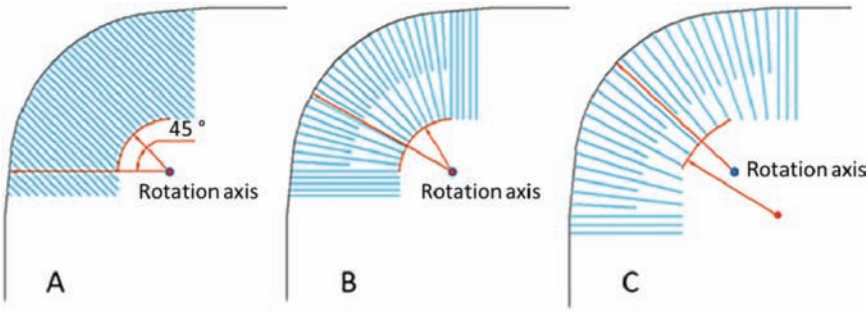

Figure 40. Different creasing patterns used by [46].

parallel score lines should be the same in order to create a smooth surface of high visual quality. This is, however, not straight-forward to achieve, and in e.g. double-curved tray corners the in-plane compressive strains vary along as well as between the crease lines.

The uniformity in the folding and closing of the pre-creased paperboard blank is a function of the macroscopic strain-field, the dimensions of the creasing tool and the physical properties of the material. Forming of an even and smooth wall requires an optimised number of creases of certain dimensions at the correct positions. Creasing pattern design, in the form of positioning of creases, the amount of creases and the width of creases are investigated by [46] evaluating different creasing patterns for (Figure 40) for five different types of trays. The effect of creasing patterns is evaluated by the quality of the fold and the flatness of the tray flange, where discarded creases were not formed properly and had large gaps in the tray flange area, (Figure 27).

It is found in [46] that the number of creases is the most important parameter in the pattern design, and that the optimum number of creases is based on the radius of the blank. Furthermore, narrower crease widths in general fold more evenly, and, thus, a wide crease cannot replace several narrow creases. Also, creases positioned radially towards the rotation axis folds more evenly cf. creasing patterns B and C with creasing pattern A in Figure 40.

4.4 Deep-drawing

Process parameters of relevance for deep-drawing of paperboard are related to the motion of the forming tools, material properties and process parameters. Examples of parameters that need to be considered in deep-drawing of paperboard are listed in Table 3. A major step forward in understanding and advancing the paperboard deep-drawing process has been published in [32]. The results attained

Table 3. Examples of parameters in deep-drawing of paperboard, condensed from [2].

Motion design	*Material properties*	*Process parameters*
Punch motion	Fibre raw material	Geometrical shape
Motion synchronization	Network structure	Drawing height
Cycle time	Mechanical properties	Tooling
Inertia	Surface properties	Drawing gap
Control deviation and quality	Sorptive properties	Tool temperatures Moisture content
	Temperature properties	Blank holder force

in this doctoral thesis, and additional developments thereafter have been published in a number of papers, and here the most important findings will be reviewed.

To implement the technological advancements, and to enable close control of process parameters, a highly flexible laboratory deep-drawing device was developed at the Institute of Processing Machines and Mobile Machines at TU Dresden. This equipment is described in detail in e.g. [2, 32] and it allows for independent control of *blank holder force* and *temperature* and *motion* of the tools. This equipment and the associated process are illustrated in Figure 41.

The complexity of deep-drawing of paperboard can be outlined based on basic considerations related to tool geometries, tool motion, material properties, moisture content and temperature. The strong anisotropy of paperboard in general leads to more severe unwanted effects compared to deep-drawing of metals and

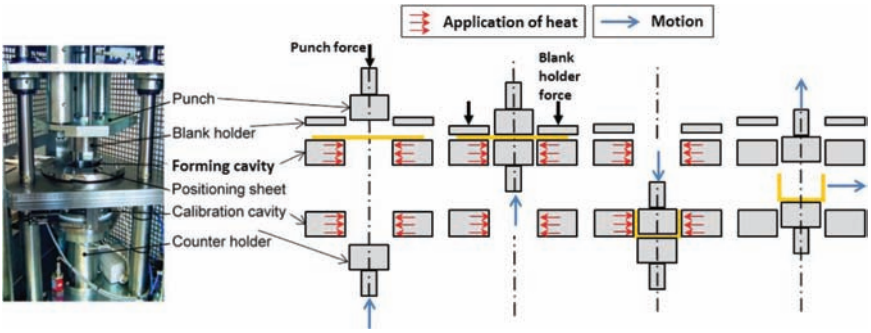

Figure 41. The deep-drawing laboratory device at TU Dresden. Typical values of process parameters are punch temperature 90 °C, forming cavity temperature 140 °C, blank holder force in the order of 500–9000 N, drawing gap 0.3 mm and dwell time 2.5 s. Picture reproduced with kind permission of Dr. M. Hauptmann, TU Dresden.

plastics. A crucial deformation mechanism for the quality of the formed parts is the immediate compression experienced by the material when being fed into the drawing gap. Obviously, this will be directly influence by the tool geometry. Temperature increases will cause thermal expansion in both the tools and the paperboard material, and moisture content and temperature will have a strong influence on formability of the material and the drying of the formed product as well as the paper-to-metal frictional properties. The choice and formation of material constituents and the conditions during papermaking offer various possibilities to design the material, but due to the lack of models and quantitative knowledge on the damage and deformation mechanisms during paperboard deep-drawing it is difficult to systematically understand the influence of different parameters.

Failure of the material is not a continuously defined output variable and [42] studied parameters that influence rupture in paperboard deep-drawing by employing a statistical analysis based on logistic regression with a binary outcome based on intact or damaged deep-drawn cups. They find that different modes of rupture (Figure 19, Table 1) can be distinguished with such a model, and conclude that the blank holder force (cf. Figure 41) is the most critical process parameters when it comes to the occurrence of rupture. A high punch velocity is beneficial when the material does not experience substantial out-of-plane compression in the drawing gap, and the occurrence of rupture is also influenced by the conditioning of the surface of the forming cavity. On the other hand, there is no significant influence of punch radius (defined in Figure 8), temperature of forming cavity and paperboard moisture content. The latter two parameters are somewhat surprising since it is well-known that they strongly affect the mechanical properties of paperboard. The reason for this anomaly has not been established, but one possible explanation is that the actual values of the temperature and moisture content of the material in the real process are different from those determined prior to testing, cf. [39]. Since it is difficult to measure these parameters in the real process, analysis using a simulation tool could perhaps be used to spread some light on this hypothesis.

The influence of five basic parameters is investigated experimentally using a multiple linear regression analysis by Hauptmann and Majschak [2]. They include blank holder force, sum of the tool temperatures (punch and forming cavity), difference in tool temperatures, and initial moisture content and grammage of the paperboard material in their analysis. The investigated ranges of the parameters are listed in Table 4. The temperatures of the tools are expected to influence the material properties since it is well-known that an increase in temperature causes thermal softening of the material. The temperature difference will influence the drawing gap with obvious consequences for the immediate compression that the material will experience when being drawn into the forming cavity.

In their analysis they use a combined quality criterion where all quality parameters relevant to shape accuracy, shape stability and visual quality, i.e. spring-

Table 4. Parameters and upper and lower values used in the paperboard deep-drawing investigation by [2].

Parameter	*Lower value*	*Upper value*
Blank holder force	500 N	3000 N
Sum of temperatures of punch and forming cavity	200 °C	300 °C
Difference in temperatures of punch and forming cavity	0 °C	100 °C
Initial paperboard moisture content	7.3%	11%
Grammage	510 g/m^2	600 g/m^2

back angle, deflection, tensile energy absorption, wrinkle distance and wrinkle distance standard deviation, are given the same weight. They find that the blank holder force, the sum of tool temperatures and the initial moisture content are the most important process parameters and the impact of them are shown in Figures 42–45. The effect of temperature difference and grammage compensates themselves in this analysis, and [2] emphasize that their conclusions are based on a linear regression analysis that do not necessarily describes the physical relations sufficiently well.

The distance between wrinkles is significantly reduced by all parameters except grammage, probably since increased grammage leads to increased sheet thickness and the drawing gap was fixed. Increasing the value of a constant blank holder force leads to a drastically better wall quality with more uniform distributed wrinkles and reduction of wrinkle distances (Figure 42). This is credited to flattening of the paperboard blank before being drawn into the forming cavity. This affects both the stiffness properties and the thickness of the paperboard, parameters that will influence both forming and compression of wrinkles. Further influences of different parameters on the formation of wrinkles are speculated on in [2] without reaching a decisive conclusion. This is not unexpected since the compressive loading in the drawing gap will be a very complex non-linear function of many parameters and, in the opinion of the author, there is not even today sufficient knowledge on the mechanical properties of the material in order to verify possible deformation mechanisms in detail.

The immediate through-thickness compression experienced by the paperboard blank when it is fed into the forming cavity is of utmost importance for the outcome of the forming operation. The magnitude of the compressive stress is the result of an increase in blank thickness due to the circumferential compressive stress, wrinkling and the difference between the radius of the forming cavity and the punch, here, defined as the drawing gap. The compressive stress that will have a positive influence on the formation of a beneficial wrinkle distribution is a

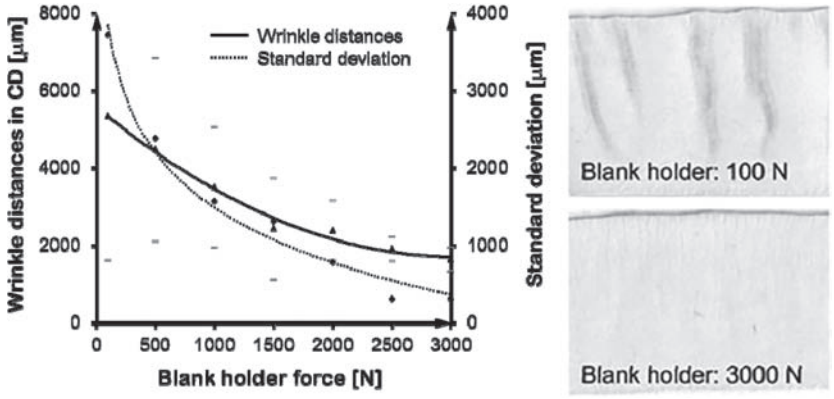

Figure 42. Typical appearance for wrinkle distance and its standard deviation as functions of blank holder force (*left*), and examples of visual appearances of the wall in the CD for blank holder forces of 100 N and 3000 N. Pictures reproduced with kind permission of Dr. M. Hauptmann, TU Dresden.

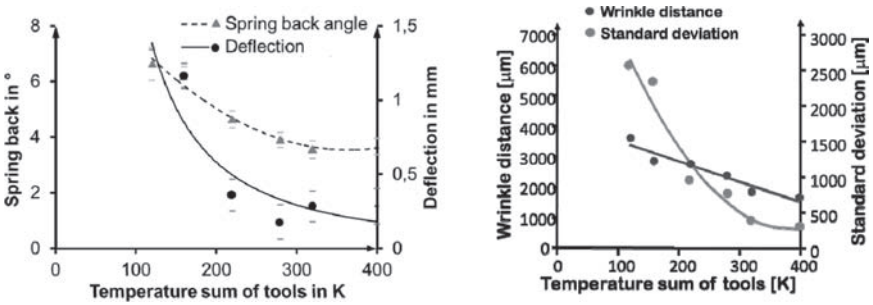

Figure 43. Typical appearances of spring-back angle, deflexion, wrinkle distance and standard deviation of wrinkle distance as functions of the sum of tool temperatures (energy input). Pictures reproduced with kind permission of Dr. M. Hauptmann, TU Dresden.

function of both the drawing gap and the paperboard blank properties such as thickness, density and stiffness properties. Typically each material and geometry combination requires an optimised drawing gap, which will require new tools for each combination. To the knowledge of the author, there is not yet an efficient approach for estimating the required drawing gap, and today one has to rely on testing and experience.

The influence of paperboard thickness in relation to drawing gap, polymer coating layer, drawing speed and temperature of the forming cavity on the quality of deep-drawn cups is investigated by [62]. They use two grammages (290 g/m^2

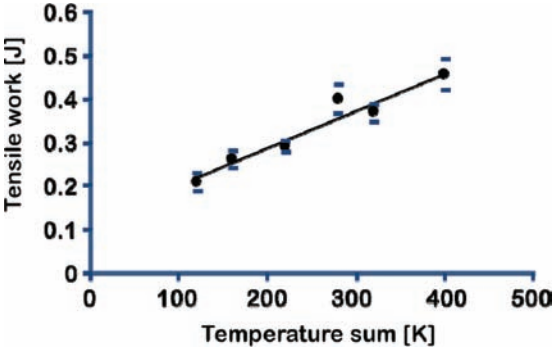

Figure 44. Typical appearance of tensile work to failure as function of sum of tool temperatures (energy input), redrawn from the data of [2].

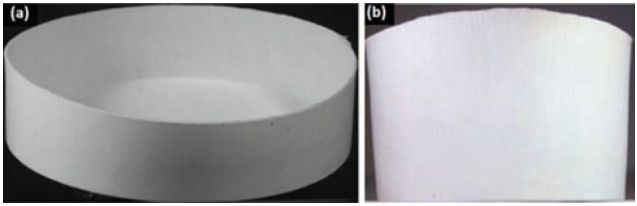

Figure 45. (a) Optimized quality of deep-drawn paperboard parts, (b) improved forming degree with a forming ratio of 0.63. Pictures reproduced with kind permission of Dr. M. Hauptmann, TU Dresden.

and 350 g/m^2) of a three-layered solid bleached sulphate paperboard with and without an extruded 40 g/m^2 PET coating representing four different blank thicknesses (318, 349, 381 and 414 μm). The drawing gap is 0.3 mm and deep-drawing is carried out at forming cavity temperatures of 100 and 180 °C and different drawing speeds (2, 25 and 50 mm/s). The number of wrinkles is evaluated using the technique developed by [53]. The results for the number of wrinkles as function of cup height are shown in Figure 46 for the four different material thicknesses.

An increased forming cavity temperature has a positive effect on the quality of the formed cups as represented by the number of wrinkles as previously observed by, for example [53]. The influence of the drawing speed is less obvious. As long as the polymer coating layer is not damaged, there is not much difference between different drawing speeds suggesting that drawing should be carried out at the highest possible speed in order to enable high production volumes. The number of wrinkles is clearly lowest for the 350 g/m^2 paperboard with a 40 g/m^2 PET coating

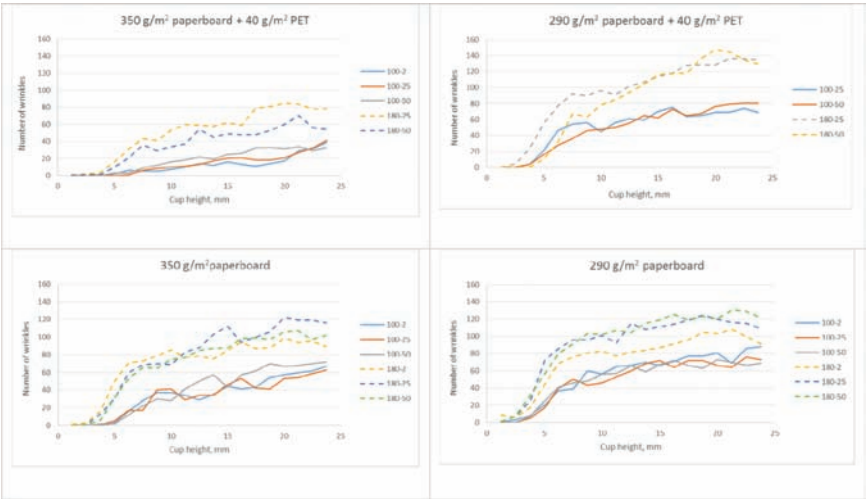

Figure 46. Number of wrinkles for different materials, forming cavity temperatures (100 or 180 °C) and drawing speeds (2, 25 or 50 mm/s) at different cup heights. The first number in the legends for the different curves is the forming cavity temperature and the second is the drawing speed, [62].

representing a thickness of 138% of the drawing gap. This is in agreement with the findings of [37] that suggest a blank thickness of 95–135% of the drawing gap for press-forming of paperboard.

A maximum in the possible number of wrinkles is expected. This number should be a function of the paperboard stiffness and damage properties, the stress state and the drawing gap, and these parameters, in turn, are affected by moisture content, tool temperatures and possibly also porosity or other parameters describing the microstructure of the material. To establish the relations between these parameters and the wrinkle distribution is a research area of importance for both process and materials design, that so far has reached limited attention. It is today, in principle, necessary to tune the blank holder force for each combination of paperboard properties and process parameters. This would require a mathematical model describing the deformation behaviour in the process with sufficient detail, and initial attempts along this line were recently presented in [63, 64], as will be discussed further below.

The shape stability, as defined by the tensile work of failure, is mostly influenced by grammage, since this leads to higher tensile strength, and the moisture content of the paperboard. Positive effects are also seen for combined increase in grammage and moisture content, while a temperature difference between forming tools and material has a negative effect on the shape stability. While the blank

holder force has a major influence on the formation and visual appearance of wrinkles, it is not believed to have a significant effect on the fixation of the wrinkles [2]. A too high blank holder force could have a negative effect on the shape accuracy, particularly the spring-back angle, as noted by [53], and possibly also lead to wall rupture (Figure 19, Mode B) because of the increase in the resisting frictional forces as the blank is drawn into the forming cavity. The parameters that influence the shape stability, as defined by the force-elongation characteristics in Figure 26, are investigated further by [45]. They study two materials with respect to process and material parameters; one commercial paperboard and one laboratory material with enhanced formability due to improved fibre-to-fibre mobility [27]. Tensile test were carried out on test pieces, cut at different positions, from the wall of cups drawn to different height as shown in Figure 47.

Their results (Figure 48) show that shape stability as expressed by the initial stiffness of the wrinkled material decreases systematically with drawing height, while the strain-at-break increases linearly with drawing height. This could be explained by the increasing number of wrinkles for the test pieces cut from positions at larger drawing heights. The linear increase in strain-at-break (Figure 48b) can be explained by the increase in material excess at higher drawing heights, and the solid line is a theoretical estimate based on the forming cavity radius and drawing height.

An adapted blank holder force as further discussed below significantly improves the wall stability and supports the exploitation of the material fixation capacity resulting in the possibility to use elevated moisture, tool temperature and through-thickness compression. The laboratory material that should support in-plane fibre movement also exhibits improved shape stability. Furthermore, it is found in [45]

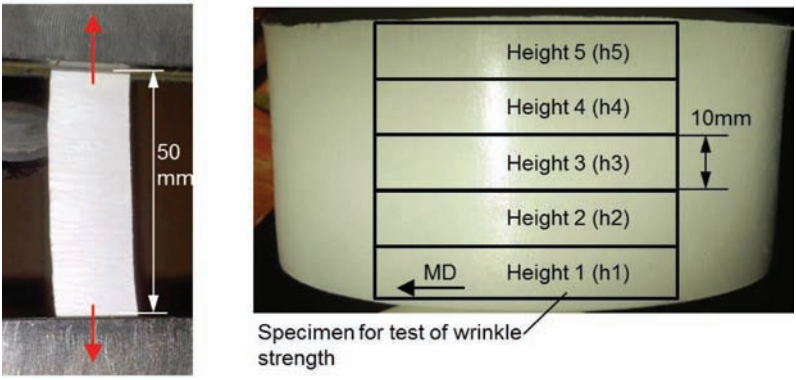

Figure 47. Illustration of tensile testing of test pieces cut from the wall of a 50 mm high deep-drawn paperboard, [45].

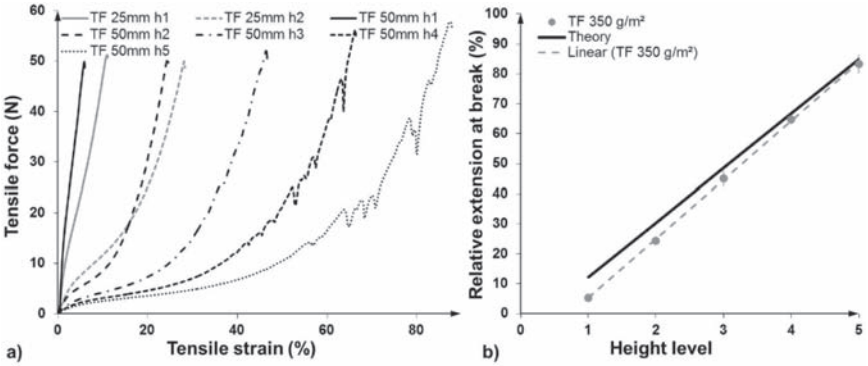

Figure 48. (a) Tensile force as function of tensile strain and (b) strain-at-break for test pieces cut at different positions (Figure 47) of 25 mm and 50 mm deep-drawn paperboard cups for a commercial paperboard with a grammage of 350 g/m^2, [45].

that higher through thickness compression improves wall stability. This is expected since successful forming at higher compression should result in a material with higher density.

Shape accuracy, as defined by the deflection of the wall of the formed parts, is strongly influenced by the thermal energy input. This indicates that the drying of the material is the major mechanism for shape accuracy. Drying of the material increases the elastic stiffness and thereby reduces the residual deformation after the forming.

A constant blank holder force does not react to the material thickening that originates from in-plane compression and formation of wrinkles, and leads to a continuous increase in pressure from the blank holder on the paperboard blank with decreasing contact surface as the blank is drawn into the forming cavity as illustrated in Figure 10. The decrease of the contact surface is quadratic in punch position, s_P (Figure 8), for circular blank and base geometries, and the contact pressure,

$$p = \frac{P_{BH}}{A_{contact}} = \frac{P_{BH}}{\frac{\pi}{4}\left(D - 2s_P\right)^2 - \frac{\pi}{4}\left(d + 2r_c\right)^2}, \tag{3}$$

is asymptotically approaching a very high value before the blank leaves the blank holder [31]. In Equation (3), P_{BH} is the blank holder force, D is the blank diameter, d is the punch diameter and r_c is the infeed radius. The decrease in contact area between the blank holder and the blank is well approximated by a linear function, and motivated by this a blank holder force decreasing linearly with punch position is used for, example in [42] and [53] with considerable success. In order to

improve the deformation experienced by the material in the forming process, it would be advantageous to adapt the blank holder force to the position of the punch. The positive effect of this is known from deep-drawing of sheet metals [65]. The influence of a variable punch force trajectory is investigated in [31] by allowing the blank holder to go over from position to force control when the blank holder comes into contact with the paperboard. Examples of different blank holder force trajectories for a certain paperboard and tool set are shown in Figure 49. It should already here be noted that different blank holder force trajectories are in general needed for different materials and tool parameters, such as the drawing gap. The maximum value of the punch position in Figure 49, 22 mm, is the value when the blank leaves the blank holder.

The *constant* blank holder force is chosen as the maximum force that does not lead to rupture, and the *linear decreasing* punch holder force is motivated by the discussion following Equation (3). The value 500 N is the lowest possible value of the blank holder force for the equipment used. The *peak* and *extended maximum* blank holder force trajectories are motivated by the possibility to increase the blank holder force due the reduction in the restraining forces below the blank holder when drawing the blank out of the blank holder. The values of the blank holder force, as function of the punch position for the blank holder force trajectories in Figure 49, were determined experimentally to avoid wall rupture. The *theoretical optimal* trajectory is based on the assumption that the load carrying ability (Figure 10) is proportional to the circumference of the material drawn into

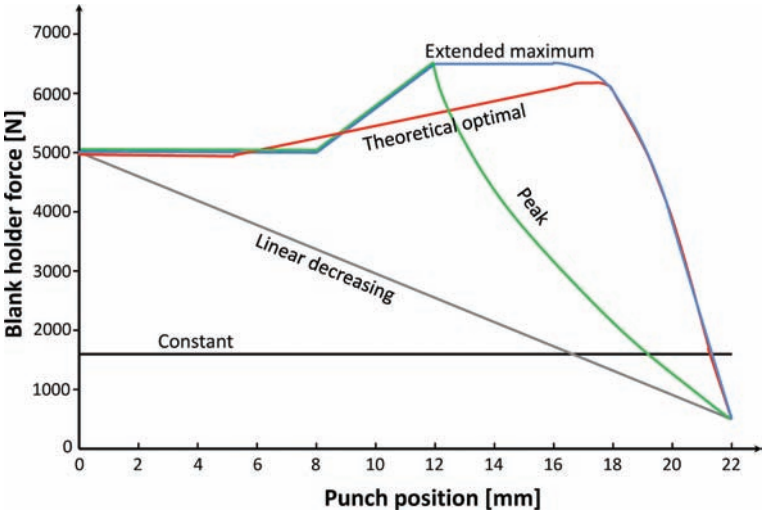

Figure 49. Different blank holder force trajectories, redrawn from [31].

the forming cavity. Although the material is forced to wrinkle the increasing cross section is not fully compensated, and it is available for additional tensile loading, and might increase the endurable tensile force continuously with a linear characteristic [31]. Using the slope of this linear function in the development of the circumference of the currently loaded cross section illustrated in Figure 10 should lead to an optimised increase in the blank holder force. The trajectories shown in Figure 49 are for a tool set with a relatively large value of the drawing gap paperboard thickness ratio. For a smaller drawing gap the optimised blank holder force, in contrast to the larger drawing gap, needs to be decreased during the initial phase of the drawing, otherwise the material ruptures [31]. A higher drawing ratio will also reduce the feasible blank holder force since a higher drawing ratio will generate additional tensile load in the tensile loaded cross section. (Figure 10)

The blank holder force trajectory affects both the drawing height at which wrinkles are formed, the number of wrinkles at the maximum drawing height and the standard deviation of the distance between wrinkles, Figure 50. In Figure 51 examples of the formed cup wall for different blank holder force trajectories for a commercial 350 g/m^2 paperboard are shown. It can be concluded that the adaption of the blank holder force trajectory to the deformation and damage mechanisms of the material in the 3D deep-drawing process leads to significant improvements in visual quality. The higher blank holder force levels possible for the adapted trajectories support the prevention of wrinkles by restricting out-of-plane fibre movements. In the design of the blank holder force trajectory, the through-thickness compression enforced by the drawing gap, and the paperboard stiffness and strength properties need to be considered.

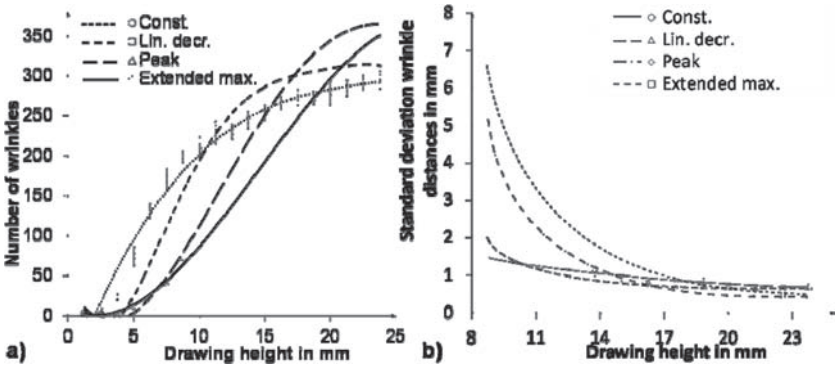

Figure 50. (a) Number of wrinkles detected over the drawing height; (b) Development of the standard deviation of wrinkle distances with the drawing height. Pictures reproduced with kind permission of Dr. M. Hauptmann, TU Dresden.

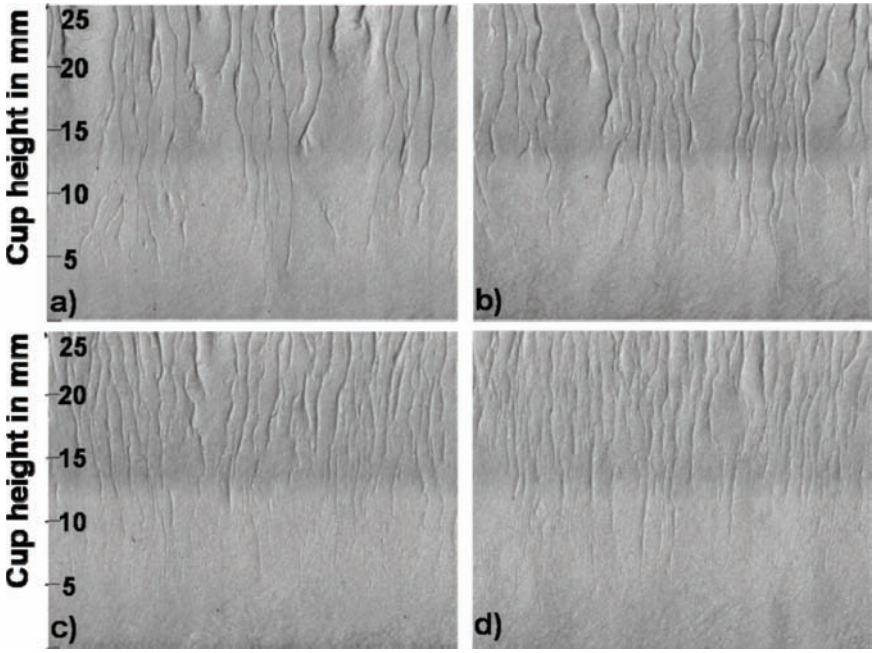

Figure 51. Sections of scanned walls of deep-drawn 25 mm high paperboard cups in CD for the different blank holder force trajectories in Figure 49: (a) Constant blank holder force of 1600 N; (b) Linearly decreasing; (c) Peak; (d) Extended maximum. Pictures reproduced with kind permission of Dr. M. Hauptmann, TU Dresden.

To advance the geometry of shapes is a key driving force in the development of paperboard packaging designs. The recent technological developments in deep-drawing of paperboard open up possibilities to improve the drawing ratio, but also to form new innovative base shapes, Figure 52. Traditionally, paperboard deep-drawing has been limited to convex base elements. In contrast to the convex sections, there will be a shortage of material in the concave sections (Figure 53) resulting in high tensile strains parallel to the base that quickly can reach the failure strain of the paperboard. The deformation mechanisms of deep-drawing of concave and straight sections (Figure 52) are studied by [25]. Of particular interest is to investigate possible overflow of material from convex sections to neighbouring straight and concave sections.

In straight sections the areas of the paperboard blank and the formed structure's wall are equal, and no in-plane compression is expected due to material overflow. However, in [25] wrinkles are observed also in the straight sections (Figure 54). This indicates a possible deformation mechanism where in-plane compression is

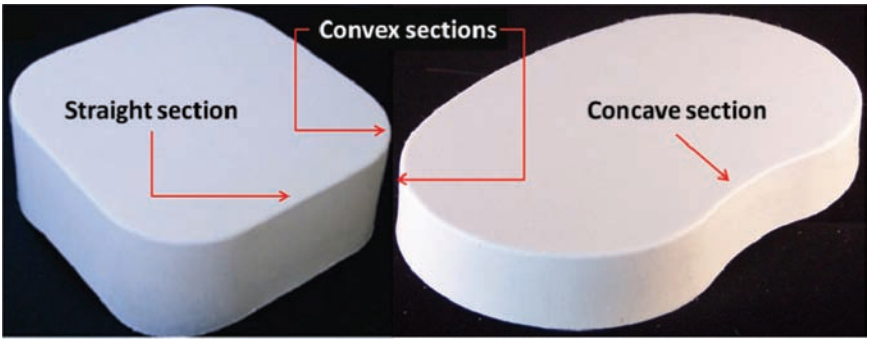

Figure 52. Innovative base shapes. Picture reproduced with kind permission of Dr. M. Hauptmann, TU Dresden.

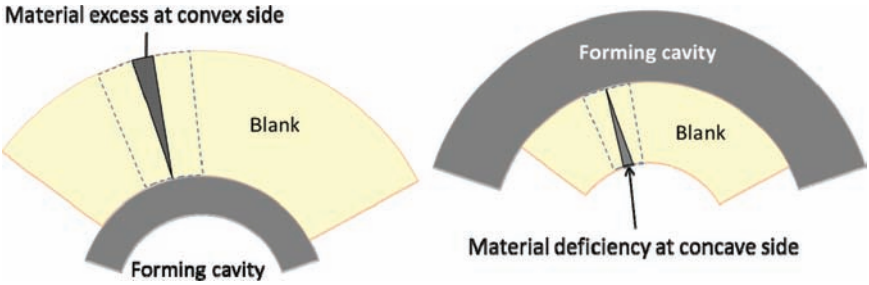

Figure 53. Illustrations of material excess at convex base shape and material deficiency at concave base shape in drawing of paperboard.

created by material overflow from the adjacent convex sections. The material overflow means that the geometrically required strain in the concave sections can be larger than the measured strain-at-break of the material. Tensile loading of concave sections leads to compressive stresses normal to the base and wrinkles can occur parallel to the base, as shown in Figure 54.

Thus, [25] demonstrates that deep-drawing can be used to produce concave three-dimensional paperboard structures if the geometrical parameters are carefully adjusted. Using recent numerical analysis tools [63] and [64] it should be possible to further elaborate on the deformation mechanisms in deep-drawing of base elements with concave parts, and particularly determine the operational window of paperboards required for a certain base shape. New fibre network materials with considerably improved strain to failure will also play an important role in the development of advanced structures with concave base elements [19].

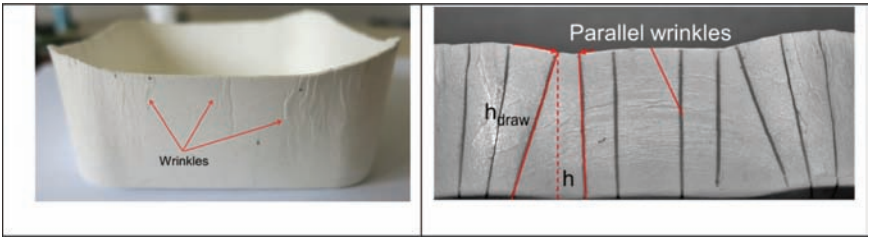

Figure 54. Wrinkles in straight sections of rectangular deep-drawn paperboard structure (*left*) and wrinkles parallel to the base in concave sections (*right*), adapted from [25].

New combinations of material, base shape geometry and drawing height require new tuning of the blank holder force trajectory and tool temperatures (thermal energy intake) [26]. In order to provide deeper insight into the limitations of deep-drawing of paperboard, [26] utilize recent advancements in blank holder force trajectory [31]. The challenge in improving the drawing ratio is to avoid fracture at the bottom of the formed part since the paperboard has to be able to carry the sum of the restraining forces in the drawing gap and between the blank holder and the forming cavity [9]. Circular base shapes, with a punch diameter of 110 mm, and punch edge radii of 5 or 10 mm, and rectangular base shapes, according to Figure 55, are used to analyse the effects of base shape radius and punch edge radius (see Figure 8). Blank preparation using creasing lines is also included in the analysis in order to deepen the understanding of the geometrical limitations.

The base shape radius is varied between 6 and 30 mm for four different drawing heights. It is important to pay attention to the fact that a certain edge radius leading to failure is always related to the drawing height [26]. An increase of the punch edge radius to 10 mm, compared to the 0.2 mm used in [31], does not influence the forming parameters, but leads to non-compressed wrinkles, at the bottom radius, (Figure 56) while the quality of the wrinkles in the walls is not affected. The appearance and number of wrinkles depend on the fibre orientation. Wrinkles formed when the material is compressed in the MD appear rougher and clearly visible. The reason for this is likely related to a lower stiffness in CD. For higher wall heights and smaller base shape radii (8 to 12 mm) in a commercial paperboard, the material excess could hardly be handled within such a small region, and increased relocation of the material to the straight sections is observed, Figure 57.

The punch edge radius is a critical point before the material is compressed in the drawing gap [26]. An increasing bottom edge radius reduces the visual quality by the presence of non-compressed wrinkles. For a large punch edge radius the initial part of the deep-drawing process closely resembles press-forming and the material will experience a stress-state similar to the one illustrated by the middle material element in Figures 13 and 14. Increasing the blank holder force and

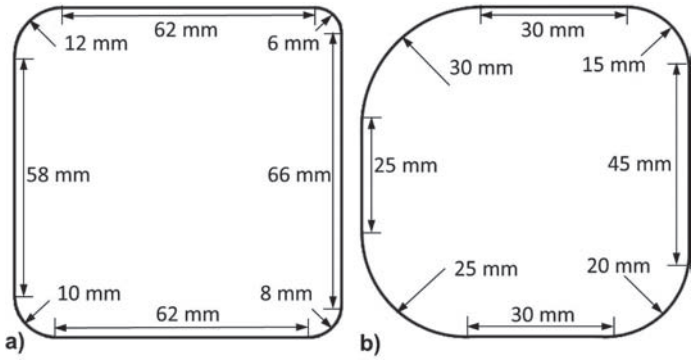

Figure 55. (a) and (b), base shape geometries with different base shape radii, [26].

Figure 56. Wrinkles at a punch edge radius of 10 mm in structures drawn at a maximum blank holder force of 5000 N and a sum of tool temperatures of 300 °C: (a) compression in MD; (b) compression in CD; and (c) compression in CD at a maximum blank holder force of 8000 N, [26].

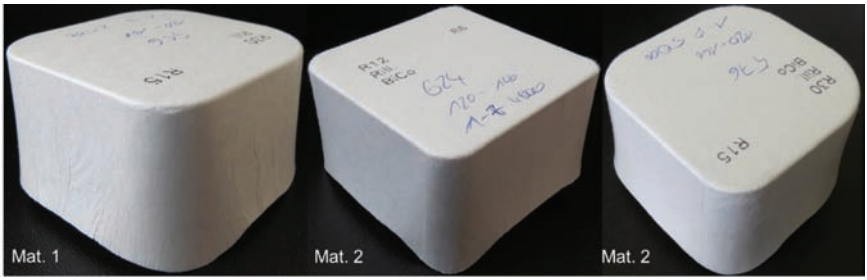

Figure 57. Formed structures of rectangular 3D-shapes with the tool sets introduced in Figure 55 for a commercial paperboard (*left*) with 15 mm radius in front, and from a laboratory biocomposite fibre material with radius 10 mm in front (*middle*) and with radius 15 mm in front (*right*), [26].

thermal energy intake reduces the non-compressed wrinkles at the bottom radius considerably, but the increase in these two variables is limited by the strength of the material. For materials with large values of strain-at-break the edge punch radius at which non-compressed wrinkles occur is increased. In contrast to deep-

drawing with immediate compression, it is for large bottom edge radii advantage to have a material that also has a high value of the failure strain.

The maximum forming ratio with a cylindrical base for a typical commercial paperboard is in the order of 0.9–1 [31]. Materials with improved out-of-plane compressive deformation behaviour are likely to provide potential for forming ratios of 1.3–1.5. The value of the punch edge radius strongly influences the height that can be drawn. Larger values of the edge radius make it possible to draw higher cups on the expense of the type of wrinkles shown in Figure 56. Using creasing lines at the edge radius supports the achievable wall height and increases the blank holder force that can be applied. Spring-back of rectangular shapes is reduced, with increasing drawing height and smaller punch edge radius leads to less spring-back and a better shape accuracy [26]. This is likely due to highly localised inelastic deformation at the base shape corners and at the small punch edge radii limiting the influence of the elastic spring-back of these regions.

Although, there have been major improvements in the performance and understanding of the paperboard deep-drawing process, there are still important problems to solve, particularly related to quantitative understanding of the deformation mechanism. It also remains to implement these developments in fast-running packaging machines, i.e. to go from laboratory scale to full production via pilot scale investigations. Two of the most important topics for the quality of deep-drawn paperboard are optimised blank holder force trajectories and elevated initial paperboard moisture content. In order to avoid motion control problems related to the switch over from displacement to force control used in the laboratory equipment [2], and time-consuming conditioning of the blank material, a spring-loaded solution for applying the blank holder force profile in displacement control and a roll preparation method for applying water to the paperboard is investigated in [66]. Covering one of the rolls in a two-sided roll solution with a sponge enables a fast moisture uptake of up to 12% moisture content. The risk for oscillations of the blank holder through harmonic oscillations in the spring-loaded system depends on a number of factors such as system layout, masses, spring-stiffnesses and drive frequencies, but appears to be manageable for an output range of 10–200 packages per minute [66]. Furthermore, these authors find that the spring package reduces the sensitivity of the blank holder force to small changes in position, due to for example the forming of wrinkles, which reduces the requirement of the accuracy of the position control, considerably.

The fixation of wrinkles formed in deep-drawn paperboard structures is enhanced by reduced material stiffness and increased out-of-plane compression. This can be achieved by increasing the tool temperatures and the moisture content of the material, and by reducing the drawing gap [45]. Being inspired by developments in sheet metal forming, [67] suggest the concept of using small

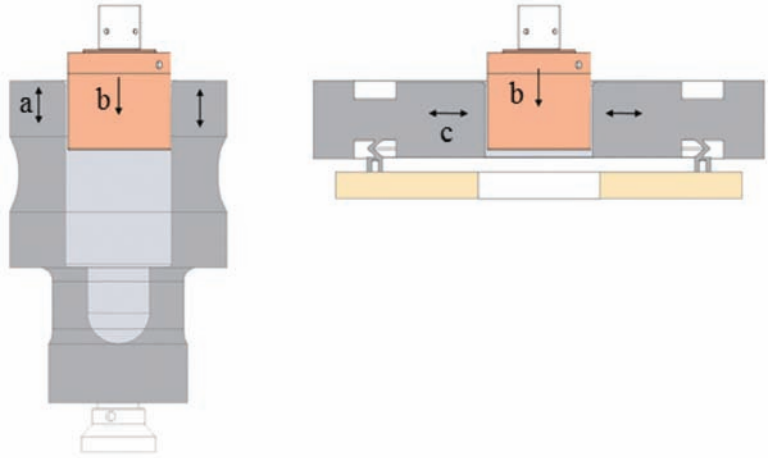

Figure 58. (a) Axial vibrations of the die; (b) Axial vibrations of the punch; and (c) Radial vibrations of the die. Picture reproduced with kind permission of Dr. M. Hauptmann, TU Dresden.

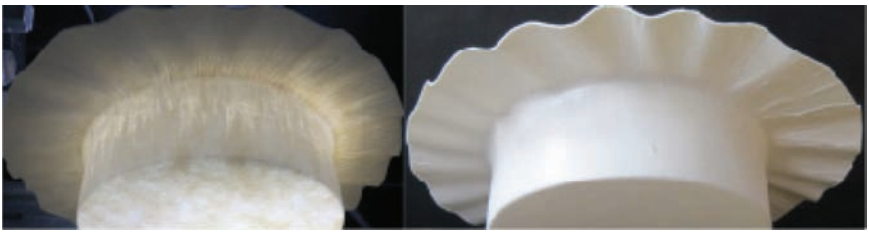

Figure 59. Ultrasonically deep-drawn paperboard cup. Picture reproduced with kind permission of Dr. M. Hauptmann, TU Dresden.

ultrasonic vibrations of the forming tools in order to generate a rapid increase in temperature. This would not only increase the temperature, but also contribute to the densification of the network structure without reducing the drawing gap. Ultimately, it can also have an effect on the frictional properties between the paperboard blank and the tool. The lay-outs of the axial vibration of the punch and the axial and radial vibrations of the forming cavity are illustrated in Figure 58. It is found by [67] that the ultrasonic vibrations have a large impact on the heat generation in the material during the forming process, and that the wall stability as well as the surface smoothness is considerably improved. However, the use of a vibrating punch may lead to relative motion between the punch and the

paperboard which can cause rupture at the bottom of the punch as described by Mode C in Figure 19. Furthermore, care is needed with respect to the material thickness in relation the drawing gap, and with respect to geometric deviations and misalignments in the process. An example of a deep-drawn paperboard cup using vibrations of the forming cavity, only, is shown in Figure 59. Note particularly, that part of the cup wall has become transparent due to the high density of the material.

4.5 Press-forming

Similarly to paperboard deep-drawing, press-forming of paperboard also involves a large number of parameters related to geometry and motion of the tools, process parameters and material properties. In Figure 60, the pressing force, the blank holder force, the tool temperatures and the pressing speed are illustrated. The mould clearance, dwell time and the moisture content of the formed paperboard are examples of other parameters that can be altered. A summary of the most important process parameters are listed in Table 5.

An important contribution to the paperboard press-forming research is carried out at Lappeenranta University of Technology. The LUT Packaging Line illustrated in Figure 61. This device has separate die-cutting and press-forming units and enables accurate control of process parameters, and also contains a unit for different types of quality control [68].

The outer dimensions of press-formed trays are investigated by [44]. They find that they are primarily affected by the temperature of the forming tools, the dwell time and the pressing speed, while the pressing and blank holder forces have only minor influences on the dimensions of the press-formed tray. These results are in line with the results found for deep-drawing [2], [30], [53]. The temperature of the forming cavity and the dwell time has a significant effect on the tray dimensions because an increase in temperature impacts the spring-back of cellulose based materials as noticed by [41] for hot-pressing. An increase in the pressing speed

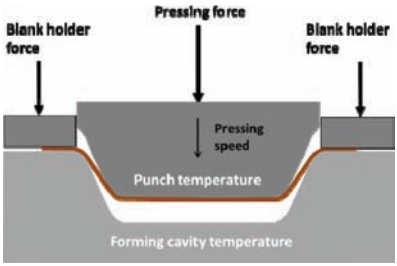

Figure 60. Process parameters for press-forming of paperboard, adapted from [10].

Table 5. Examples of parameters that needs to be considered in paperboard press-forming

Motion design	*Material properties*	*Process parameters*
Punch motion	Fibre raw material	Geometrical shape
Cycle time	Network structure	Drawing height
	Mechanical properties	Tooling
	Surface properties	Mould clearance
	Sorptive properties	Blank holder force
	Temperature properties	Tool temperatures
		Moisture content

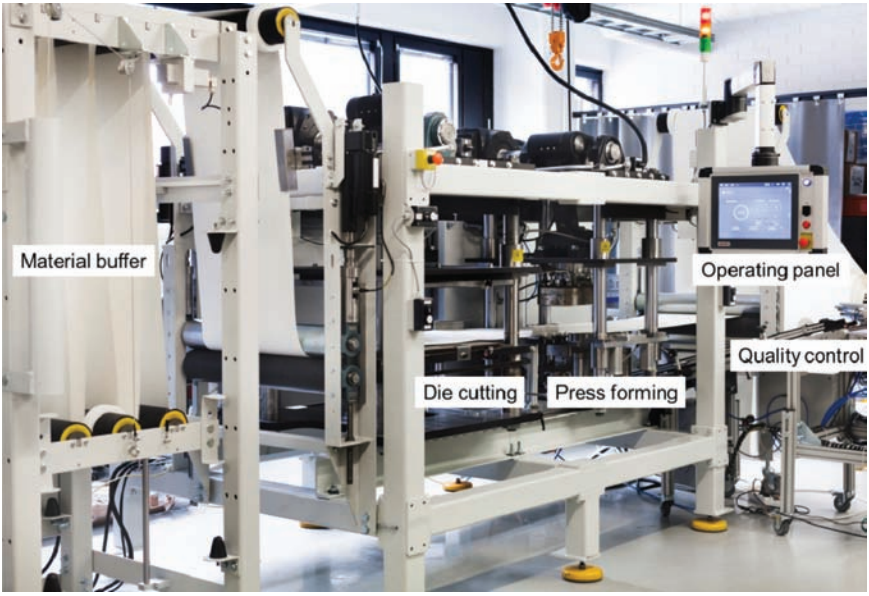

Figure 61. LUT Packaging Line, [68]

results in larger trays since this reduces the time in contact between the blank and the heated forming cavity. The dimensions of the press-formed trays are also in general larger than the design values, [44]. Thus, in order to produce trays of the correct shape and size it is necessary to use tools with smaller design values. This requires an iterative process, depending on process parameters and material properties, which would benefit immensely from a computational design tool capturing the deformation mechanism in a physically sound way. The shape stability of

press-formed paperboard trays is studied by comparing the dimensions of the trays unloaded and at a compressive loading caused by a weight of 4 kg, [44]. The results in Figure 64 show that for a sufficiently long dwell-time, the dimensional changes is relatively unaffected by the dwell-time. Also, the dimensional change of the long side of the tray is smaller than of the short side that follows from the fact the long side of the tray is oriented in the MD of the material.

The blank holder force is similarly to deep-drawing one of the most important parameters for successful press-forming of paperboard [9], [36], [37]. Too low values of the blank holder force cause visually unacceptable wrinkling, and too high values can similarly to deep-drawing lead to rupture in tray corners reducing the applicability of this parameter to adjust tray dimensions [44]. The blank holder force will also have an effect on the flatness of the flange, which in turn will affect sealing and gas tightness of modified atmospheric packaging (MAP) as further discussed below. The blank holder force has a limited effect on the outer dimension of press-formed tray. While the use of a high value of the pressing force reduces the tray size, the tray quality is in general not sufficient for high values of the pressing force [44]. Thus, as long as blank holder and pressing forces, respectively, are within the operational window of a certain press-forming operation, they are not critical for the outer dimensions of the trays. One plausible explanation for the limited influences of the press force and blank holder force are that the press-forming process is displacement controlled. Thus, as long as the paperboard blank is filling the forming cavity properly, additional press and blank holder forces will not significantly change the outer dimensions of the tray.

Control of the blank holder and the pressing forces are of utmost importance for the quality of press-formed products. In order to improve the control of the forming operation, the original punch, equipped with a centrally positioned load cell, is replaced with a punch having one load sensor in each corner of the punch according to Figure 62 [35]. One application of this device is for detection of rupture in the formed product. In general rupture is associated with a drop in the pressing force-forming depth curves registered by the individual force sensors as illustrated in Figure 63.

Similarly to deep-drawing, the ratio between paperboard thickness and mould clearance play a significant role in the outcome of the press-forming process. This is investigated by [37] using four commercial polyethylene terephthalate (PET) extrusion-coated paperboards of grammages 190, 230, 310 and 350 g/m^2, respectively. The grammage of the PET-layer was 40 g/m^2. The paperboard blank was pre-creased with a creasing pattern representing a typical lay-out for tray pressing processes, and the tray wall quality was observed at different wall positions (Figure 65) using the subjective grading scale introduced in Table 2 and Figure 30. Each tray wall position (A–J) represent different mould clearance and in-plane compression, and the press-forming was carried out using a forming

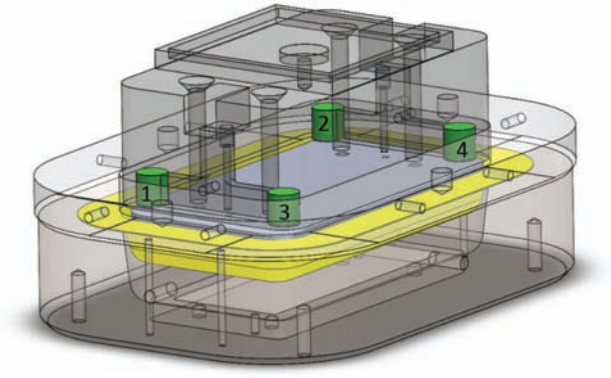

Figure 62. Location of the four force sensors at the corners of the punch. Picture reproduced with kind permission of Dr. P. Tanninen, Lappeenranta University of Technology.

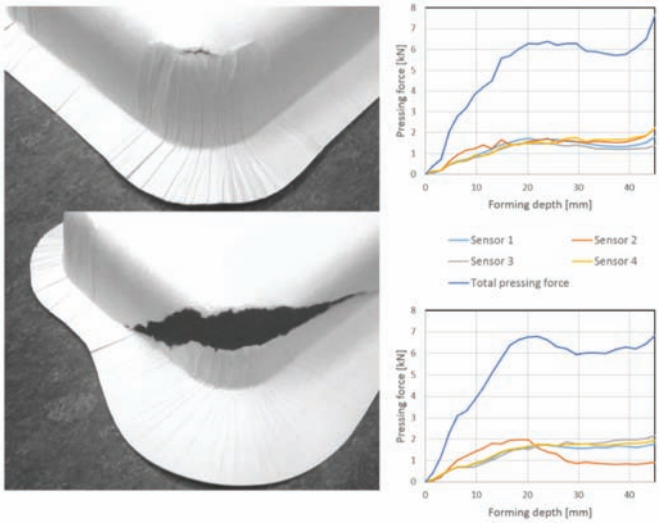

Figure 63. Graphs from the individual force sensors. *Above*: A small fracture detected by sensor 2 using a 1.7 kN blank holder force. *Below*: A large rupture detected by sensor 2 with a 2.5 kN blank holder force. Picture reproduced with kind permission of Dr. P. Tanninen, Lappeenranta University of Technology.

cavity temperature of 170 °C, pressing dwell time of 1 s, blank holder force of 1.16 kN, pressing force of 135 kN and pressing speed of 130 mm/s.

It is found by [37] that for the particular paperboard used, a blank thickness between 95 and 135% of the mould clearance performs best. However, they also

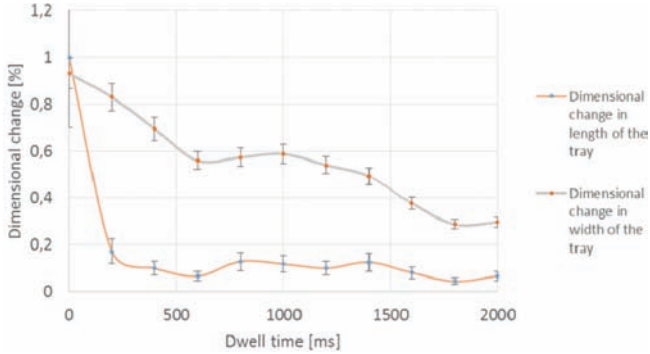

Figure 64. Dimensional changes of press-formed paperboard tray loaded with a weight of 4 kg as functions of dwell-time, from [44].

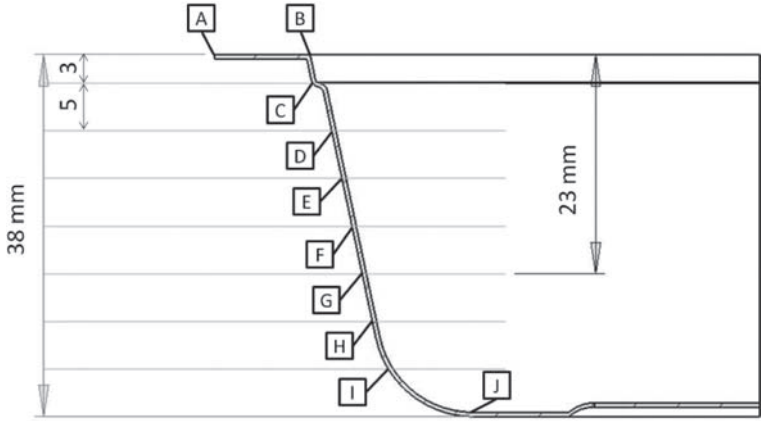

Figure 65. Observation points for evaluation of the quality of the press-formed tray corners, [37].

state that this result is not immediately transferable to other material without testing, which clearly illustrates the need for predictive tools that can handle different types of materials and tools geometries and take temperature and moisture content into account. It is also found that the width of the pre-formed creases decreases with increasing material thickness. Not unexpectedly, these results indicate that the ratio of paperboard thickness and mould clearance is a key parameter for the outcome of the forming process, and that there is a strong need for a more detailed analysis of the deformation mechanisms in press-forming.

A key runnability property in MAP is the ability to form structures that are gas tight after heat-sealing with a transparent polymer lid. The influence of the blank holder force on this property is investigated in detail by [36]. They follow the oxygen content of the press-formed paperboard trays (Figure 66) and use a penetrant colouring solution (Figure 67) to detect possible leaks. The press-formed trays are sealed using an industrial sealing machine. They find, not surprisingly, that the blank holder force directly affects the quality and smoothness of the surface of the tray rim, and therefore directly the gas tightness. They also find that the particular geometry of the press-formed structure plays a role, and that more advanced geometrical shapes require more careful parameter optimisation.

Heat-sealing also requires the formed structure to be dimensionally correct. Trays with varying dimensions and different weights to simulate the products are analysed by [44]. The trays are flushed with a protective gas used for food applications and the oxygen content is measured one minute after sealing. Figure 68 shows that both tray size and product mass has an influence on the gas tightness as represented by the oxygen content 1 s after sealing. The reason for this is that an incorrect dimension of the press-formed tray does not fit the sealing tools properly when the vacuum chamber is closed. (Figure 69) This will be compensated by a large mass of the product, but when the dimension of the tray is too large this will not be sufficient [44].

Control of the mould temperature is a crucial part of the press-forming process and a prerequisite for successful manufacturing of trays and other structures. Heating of the forming cavity is in general acquired by adding heating elements of different shapes and sizes into the mould. In order to analyse the influence of the temperature distribution on the quality of formed trays, [69] use thermo-

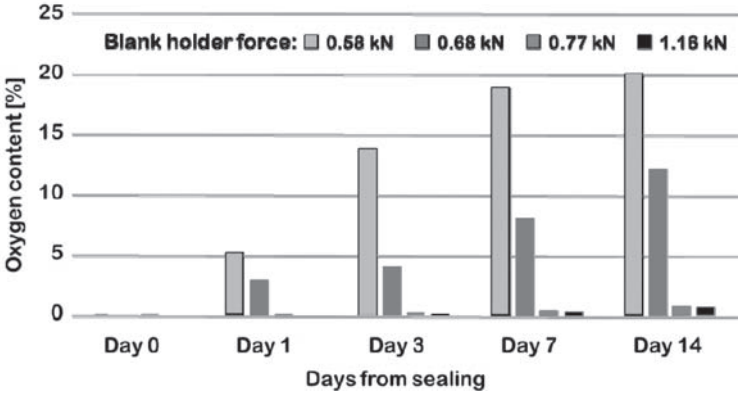

Figure 66. Oxygen measurement averages for heat-sealed press-formed paperboard trays at four different blank holder forces, redrawn from the data of [36].

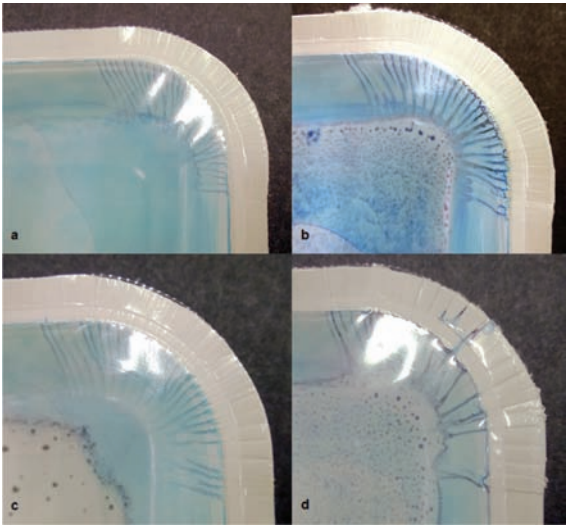

Figure 67. Leak detection by colour penetrant in corners of heat-sealed press-formed paperboard trays at four different blank holder forces: (a) 1.16 kN, (b) 0.77 kN, (c) 0.68 kN, and (d) 0.58 kN, [36].

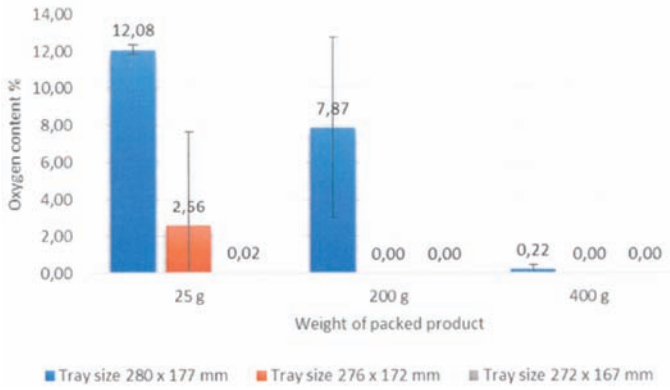

Figure 68. Oxygen content of heat sealed and gas flushed packages with different size and product mass, [44].

graphic imaging. They find that the temperature distribution in general is uneven, that measurements of the temperature are inaccurate and that hot spots such as heads of screws influence the surface of the formed structure. Therefore, they suggest a new structurally less complex mould tool design, based on adding an oil

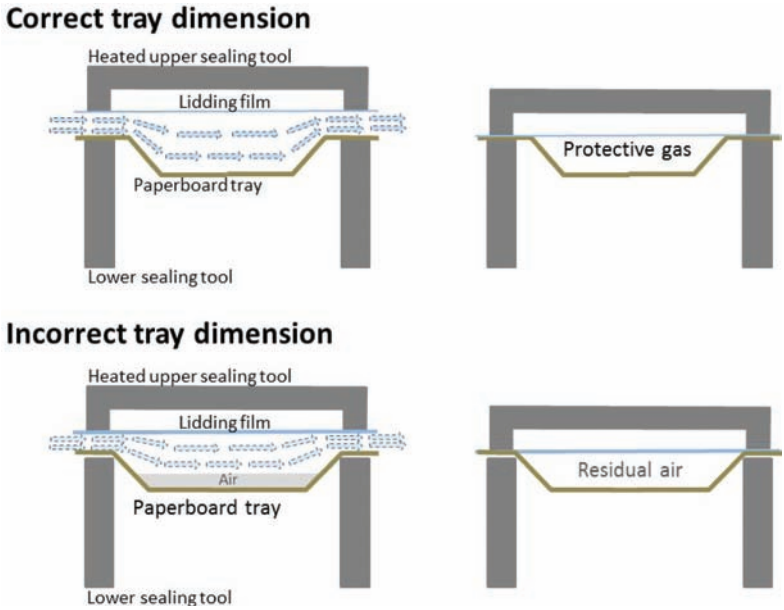

Figure 69. Schematic illustration of flushing with vacuum and sealing of Modified Atmosphere Packaging (MAP) paperboard trays of correct and incorrect (too large) dimensions, redrawn from [44]. A product inside the tray will improve the position of the tray in the heat-sealing equipment, but not necessarily completely compensate for an incorrect tray dimension.

chamber to the cavity mould. In this new mould, the heating elements can be controlled individually according to data from temperature sensors, and the oil distributes the heat more evenly, as illustrated in Figure 70. In the new mould design the decrease in temperature after production runs is reduced due to the large heat capacity of the oil used; resulting in improved quality and less variance in dimensions of the formed structures. However, too long dwell times at too high mould temperatures cause damages to the polymer layer, and [44] find that the entire dwell time range is only available at a forming cavity temperature below 160 °C.

While there have been major improvements in the performance and understanding of the paperboard press-forming process as illustrated here, there are still important problems to solve, particularly related to quantitative understanding of the deformation mechanism such as folding of creases, and also to tailor the mechanical properties of paperboard materials to the particular requirements of paperboard press-forming.

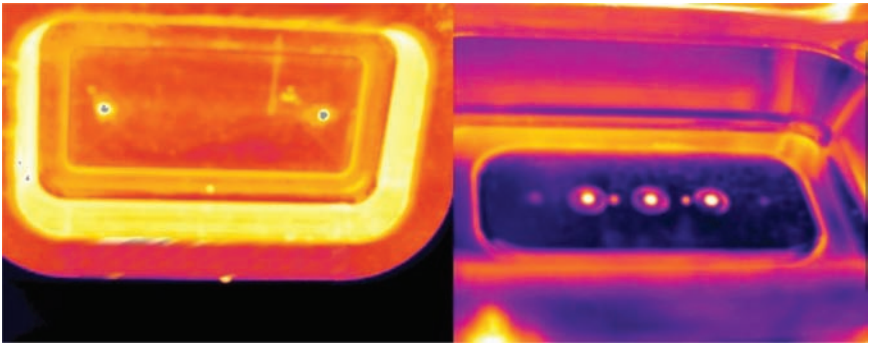

Figure 70. Temperature distributions in mould with individual control of heating elements and an oil chamber (*left*) and traditional mould with bar-shaped heating elements (*right*), Picture reproduced with kind permission of Dr. P. Tanninen, Lappeenranta University of Technology.

4.6 Hydroforming

Process parameters of relevance for hydro-forming or stretch-forming of paperboard are related to the shape of the forming cavity, material properties and process parameters. Typical parameters that need to be considered are listed in Table 6.

The influence of different parameters on the hydroforming of paperboard has recently been studied independently by research groups at KTH Royal Institute of Technology, Sweden and TU Darmstadt, Germany. A laboratory device for hydro-forming developed by [70] (Figure 71) is the foundation for several investigations on hydro-forming of paper materials using forming cavities of different shape and complexity [39], [43], [51], [71]. The equipment developed by the group at TU Darmstadt is schematically illustrated in Figure 72.

The influence of basic process parameters and material properties is investigated by [39]. Phenomena such as rupture, wrinkling, shape stability and shape accuracy are studied by varying type of fibre raw material, sheet grammage, paperboard moisture content, temperature of forming cavity, forming pressure and forming rate. The materials include different commercial and laboratory papers and boards with grammages ranging from 80 to 350 g/m^2.

The outcome in terms of rupture for different moisture ratio and grammage are presented in Figure 73. For the 80, 180 and 300 g/m^2 materials, the results for different moisturising techniques are distinguished in the graph by plotting test pieces moisturised on the bottom side of the blank just below the particular moisture content on the horizontal axis, while specimens moisturised on their upper

Table 6. Examples of geometrical, material and process parameters in hydro-forming of paperboard

Geometrical design	*Material properties*	*Process parameters*
Forming depth	Fibre raw material	Blank holder force
Nominal stretch	Network structure	Forming pressure
Local strains	Mechanical properties	Temperature of forming cavity
	Surface properties	
	Sorptive properties	
	Temperature properties	

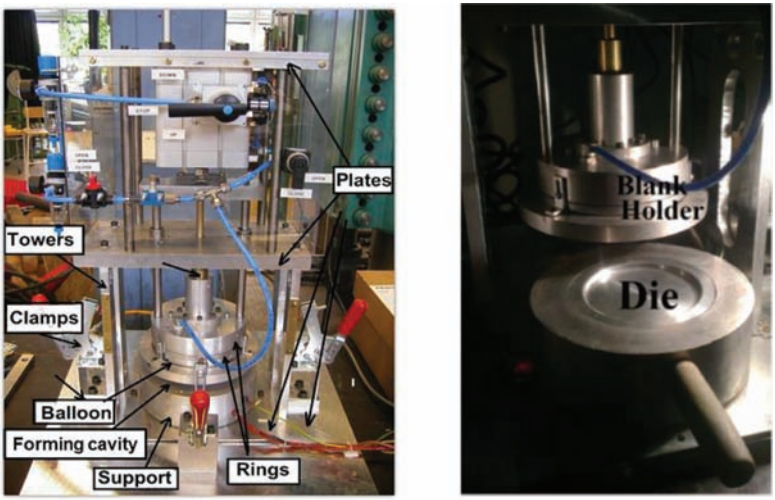

Figure 71. Laboratory device for hydro-forming of paperboard at KTH Royal Institute of Technology, Stockholm (*left*) and close-up of blank holder and forming cavity/die (*right*), [70].

side are plotted just above. For the 80 g/m^2 paper, all test pieces moisturised on both sides fracture and the rare few that did not fracture are evenly distributed between the two types of one-sided moisture application, and this only for moisture ratios in the interval 80–90%. For paperboards of higher grammage the outcome in terms of successfully formed structures is better and the advantage of one-sided moisturising is even clearer. Thus, the way the moisture is applied appears to be more important than the exact moisture ratio. One interpretation would be that the specimens that fail do so because of friction intended to draw

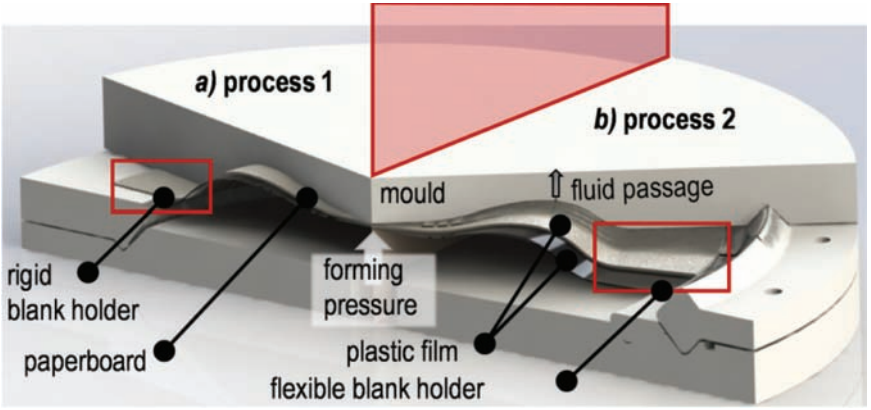

Figure 72. Laboratory device for hydro-forming of paperboard at TU Darmstadt, [72].

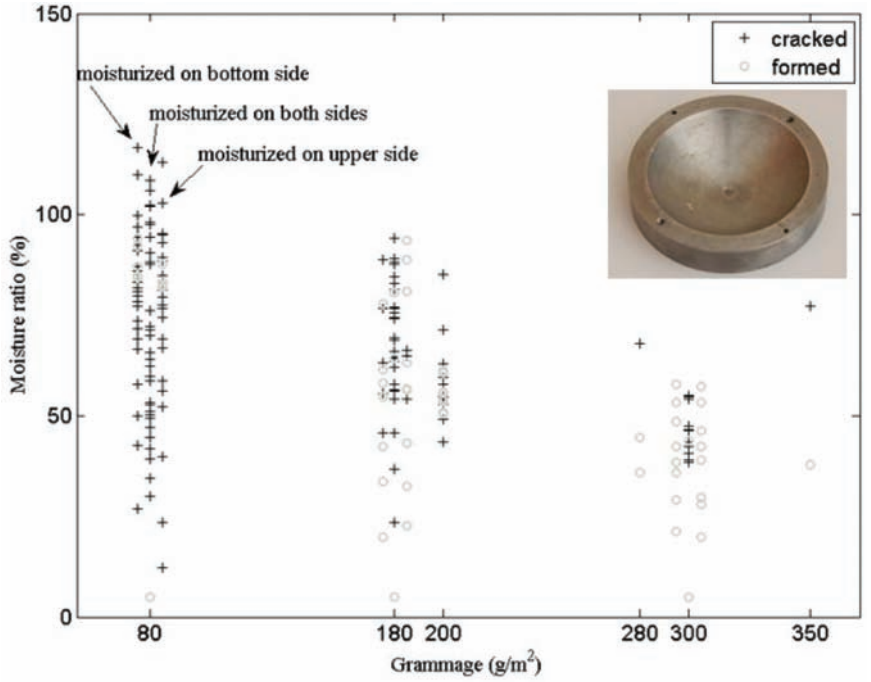

Figure 73. Outcome of hydro-forming trials with papers of different grammage at varying moisture ratio. The forming cavity has a diameter of 100 mm and a depth of 15 mm (nominal stretch 1.06 if the edge of the blank is fully restrained). The temperatures of the forming cavity are between 130 °C and 170 °C, [39].

the material into the double-curved region. It would seem that wet strength is necessary to withstand the friction, and that is why a dry layer in the specimens is beneficial. The possible influence of moisture ratio by estimating how much water that is evaporated from the sheet before forming is also investigated by [39] and their results indicate that for the 80 g/m^2 paper, the real moisture ratio was around 35%.

Obviously, the influence of the value of the forming pressure is related to the grammage of the blank material. Low values work fine for low grammage materials, while high grammage materials will not fill the forming cavity properly. High values of forming pressure form high grammage materials well, but lead to fracture for low grammage materials. It should be noticed that the forming pressures used in Figure 73 are optimised for the respective grammage. No influence on forming of wrinkles or any other results was found for the forming rate, as characterised by the air flow rate used to fill the rubber balloon.

Two major types of wrinkles are observed in hydro-forming of paperboard (Figure 74). Small wrinkles around the edges of the forming cavity are probably caused by buckling during forming (Figure 74(a)). The small wrinkles have a sort of wavy appearance and appear when forming with additional moisture on the upper surface of the blank. There is a possibility that this is related to the sample decreasing its circumference during forming. If the opposite side of the specimen was moisturized this type of wrinkles did not appear which may indicate that the forming of the wrinkles is initiated at the side of the paperboard with lower or even compressive strains during the deflection. The larger wrinkles were probably the result of material being forced into the forming cavity during forming as seen in Figure 74(b). This is probably caused by the insufficient clamping force, which results in too low friction to prevent paperboard slippage. Thus, the smaller type of wrinkles appears when forming with added moisture while the larger wrinkles appear when forming using dry paperboards.

Spring-back was typically not a major issue in the hydro-forming experiments as long as heat was applied during the final drying indicating that the elastic region

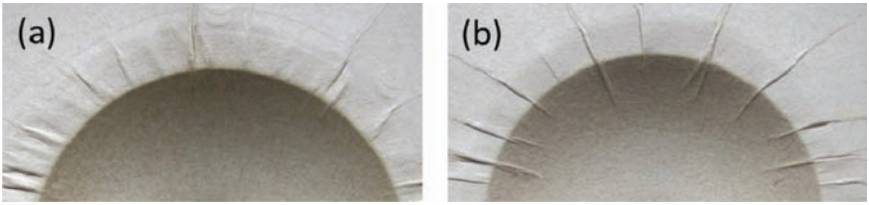

Figure 74. Two types of appearances of wrinkles, (a) small wrinkles at the edge and (b) shows, but fewer, wrinkles that stretches inwards towards the formed part.

Table 7. Pulp types and average thickness of 300 g/m^2 laboratory boards, data from [39].

Type	*Average thickness,* μm
PL (unbeaten hardwood)	451.4
PB (unbeaten softwood)	582.0
LEM (commercially beaten hardwood)	324.7
BEM (commercially beaten softwood)	443.0
BS (bleached chemical pulp)	474.6
OS (unbleached chemical pulp)	475.6
CTMP (chemo-thermo-mechanical pulp)	736.4
3S (three-ply board made of OS, CTMP, BS)	517.3

of deformation at such conditions was small. The influence of different types of pulp is also investigated by [39]. Laboratory sheets of 300 g/m^2 were produced from hardwood and softwood, according to Table 7, in order to obtain paperboards with different physical and mechanical properties. Hydro-forming was performed at three different forming pressures (1, 2 and 3 bars) for a forming cavity temperature of 130 °C and an additional moisture of about 25%. The evaluation of formability and shape stability considered only general characteristics of the paperboards, such as thickness, elastic modulus; strain-at-break, tensile strength and yield stress that were measured prior to forming and on test pieces cut from successfully formed structures. The results for unformed and formed paperboards are given in Table 8. Typically, sheets from short-fibre hardwood performed worse than other sheets. The weakness of the formed samples in comparison with unformed samples is clearly seen, but from a shape stability point of view also the geometric stiffness due to the curved shape needs to be considered before declining the properties of the formed structures.

In a series of papers, groups at TU Darmstadt investigated the influence of paper and process parameters on hydro-forming of paperboard. In [73], a new test device called the paperboard bulge test (PBT) was proposed for characterisation of quasistatic biaxial loading of paperboard relevant for 3D forming of paperboard structures. This equipment is by itself a type of hydro-forming device and they find that the PBT always predict a higher strain-at-break compared to uniaxial tensile tests, and also that at low paperboard moisture content there are variations in flow curves derived from the PBT and tensile tests. This raises some concern regarding the clamping system used in the PBT, but contributes also to the frequent observation that failure strains in 3D forming processes are higher than measured in standard tensile tests. The PBT exhibits similarities with the

Table 8. Comparison of the mechanical properties of unformed and formed paperboards according to Table 7, data from [39]

Board type	*E-modulus,* GPa	*Strain at break,* %	*Tensile strength,* MPa	*Yield stress,* MPa
PL Unformed	4.12	2.60	31.6	7.9
PL Formed	2.24	1.61	24.1	13.6
PB Unformed	2.20	3.46	16.7	3.9
PB Formed	0.95	2.72	13.6	3.0
LEM Unformed	6.57	2.26	50.5	12.4
LEM Formed	3.98	1.82	43.8	18.6
BEM Unformed	3.92	4.15	37.0	7.5
BEM Formed	2.33	2.90	33.8	13.7
BS Unformed	2.39	4.20	18.6	3.8
BS Formed	1.17	1.95	13.5	6.5
OS Unformed	2.89	3.98	25.6	5.2
OS Formed	1.65	2.23	21.1	5.9
CTMP Unformed	1.55	1.50	13.1	3.3
CTMP Formed	1.19	1.11	10.2	6.1
3S Unformed	3.84	2.37	30.8	8.3
3S Formed	2.89	1.77	31.3	16.2

well-known burst strength test, and an extension of the burst strength test has also recently been presented in [74].

In [15] the material behaviour of two different types of paperboard was characterized in tensile tests, PBT and friction tests, and a particularly adapted hydroforming process illustrated in Figure 72 was used to produce 3D paperboard structures. They compare finite element simulations with hydroforming experiments in terms of blank holder force, mould filling pressure, mould filling (using an online measurement device to determine the filling behaviour), and coefficient of friction. Based on their results, they conclude that simulations can be used for the definition of the blank holder force, as well as the material behaviour in the forming process, and that it is possible to produce paperboard structures without wrinkles or cracks in the proposed hydroforming process, but also that the interaction between paperboard and forming cavity for higher normal stresses is not sufficiently well characterised by standard friction tests.

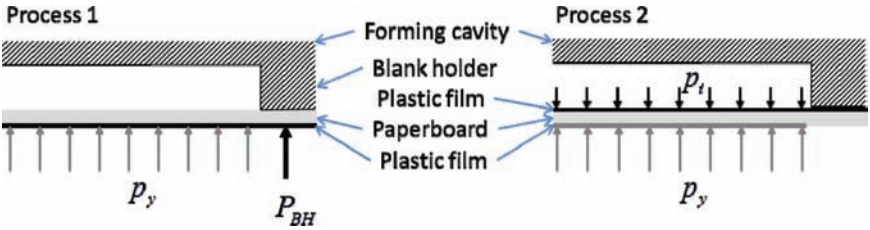

Figure 75. Hydro-forming processes used at TU Darmstadt, adapted from [72].

In contrast to paperboard deep-drawing and press-forming, the technological development of the forming process has, as of today, undergone fewer and less detailed development. Perhaps this is motivated by higher demands on paperboard stretchabilty and therefore being further away from applications. The recent development of paperboard materials with enhanced deformation properties will most likely change this situation.

The benefits of the through-thickness compression during, for example, paperboard deep-drawing are obvious as depicted above. Thus, it is expected that similar advantages would follow also for other forming methods. This has been considered by [72] in their comparison with sheet metal forming. The hydro-forming device developed at TU Darmstadt (Figure 72) is prepared for two different processes as illustrated in Figure 75. In Process 1, the blank is formed with pressurised air and the paperboard is separated from the air with a plastic film. The blank holder force P_{BH} is controlled and the blank holder can be heated. In Process 2, a liquid is used for the forming process, and a counter pressure p_2 can be applied in order to compact the paperboard during the process. The counter pressure supports the paperboard during the forming and also suppresses wrinkling by enabling the material to flow from the edge of the blank inwards.

5 MATERIAL PROPERTIES

Formability is defined by [28] as a mechanical property that determines the performance of the paperboard material in the forming process. This property is in general a very complex function of more fundamental paperboard properties such as stiffness, damage and strength as well as paper-to-metal friction. Formability requirements are different for the different manufacturing processes (Figure 76) as discussed above. Thus, a thorough understanding of the deformation and damage mechanisms experienced by the paperboard materials in 3D forming is essential for a correct choice of material and for materials design.

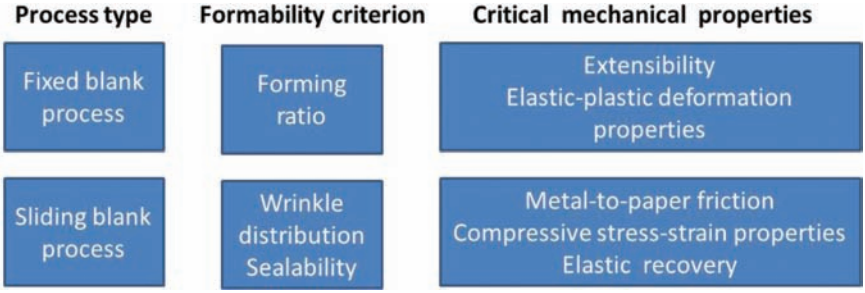

Figure 76. Illustration of relations between forming process, criteria of good formability and required paper material properties, redrawn from [47].

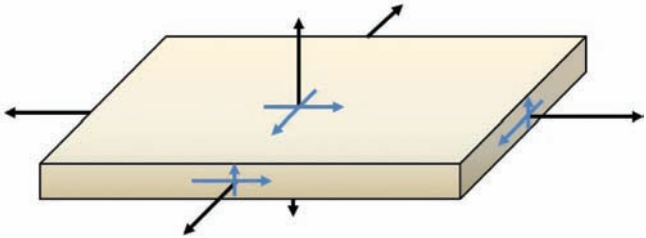

Figure 77. Schematics of general three-dimensional stress-state in a sheet material. Black arrows indicate normal stresses and blue arrows indicate shear stresses.

Paper and paperboard are heterogeneous materials with a considerably more stochastic structure compared to other materials used in three-dimensional forming operations, [1]. In forming of three-dimensional structures using deep-drawing, press-forming, hydroforming or other applicable methods, material elements will be subjected to a multiaxial stress-state comprising both in-plane and out-of-plane normal and shear strains as illustrated in Figure 77.

Although, there are numerous parameters, related to both the fibre raw materials and manufacturing methods, which impacts the mechanical properties of paper and board it is possible to identify primarily three primary factors that have an effect on the strainability of paper materials: fibres, fibre-fibre interactions and fibre network structure [75], [76]. Beside these, there are also secondary factors, such as fines, that have a profound effect on the mechanical properties of paper and board. However, they will not be considered separately in the present analysis, but considered as contributing to the general fibre-fibre interaction.

Today, with some important exceptions such as FibreForm® [19], most commercial paperboard materials have relatively poor extensibility. Typical values of the ultimate strains are 2–4% in the machine direction (MD) and 3–6% in the cross machine direction (CD). There is always a region in which inhomogeneity of the material will have a strong influence on the forming result [31]. This is also supported by results showing that materials with more uniform deformation fields in general show improved material properties of importance for 3D forming, such as the strain to failure [77], [78].

The limited ability of paperboard materials to withstand plastic deformation under multiaxial stress-states is an important origin of defects in three-dimensional paperboard forming. However, the success for paperboard in forming of advanced geometrical structures is also limited by lack of knowledge on the mechanical response of the material to relevant multiaxial stress-states. In forming operations, the mass density may change resulting in a change in stiffness and strength properties. Macroscopic and microscopic internal damage, such as delaminations and bond failure, will also change the macroscopic behaviour of the material, and on top of this there are also changes in the material behaviour due to variations in moisture content and temperature.

5.1 Tensile properties

Forming of advanced paperboard structures is in general associated with subjecting the material to considerable in-plane plastic strains as illustrated by large values of the nominal stretch required to form certain structures as given by Equation (1). Tensile elongation (strain-at-break) in general correlates with the formability of paper, at least for forming operations having a considerable contribution from a fixed blank process as illustrated in Figure 78 for the 2D formability tester and 3D spherical forming device, respectively.

The deformation mechanisms in 3D deep-drawing, being based primarily on the sliding blank principle, is different from the 2D formability tester and the 3D spherical forming device. Here, the paperboard is subjected to a combination of shear, tensile, compressive and frictional stresses, and therefore [28] did not find any correlation between strain-at-break and the distance between wrinkles. This is not surprising since forming of wrinkles from a material property point of view is related to stiffness and not strength.

The compressive properties of paper have a strong influence on the formation of wrinkles in 3D deep-drawing [28]. The stiffness properties are important, but, it should be emphasized that the deformation and damage mechanisms in this sliding blank process are multi-dimensional and complex, and the compressive loading of the material is function of the thickness of the paper, the drawing gap and the stiffness properties of the material.

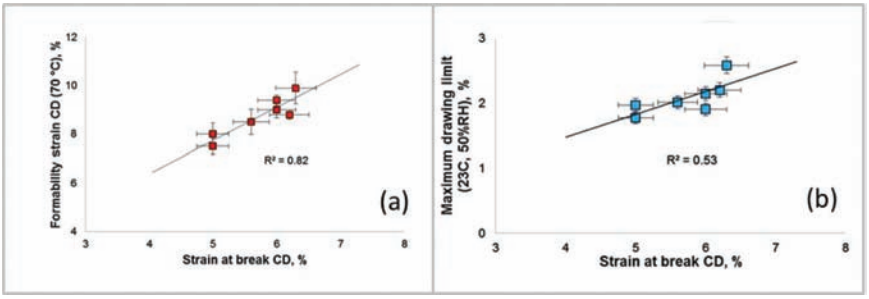

Figure 78. (a) The correlation between formability strains in CD measured at 70 °C and strain-at-break (CD) and (b) the correlation between the maximum drawing limit at 23 °C, 50% RH, and the strain-at-break value (CD) for different commercial samples, [28].

5.2 Biaxial yield and failure criteria

The limited use of paperboard in industrial forming operations is according to [72] attributed to the lack of knowledge concerning material forming limits and design of forming operations. To remedy this situation, they apply established design strategies and material characterisation methods from metals to paperboard, particularly the concept of forming limit diagrams (FLD), [79]. An FLD is established by plotting the major and minor in-plane principal strains at failure for different test setups and geometries. This plot defines the forming limit and typically if strain-states near or above the forming limit are experienced during the forming operation, the structure will fail.

In [73], tensile tests with and without notches, Nakazima tests [80] and paperboard bulge tests with a carrying layer and perforated samples [81] are carried out. Since the failure properties of paper and board are strongly dependent upon the principal material directions, MD and CD, they find that an FLD based on the material directions is more suitable. Such an orientation based FLD is shown in Figure 79. The FLD is strongly dependent on a through-thickness compressive loading as discussed earlier, and this is explored by a hydraulic bulge test with the paperboard sample sandwiched between two metal layers as discussed in the previous chapter.

Inspired by [74], the concept of FLD is also explored by [82] in a study of the biaxial in-plane yield and failure surfaces of paperboard. They use biaxially loaded cruciform specimens containing a reduced thickness region in order to increase the probability of failure in this region. The experimental result in the form of strain-based failure surface with a bilinear curve fit and strain limits for different material tests and 3D forming operations are shown in Figure 80.

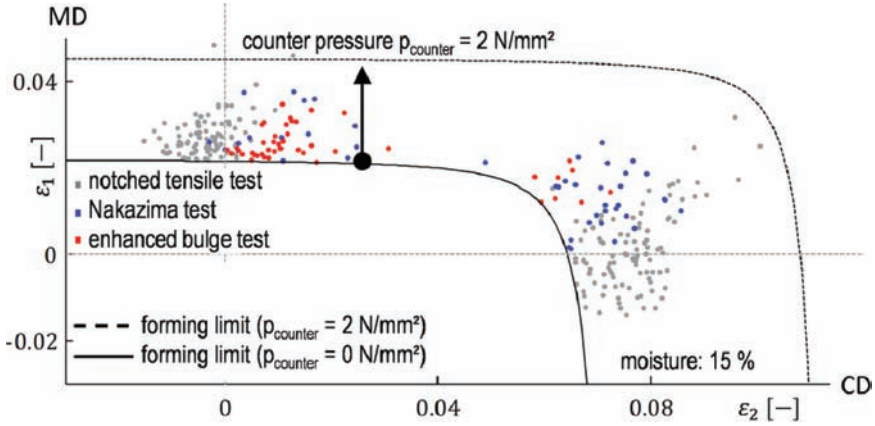

Figure 79. Orientation based forming limit diagram, [73].

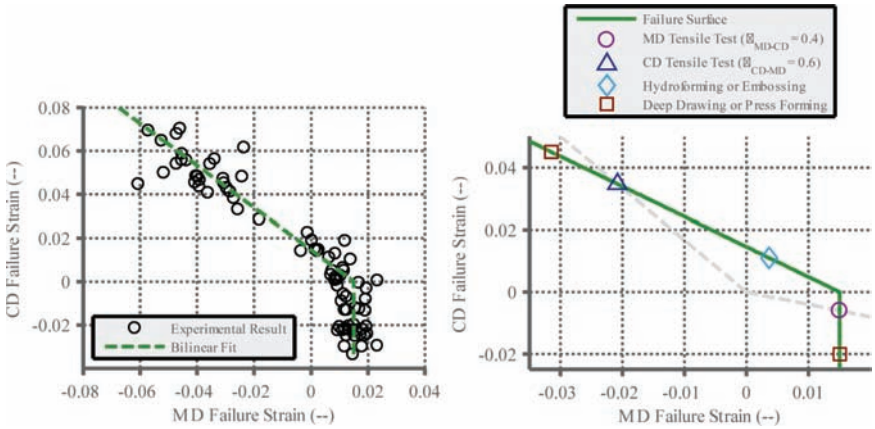

Figure 80. Strain-based failure surface with a bilinear curve fit and strain limits for different material tests and 3D forming operations, [82].

5.3 Methods for improving the 3D forming behaviour of paper and paperboard

The extensibility of paper and paperboard depends apparently on the mechanical properties of the fibres, fibre-to-fibre joints and the fibre network structure. These factors, in turn, can be influenced by a large number of parameters in order to improve the deformation characteristics of the material for certain applications. Fibres can, for example, be affected by different types of mechanical deformation

and damage processes. The properties of the fibre-to-fibre joints can be affected by chemical modifications of the fibres and by application of particular additives, and the network structure can be affected by, for example, creping, compaction and drying strategies as illustrated in Figure 81. The objective of materials design for forming of advanced three-dimensional paperboard structures is to combine these methods to meet the particular requirements of different manufacturing processes. Due to the particular properties of fibre network materials, such as anisotropy, porosity, heterogeneity etc. transfer of knowledge from other materials such as fossil-based polymers and metals is difficult or at least not straight-forward.

It is claimed by [52] that maximising the shrinkage during drying is the most efficient way to enhance the strain at failure of paperboard. Free shrinkage reduces tensile strength and stiffness of paperboard, but these losses can be compensated for by additives. Optimising forming conditions in terms of moisture level and temperature can have a positive effect on the formability. This, however, requires control of these parameters as well as their influence on the mechanical properties of the network material.

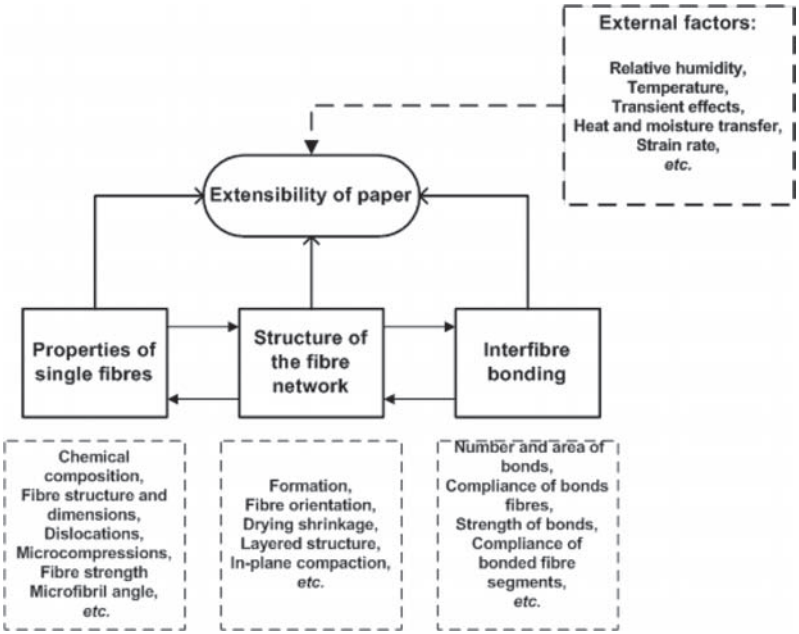

Figure 81. Factors that affect the extensibility of paper, [76].

Methods for boosting the extensibility of paper and board have been on the agenda for papermakers for a long time and are recently reviewed by [76]. Therefore, the objective of this chapter is not a complete review of this literature, but only to include only some recent results of particular relevance for 3D forming of paper.

5.3.1 Mechanical treatment of fibres

Curled fibres improve the elongation properties of paper, but simultaneously reduce the tensile strength. The deformation and damage mechanisms in forming of advanced structures in general requires both strainability and strength, therefore, curled, crimped or micro-compressed fibres are in general less suitable for three-dimensional forming of paperboard, at least for processes such as hydroforming where both strainability and strength are needed. High-consistency refining (HCR) or a combination of HCR and low-consistency refining (LCR) can be used to obtain the optimal curl in the fibres and improve elongation [1]. Mechanical treatment at high consistency is known to introduce fibre deformations that contribute to the elongation properties of paper, and an appropriate combination of high- and low consistency mechanical treatments of the fibres is a well-known strategy for improvement of the extensibility of sack paper grades.

Successive treatment at low consistency will recover some of the strength properties lost during the HC refining. How and to what extent fibre deformations induced by HCR and LCR affect the elongation potential of paper is investigated by [83]. They use the wing defibrator, the E-compactor and the Valley beater to induce different types of fibre deformations in chemical softwood pulp, and they find that the type and intensity of the mechanical treatment has a significant effect on the fibre deformations and the resulting paper properties. A strong relation between strain-at-break and tensile index is found for the different fibre treatments as illustrated in Figure 82 for restrained and free drying, respectively.

It is also found by [83] that high-consistency refining with the wing defibrator in combination with subsequent low-consistency refining with the Valley beater gives paper with high strength properties without impinging on the strength and dewatering properties (Figure 83).

5.3.2 Mechanical treatment of fibre network structure

One way to achieve improved strainability of paper and board materials is by building a tensile strain-potential into the fibre network different types of treatments. Typically, this involves either a mechanical treatment including in-plane

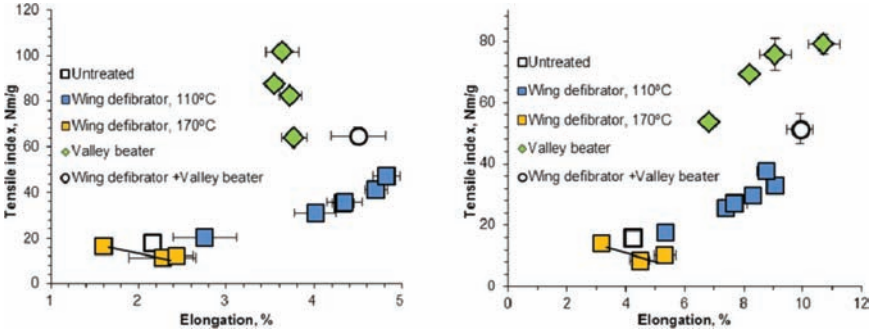

Figure 82. Tensile index as function of strain-at-break for different mechanical treatment of the fibres at restrained drying (*left*) and free drying (*right*), [83].

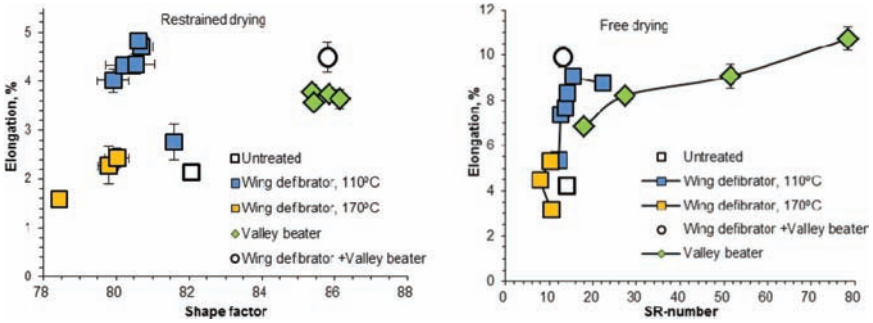

Figure 83. (*Left*) Effect of fibre curl on the strain-at-break for restrainedly dried handsheets, and (*right*) effect of drainage property (as characterised by the Schopper-Riegler number) for freely dried handsheets, [83].

compression, resulting in a network with a residual deformation that promotes additional tensile straining, or a drying strategy that leads to more shrinkage, and a less activated network. There are several patents based on this strategy, cf. [84]–[97]. More shrinkage is typically illustrated by the improved strainability of freely dried networks compared to networks dried under restraint. This way of improving the strainability is, in general, associated with reduced tensile stiffness and strength. For the interested reader, the early development of extensible papers is described by [98].

In creping, semi-dried paper (typically dried on a Yankee cylinder) is folded, partially damaged and buckled when being released from the drying cylinder with a creping blade [76]. Due to its poor surface appearance, low stiffness and reduced strength, its use in packaging is limited, but due to high softness, it is frequently

used in tissue products. Typical appearances of uncreped and creped paper are shown in Figure 84.

In compaction, moist paper is subjected to in-plane compression. In the Clupak® process [84], the paper is stretched by a moving rubber blanket fed into a nip consisting of a steel roll and a non-rotating nip bar. When exiting the nip, the paper web will shrink as illustrated in Figure 85. Strain-at-break values of 87% are reported after processing the paper in several Clupak steps.

In the Expanda® process the paper is fed between a rubber cover steel roll and a heated steel roll. This process is similar to the double-roll compaction process [100]. Preliminary non-published investigations indicate that it is possible to achieve values of strain-at-break of 50% or more with optimal tuning of process parameters e.g. nip load, moisture content and speed difference between the rubber and steel roll. Cross-sectional micrographs of compacted paper are illustrated in Figure 86. Although not traditionally used, it is possible to feed paper sheets through in-plane compaction units in both MD and CD in order to affect

Figure 84. Cross-sectional images of uncreped and creped paper, [96].

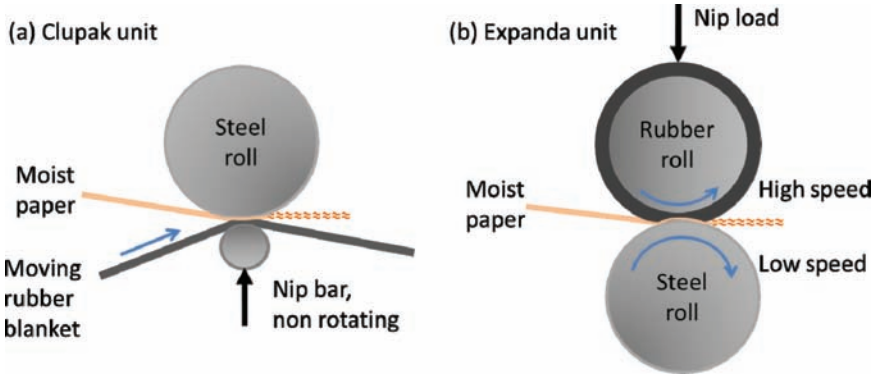

Figure 85. Schematic illustration of (a) Clupak® compaction process, and (b) Expanda® process for in-plane compaction of paper.

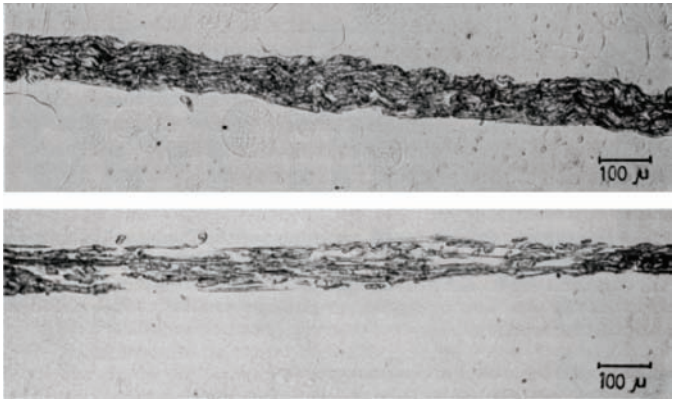

Figure 86. Cross-sectional micrographs of compacted paper before (*top*) and after straining (*bottom*), [100].

the strainability not only in one of the material directions. There is today a large interest for development of extensible paper and board grades using in-plane compaction, and there are also laboratory equipments available [101].

Finally, it is in this context appropriate to once again mention the recent development of commercially available highly strainable paperboard, FibreForm® [19]. Although this material has not yet reached the values of strain-at-break achievable in the laboratory scale, it has considerably improved elongation properties in both MD and CD.

5.3.3 Chemical modifications of fibres

The chemical composition of the pulp affects both the mechanical properties and the moisture uptake of paper-based materials. The strain-at-break and the tensile strength is typically lower for sheets made of mechanical pulp compared to sheets made of chemical pulp [75], and the lignin and hemicellulose content will influence the effect of moisture on elongation properties of the paper sheet [52]. There are a large variety of chemical modifications of the fibres that influences elongation properties of fibre network materials. It is beyond the scope of this paper to discuss all of them, and the presentation will be limited to concepts recently presented within research groups aiming at new materials for 3D forming of paperboard. It should also be noticed that there are relevant patents also in this area, e.g. [102].

In order to enable manufacturing of 3D-shapeable paper products [71] investigates the possibility to improve the thermoplastic properties of paper materials by adding various chemicals known to improve both tensile strength index and

strain-at-break. They find that adding polylactide latex to a bleached softwood kraft pulp significantly improves both strength and elongation properties. The tensile index for freely dried sheets was increased from 30 Nm/g to values in the order of 70–80 Nm/g and the strain-at-break was similarly increased from 0.03 to 0.08. It is hypothesised that the improved strainability is related to the spreading of the polylactide latex on the fibre surfaces, thereby increasing the relative bonded area. Therefore, curing of the sheets was carried out at 150 °C, well above the film forming temperature of the polylactide. By adding 20% of polylactide latex it was possible to fabricate more or less wrinkle-free double-curved structures with a stretch above 1.2 by hydro-forming (Figure 87) using a forming cavity temperature above the film forming temperature.

In [103] the Layer-by-Layer deposition technique is used to build-up of a polymeric film by deposition of alternating cationic and anionic polyelectrolytes onto a charged substrate in order to produce a highly strainable paper. They study two systems: polyethyleneimine (PEI)/nanofibrillated cellulose (NFC) and PAH/hyaluronic acid (HA), and Figure 88 shows the achieved stress-strain curves as function of the number of layers. A considerable improvement compared to the untreated reference material, and, although, the presented strains are, perhaps, not sufficient for 3D forming of paperboard, it is a technique that definitely can contribute to the tailoring of the paperboard properties by being combined also with other strategies.

It is found by [104] that gelatin protein enhances the thermoformability of paper. Both the strength and the strain at failure are affected by adding different amounts of gelatin to the paper, (Figure 89a). According to [104] it is reasonable to attribute the increase in extensibility to the increased shrinkage of the gelatin-modified paper for higher gelatin loadings. Combining gelatin with glutaraldehyde cross-linking produces an additional, but minor, improvement of both the strength and elongation behaviour compared to a gelatin content of 4%, as

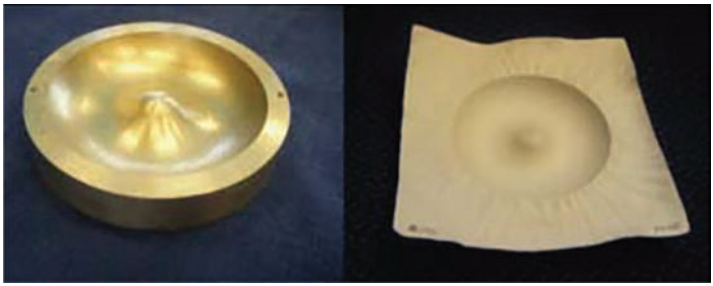

Figure 87. Forming cavity (nominal stretch 1.21) and formed bleached softwood kraft pulp sheet with 20% polylactide latex, [71].

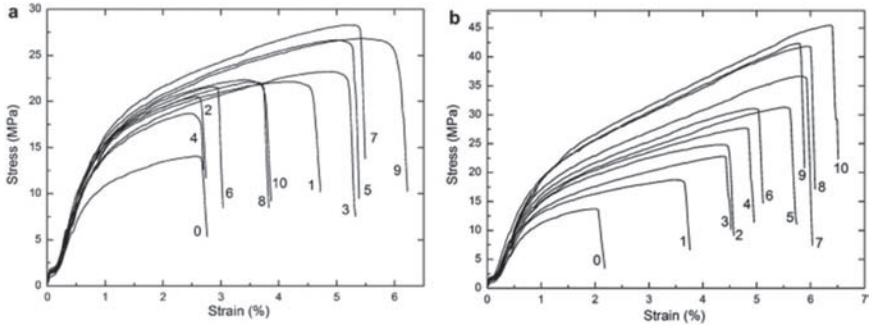

Figure 88. Stress-strain curves for (a) PEI/NFC, and (b) PAH/HA systems, both with 10 mM NaCl. The number assigned to each curve corresponds to the number of layers. The reference material was a bleached kraft pulp from softwood, [103].

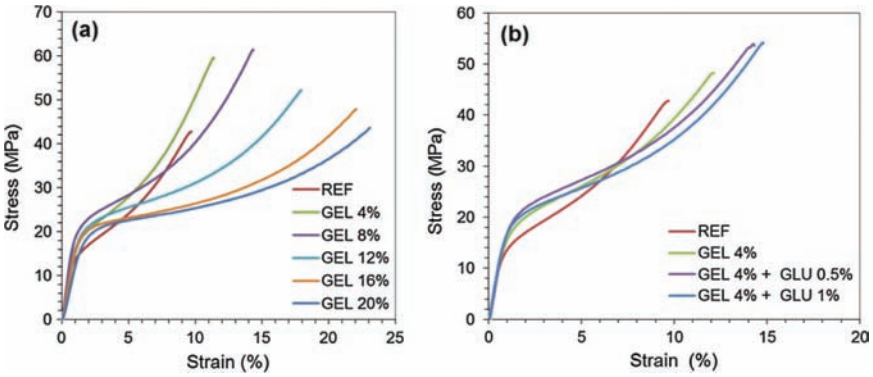

Figure 89. (a) Stress–strain curves of gelatin-modified paper, and (b) glutaraldehyde cross-linked gelatin-modified paper, [104].

illustrated in Figure 89(b). The use of spray application of agar (a substance derived from the polysaccharide agarose found in species of algae) on wet paper sheets is used by [105] to improve the extensibility of paper. They find that this has a positive effect on both the strain-at-break and the tensile strength as illustrated in Figure 90.

These authors [105] also find that other mechanical and functional properties such as wet web strength, air permeability and grease barrier can also be improved by agar addition. Extensibility of unrestrained dried paper was increased from 9% to 13%, and it can be concluded that paper treated with agar exhibited an excellent performance in the preparation of the 3D-shapes. Examples of such structures are shown in Figure 91.

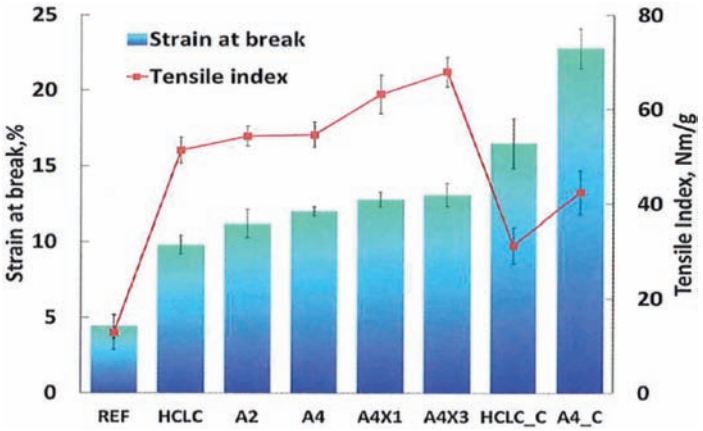

Figure 90. Influence of addition of agar of unrestrained-dried paper. HCLC are sheets from a high and low consistency reference pulp. A2, A4: 2% and 4% agar to fibres. A4X1, A4X3: agar and 1 and 3% of crosslinker. HCLC, A4_C: In-plane compaction treated samples at 45% dry solids content, [3].

Figure 91. Examples of the shapes fabricated from the 200 g/m^2 extensible paper formed in the sliding (*left*) and fixed (*right*) blank processes, [105].

It is shown by [105] that spray addition of agar on wet webs improves the extensibility of paper, and [104] find that spray addition of gelatine on wet webs also improves the extensibility of paper. The question that is investigated by [106] is whether the two mechanisms contributing to the improved extensibility for

each of them can be combined for an additional positive effect. Gelatine easily penetrates into the fibre network [104], while agar forms a film on the surface [105]. Because of this it is found that gelatine must be added first, because otherwise it cannot penetrate the agar film. The results for the strain-at-break and the tensile index are given in Figure 92, and typical stress strain curves are shown in Figure 93. It is shown by [105] that agar increases the dry shrinkage of unrestrained dried paper while gelatine does not significantly influences the drying shrinkage of paper [106]. Thus, the change of tensile stiffness of the combined spray addition of gelatine and agar is a combination of increased drying shrinkage due to agar and improved bonding due to gelatine.

It is reported by [3] that certain treatments on the fibre and fibre structure levels are additive. This will results in both improved extensibility and potentially also increased formability as illustrated in Figure 94. By combining high consistency treatment, low consistency refining, spraying with polymers, compaction of the fibre web and unrestrained drying [3] achieved strains to failure of 20–25% in MD and 15–20% in CD.

A material of interest for the production of bio-based, complex, double-curved surfaces is recently presented by [107]. They show that by partly converting cellulose fibres to dialcohol cellulose it is possible to fabricate high-density materials by conventional papermaking techniques that are strong and ductile (Figure 95),

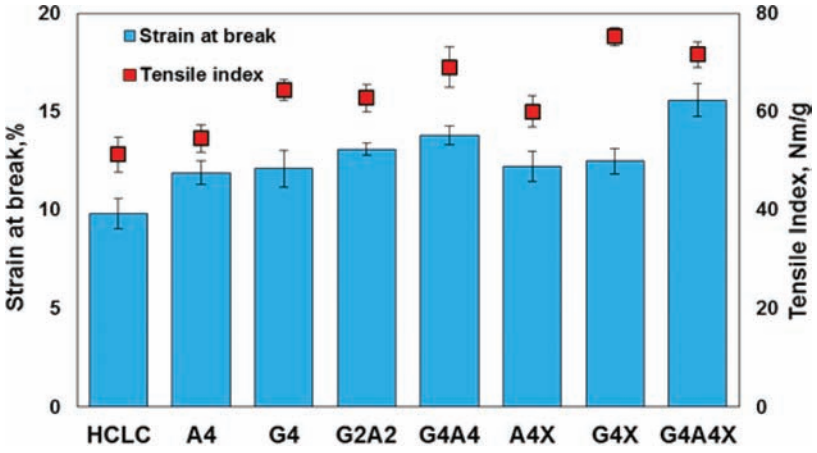

Figure 92. The influence of agar (A) and gelatine (G) addition in the presence and absence of the crosslinker (X) on the tensile strength and strain-at-break of unrestrained dried paper. HCLC stands for high and low consistency refined pulp. The numerals indicate the addition level (% relative to fibre mass), [106].

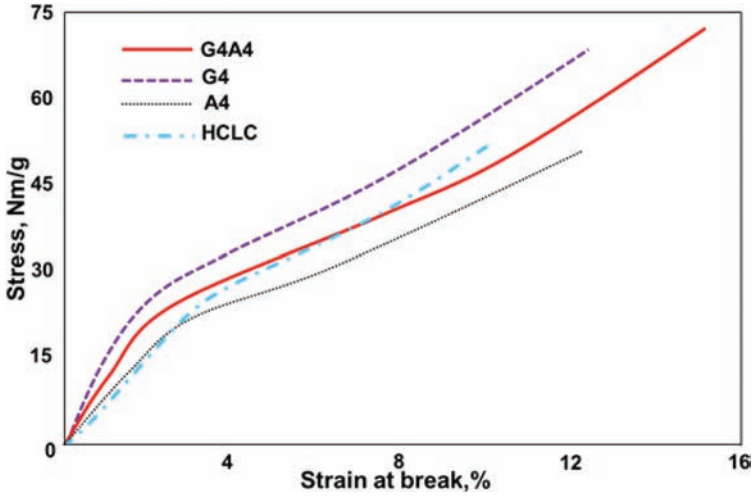

Figure 93. Selected stress-strain curves of untreated unrestrained dried paper (HCLC), paper sprayed with agar (A4), gelatine (G4), gelatine followed by agar (G4A4), [106]

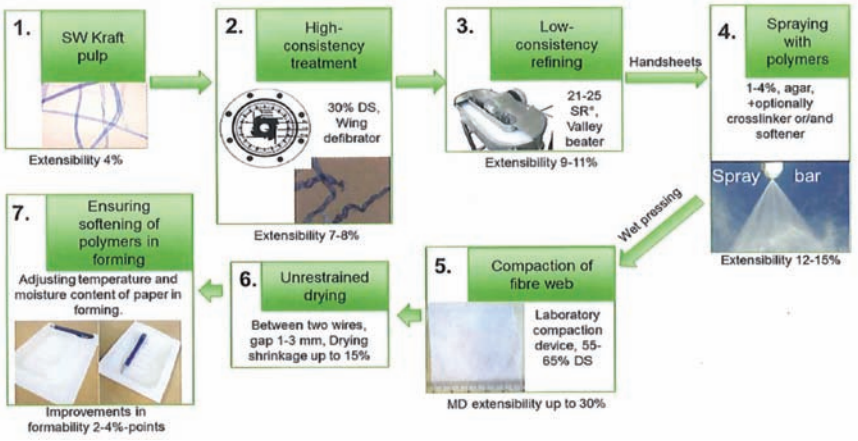

Figure 94. Synergetic approach to improved extensibility, from [3].

but also provide some barrier properties and be transparent. This material has been identified as a potential breakthrough material due to its extensive strain-at-break characteristics and hydro-forming trials using this material is recently reported in [43].

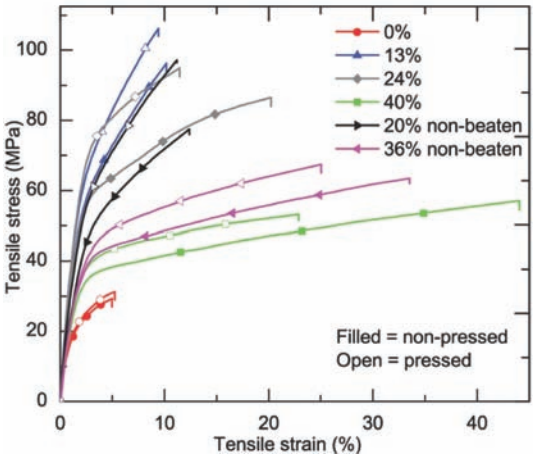

Figure 95. Tensile stress-strain curves for oxidised-reduced paper/film at different degree of oxidisation, [107].

5.4 Tailoring material properties for deep-drawing

A review of the role of material properties in paperboard deep-drawing is recently presented by [1]. An important observation therein, is that materials with a lower density are likely to perform better in deep-drawing [108]. This is mechanically motivated by the lower resistance to transverse shearing and fibre-to-fibre movement in line with the results of [27] showing that an increased pore volume and reduced bonding strength and capacity will lead to improved formability.

Conventional test methods for the mechanical properties of paperboard at standard climate do not in general describe the behaviour under 3D forming process conditions. The influence of different constituents is in general affected by variations in moisture content and temperature as well as by the complex multiaxial states of loading as described above. Thus, it is today not straight-forward to predict the performance of a certain paperboard material in deep-drawing or to adjust the paperboard design to improve the performance in 3D forming operations.

In an attempt to remedy this situation [27] report an excellent analyses of the deformation mechanisms in paperboard deep-drawing. Experiments with different fibres and material network structures on laboratory and pilot scales paperboards were conducted in order to determine critical material properties for the formability of paperboard using the laboratory paperboard deep-drawing equipment at TU Dresden, (Figure 41).

As a reference material, a 350 g/m^2 commercial tray forming paperboard is used. The deep-drawing experiments are carried out with a linearly decreasing value of the

blank holder force, (Figure 49). The maximum values of the blank holder force and the tool temperatures are optimised for each tested material. The quality analysis is carried out using the optical tool developed by [53] and the wall stability is examined by tensile testing of test pieces cut from the walls of the formed structures [2].

To investigate the influence of material thickness and density on the through-thickness compressive behaviour in the drawing gap, laboratory handsheets made of Northern Bleached Softwood Kraft (NBSK) pulp and Bleached Eucalyptus Kraft pulp (BEKP) are used. Sheets from Pressurized Ground Wood (PGW) pulp are also included. The handsheets are prepared to a grammage of 350 g/m^2 with different levels of wet pressing and refining (Table 9).

The results are shown in Figure 96 and indicate that the sheets with no refining and minimal wet pressing show a significant increase in the drawing height at which wrinkles appears in the walls of the formed structures. In general, reduced treatment of the pulp by refining and wet pressing results in sheets with higher pore volume, and it can be speculated that in-plane fibre-to-fibre movement is improved in more porous structures due to fewer fibre-to-fibre joints and less hindrance for the deformation in the network structure [27]. When the fibres are refined and the network structure wet-pressed, the visual quality is considerably reduced as shown in Figure 96. All formed (wrinkled) samples made from laboratory sheets provide higher stiffness than the reference material, when tested according to the procedure described in Figure 26, and, thus, better shape stability, (Figure 97).

Pilot scale paperboard materials were also prepared in a Fourdrinier paper machine. Material composition and additives used in the samples from the pilot paper machine included different amounts of BSK in top and bottom layers and different chemical additives. The bottom layers are prepared using combinations of BSK with different amounts of BEK, Lyocell fibres and PET fibres. Finally,

Table 9. Material and parameter variations for the experiments with laboratory sheets [27]

Number	*Material*	*Wet pressing pressure* (MPa)	*Refining*
1	BEKP	0.1	No refining (NR)
2	BEKP	89	No refining (NR)
3	BEKP	0.1	SR (Schopper Riegler) 35
4	BEKP	89	SR35
5	NBSK	0.1	No refining (NR)
6	NBSK	89	No refining (NR)
7	NBSK	0.1	SR35
8	NBSK	89	SR35
9	PGW	0.1	SR63

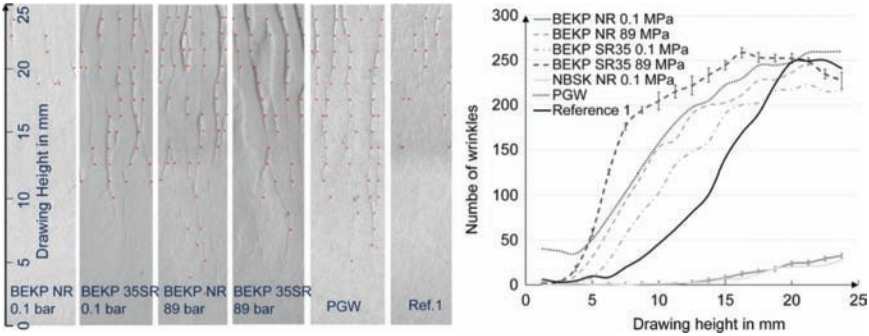

Figure 96. Measured number of wrinkles around the wall of formed samples from laboratory sheets as functions of drawing height for different types of paperboard materials. The notation for the different materials is given in Table 9, [27].

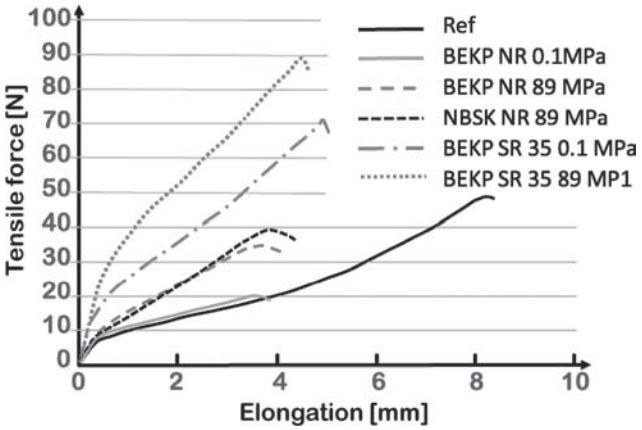

Figure 97. Force-elongation curves of deep-drawn samples made from laboratory sheets (Table 9), redrawn with data from [27].

one material is produced entirely from a combination of 90% BSK and 10% bi-component (BiCo) fibres. The BiCo fibres consist of PET fibres with a full Co-PET binder sheath, (Table 10).

Materials mixed with stiff fibres offer a considerably improved drawing height at which wrinkles occur and also a very flat wrinkle distribution (Figure 98). A material structure consisting of a mixture of cellulose fibres and a low mass percentage of stiff regenerated cellulose of synthetic fibres in combination with alkyl ketene dimer (AKD) or cationic wax as an additive lead to a wrinkle-free wall at a drawing ratio of at least 0.22. Materials combining the advantage of

Table 10. Material composition and conditions of samples from the pilot paper machine, the additives x are listed in Table 11, [27]

Number	*Variation of additive*	*Top layer*	*Top layer*
1.x	x: 1, 2, 3a, 3b, 4	NBSK 100%	NBSK 100%
2.x	x: 2, 3a, 3b, 4	NBSK 100%	NBSK 70%/BEKP 30%
3.x	x: 2, 3a, 3b, 4	NBSK 100%	NBSK 70%/Lyocell 30%
4.x	x: 2, 3a, 3b, 4	NBSK 100%	NBSK 80%/PET 20%
5.x	x: 2	NBSK 90%/BiCo 10%	NBSK 90%/BiCo 10%

Table 11. Additives used in the samples from the pilot paper machine, [27]

Additive x	*Additive*
1	Internal sizing (AKD; 22-C-AKD, melting point: *ca.* 67 °C)
2	Arbocel (6% AKD-content, melting point: 50–60 °C)
3a	Wax dispersion, cationic, melting point: 60 °C
3b	Wax dispersion, cationic, melting point: 60 °C
4	Hot melt adhesive dispersion: EPOTAL®

AKD application and the use of stiff fibres show the best forming results. Heating the adhesive cover of the BiCo fibres during the forming process possibly leads to improved sliding behaviour that supports the deformation of fibre network structure. Formed (wrinkled) materials with stiff fibres and AKD showed considerably improved stiffness compared to the commercial reference material, although there were only minor differences in ultimate strength as illustrated in Figure 99.

Sample material 5.2 exhibits the highest initial slope. Despite remarkable anisotropy, this material shows only slight deviation from the given shape comparable to the isotropic laboratory sheets. The improved accuracy of the final shape indicate that new joints are formed during the compression of the material, at least near the surface, or that some other strengthening mechanism is activated, [27]. Based on their observations, [27] break down the deformation mechanisms into three phases.

1. In the first phase of the deep-drawing process, the network structure is deformed and/or damaged and the material density is reduced due to fibre-to-fibre movement. Possible delaminations also increase the available space in terms of pore volume.
2. In the second phase, wrinkles occur.
3. In the third phase a restructuring of the network structure and a fixation of the wrinkles by forming new fibre-fibre joints in the limited wrinkle areas occurs.

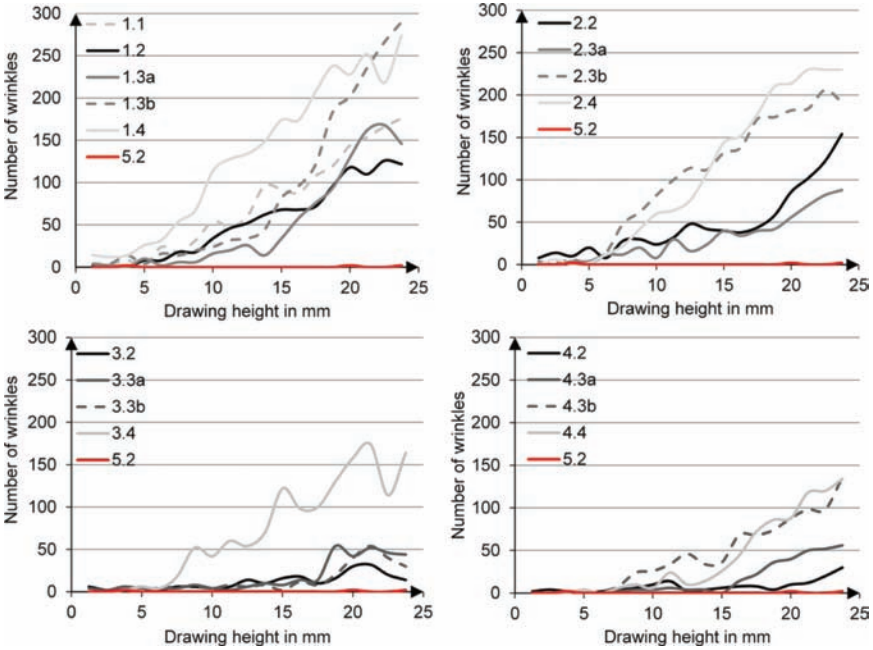

Figure 98. Measured number of wrinkles around the wall of formed samples from pilot paper machine sheets as functions of drawing height for different types of paperboard materials. The notations for the different materials are given in Table 9–Table 11, [27].

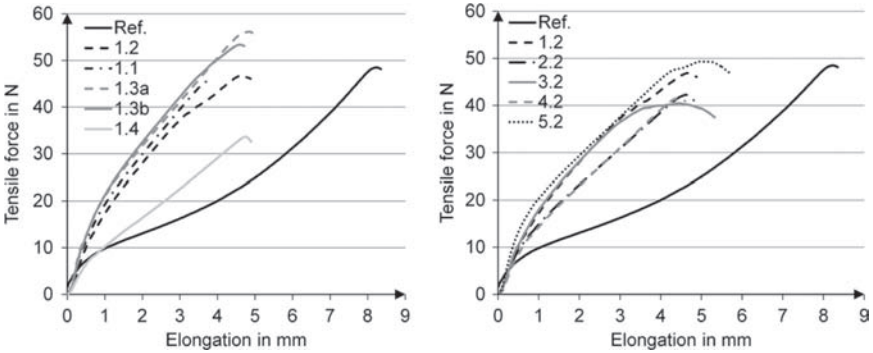

Figure 99. Force-elongation curves of formed samples made from pilot paper machine sheets (Table 9). The notations for the different materials are given in Table 9–Table 11, [27].

This description relies heavily on indirect experimental observations, and there is presently, to the knowledge of the author, no completely verified model that can confirm this description. Such a model would of course also be useful for both efficient process and material designs.

In the first phase, compensation for excess material depends on fibre-to-fibre mobility. Refining and wet pressing decrease the pore volume and increases the number of fibre-to-fibre joints, thereby hampering fibre-to-fibre movement. The use of stiff fibres increases pore volume and results in fewer fibre-to-fibre joints and/or fibre joint strength. This is demonstrated by the systematically lower tensile index for such materials, (Figure 100).

In the second phase, wrinkle formation is a complex instability phenomenon that is related to the bending properties of the network structure, but is also dependent on the particular boundary conditions that the blank is experiencing in the forming operation. Intuitively, too high sheet stiffness would not lead to an advantageous wrinkle distribution with many wrinkles of low amplitude, and this is confirmed by the investigations reported by [27]. They find that the bending stiffness scaled by sheet thickness to the power of three seems to be the most suitable test method that under standard climate conditions gives a rough tendency on the material behaviour during deep-drawing.

The results by [27] indicate that low strength and low bending stiffness has a positive effect on the formability in deep-drawing. This indicate that fibre-to-fibre

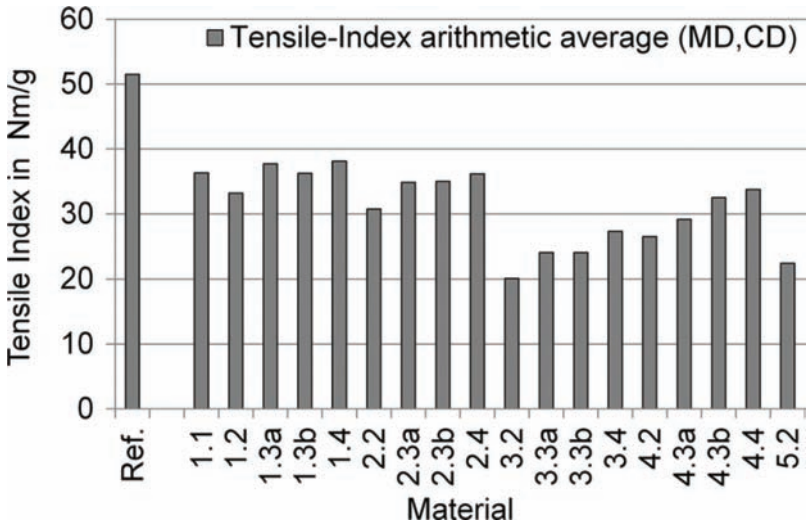

Figure 100. Tensile index of pilot paper machine samples (Table 10 and Table 11) compared to commercial reference material, [27].

mobility is advantageous for paperboard deep-drawing, or at least that increased strength through improved fibre-to-fibre joint strength is not beneficial. Decreased tensile strength and especially a decreased bending stiffness indicate improved formability. This is in complete opposition to the criteria governing the design of paperboard today, where particularly high bending stiffness is what every board maker is striving for.

In the third phase, the strength of the fixation of the wrinkles is increased by the use of refined fibers or additives with low melting temperatures (Figure 98). Overall, the observations by [27] promote the benefits of having paperboard materials where the deformation and damage mechanisms exhibit different behaviours at different stages in the process. Theoretically, this would be possible to achieve with different types of external stimuli, and this is an exciting area of future research.

6 SIMULATION OF THREE-DIMENSIONAL FORMING OF PAPERBOARD

Up until recently, insufficiencies in the constitutive modelling of paper have promoted, to a large extent, a trial-and-error approach for design of products, processes and paperboard materials, [72]. There has, however, during the last 20 years been a strong progress in the development of material models for paper, and today computational design tools will further enhance product development.

The driving force for this development is primarily issues related to packaging performance such as tools for prediction of the stacking strength of boxes, and the creasing and folding performance of paperboard and due to its practical importance there has been particular interest for modelling creasing and folding of paperboard. Continuum mechanics elastic-plastic models, sometimes in combination with interface delamination models, have proven successful in modelling of creasing and folding, cf. [57]–[58], [109]–[110]. The literature on modelling and simulation of advanced forming operations is scarce since fibre network materials are not traditionally used in such applications. However, recent development of paperboard with enhanced deformation properties has initiated interest for using such materials in forming of advanced sheet structures, and numerical simulations have been reported for both deep-drawing, press-forming and hydro-forming of paperboard.

The key concept in all forms of numerical simulations of the mechanical performance of structures is relevant and robust constitutive equations relating stresses and strains, and preferably also including the influence of temperature and moisture content of the material. In addition, the constitutive equations need to be combined with appropriate structural models and local as well as global damage and failure criteria.

6.1 Constitutive equations

Paperboard is a heterogeneous material, where the inhomogeneity and anisotropic material behaviour is due to the fiber distribution and drying condition of the network. In converting and forming operations, such as creasing, folding, deep-drawing and hydroforming, paperboard is subjected to complex mechanical and climate loading histories. Simulation of the paperboard performance in such operations is a demanding task that requires proper choices of structural and material models. Of particular importance for forming of advanced paperboard structures is a model for the interaction between the surfaces of the fibre network material and the forming tools, constitutive models that captures relevant deformation and damage mechanisms with sufficient accuracy, and the influence of moisture content and temperature.

In contrast to many other paper and board end-use and converting operations, forming of advanced three-dimensional paperboard structures, similarly to creasing and folding, requires three-dimensional constitutive equations. The foundation for much of the work on the elastic-plastic deformation of paperboard is Hill's yield criterion [111] that originally was developed for anisotropic metals. However, it is early noticed that this yield criterion does not ideally capture the elastic-plastic behaviour of paperboard due to the particular deformation mechanisms of paper and paperboard, since fibre network sheets are orthotropic by nature, i.e. the in-plane mechanical properties distinctly differ from the out-of-plane ones.

It is, however, established that recent three-dimensional continuum based approaches are able to represent the mechanical response of paperboard in many applications [60], [112], [113]. Furthermore, it is well-established that the mechanical properties of paperboard are strongly dependent on moisture content and temperature, but it is not until recently that both these parameters have been simultaneously considered in continuum mechanics modelling of paperboard. Anisotropic viscoelasticity and viscoplasticity is also considered, and particular care is taken when considering the effect of out-of-plane normal loading, which will influence the porosity of the material and, hence, the in-plane and transverse shear properties due to changes in fibre network density [60], [113].

6.2 Deep-drawing

In deep-drawing of paperboard, compaction is activated by circumferential in-plane compression and deformation constraints enable excessive wrinkling. These wrinkles lead to a thickening of the material that generates a through-thickness compressive loading that in its turn will affect the in-plane deformation. Efficient advancement of these complex manufacturing processes and accompanying tailored design of paperboard materials require relations between tool

geometry, material properties and process parameters. Today, these quantitative relations are missing, being a severe limitation for further progress.

The first attempts to quantitatively model paperboard deep-drawing using continuum mechanics and the Finite Element Method (FEM) are presented by [63] and [64]. They develop an explicit finite element model utilising a custom, yet simple, material model considering the anisotropy and the elasto-plastic behaviour of paperboard. In [64] formation of wrinkles are taking into account by utilising a one-dimensional model for a fully plasticised hinge introducing only one additional parameter in the form of the yield strength of the hinge, σ_y, (Figure 101). The out-of-plane behaviour is assumed to be elastic, while the plastic deformation of the non-wrinkled material is captured by an orthotropic in-plane maximum stress yield surface (Figure 102).

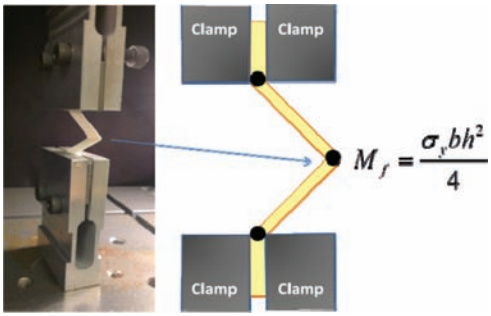

Figure 101. Modelling wrinkles using fully plasticised hinges marked by black circles. The corresponding bending moment is given by M_f, adapted from [64].

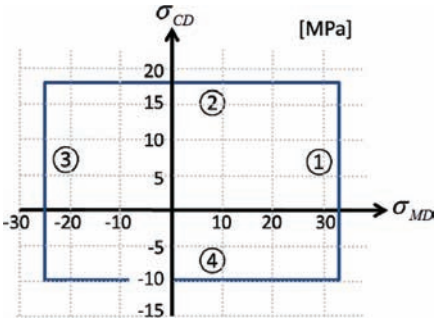

Figure 102. In-plane yield surface in MD and CD normal stress space, adapted from [63].

In-plane shear stress is known to reduce the size of the failure surface [114] and this is considered by formulating the four surfaces of the yield surface as

$$f = \begin{cases} k_1 = \dfrac{\sigma_{MD}}{\sigma_{MD,t}} + \dfrac{\tau^2}{\tau_y^2}\sigma_{MD} > 0 \\ k_2 = \dfrac{\sigma_{CD}}{\sigma_{CD,t}} + \dfrac{\tau^2}{\tau_y^2}\sigma_{CD} > 0 \\ k_3 = \dfrac{\sigma_{MD}}{\sigma_{MD,c}} + \dfrac{\tau^2}{\tau_y^2}\sigma_{MD} < 0 \\ k_4 = \dfrac{\sigma_{CD}}{\sigma_{CD,c}} + \dfrac{\tau^2}{\tau_y^2}\sigma_{CD} < 0 \end{cases} . \quad (4)$$

In Equation (4), k_{1-4} are parameters representing the amount of yielding in each material direction, σ_{MD} and σ_{CD} are, respectively, the normal stress in MD and CD, $\sigma_{MD,t}$ and $\sigma_{CD,t}$ are, respectively, the tensile yield stress in MD and CD, $\sigma_{MD,c}$ and $\sigma_{CD,c}$ are, respectively, the compressive yield stress in MD and CD, τ is the in-plane shear stress, and τ_y is the yield shear stress. Additionally, the non-wrinkled constitutive model assumes linear hardening and linear decomposition of the total strain into elastic and plastic strains. Prior to plastic deformation, the parameters k_{1-4} have the value unity, and thereafter increase independently with plastic deformation. The geometric structure and the finite element mesh used in the analysis are illustrated in Figure 103.

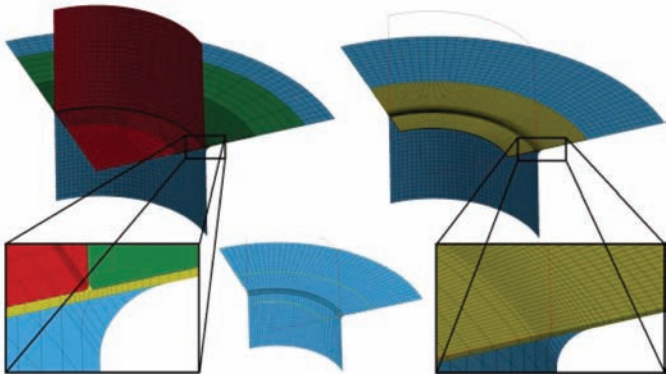

Figure 103. Finite element mesh of punch (red), blank holder (green), die (blue) and blank (yellow), from [63]

Contact between paperboard and tools are modelled by surface-to-surface paper-steel contact. Since heating of the paperboard from the tools plays an important role in paperboard deep-drawing the contacts include thermal interaction between the tools and the paperboard through conduction and radiation. The specific heat capacity and the thermal conductivity of paperboard as well as the friction coefficients were all modelled as temperature dependent. The model also relies on the observation that the effects of temperature and moisture content are uncoupled for elastic modulus, tangent modulus, hardening modulus tensile energy absorption and approximate plastic strain at break [50].

The applicability of the proposed model is illustrated in Figure 104 which shows a comparison between the simulated and experimentally determined wrinkle distributions. The model results exhibit good quantitative agreement with experiments also for other quality parameters.

The model presented by [63] and [64] provides quantitative insight into how tools and materials can be designed to reduce the failure probability, and it has been used to study the influence of e.g. blank thickness and coefficients of friction. Furthermore, model simulations indicate that the only model parameter that simultaneously can improve all three quality measures introduced by [2] is the yield strength of the hinge. It should, however, be noticed that the validity of this conclusion is governed by the limitations of the model. Conceivably, there are phenomena of significance that presently are not included in the model.

6.3 Press-forming

Despite being of large practical importance, there is to the knowledge of the author only one recent publication on modelling and simulation of paperboard

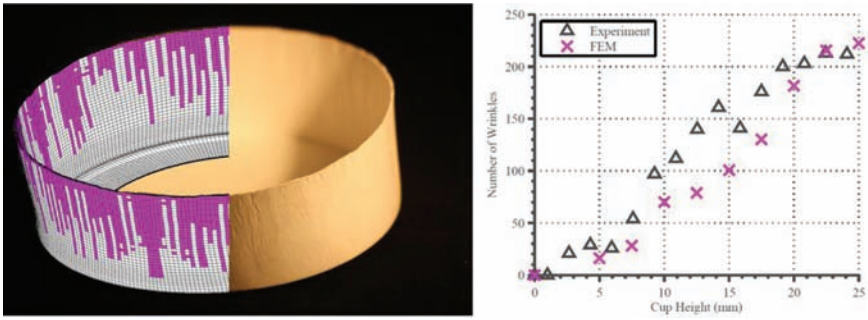

Figure 104. Overlay of experimental and simulated deep-drawn paperboard cup where white elements are non-wrinkled and magenta elements are wrinkled (*left*) and experimental and simulated number of wrinkles as function of cup height (*right*), [64].

press-forming, [115]. The potential of modelling and simulations are illustrated in Figure 105 that shows predictions of geometry and wrinkling defects using a modelling approach based on Hill's anisotropic yield criterion [111], and modelling of the creases as hinge joints that allow for rotation along the axis of the crease.

6.4 Hydro-forming

In [51] a parametric study of hydroforming of paperboard using the explicit finite element method is performed. They use the moisture and temperature dependent constitutive equations based on the orthotropic in-plane maximum stress yield surface illustrated in Figure 102 and Equation (4). The finite element model is illustrated in Figure 106.

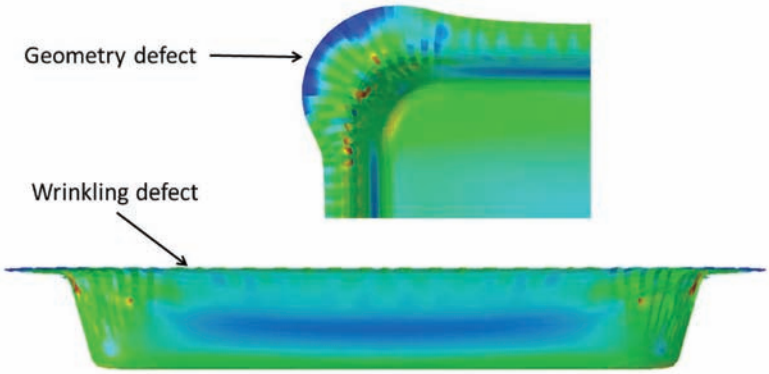

Figure 105. Simulation results illustrating geometry and wrinkling defects in paperboard tray press-forming, [115].

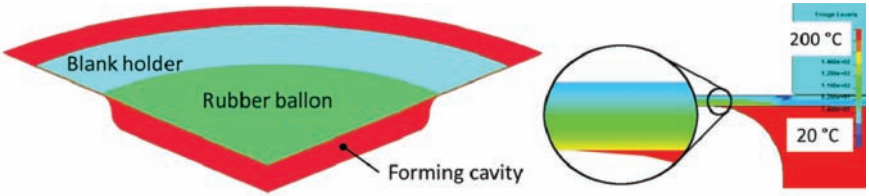

Figure 106. Finite element model of hydroforming (*left*). Due to symmetry conditions only one quarter of the circular structure needs to be modelled. The paperboard blank is below the rubber balloon, [51], and the predicted through-thickness temperature gradient at the edge of the forming cavity for a tool temperature of 200 °C (*right*).

The results from the finite element simulations are compared to experimental results for isotropic handsheets by comparing the maximum depth and the volume of the formed structure. The maximum depth and the shape of the formed structure are measured using a 1D laser scanner. The analysis is carried out using four different combinations of hydro-forming parameters according to Table 12.

The experimental results indicate that the temperature of the forming cavity has a much greater effect on the degree of forming than hydro-forming at various moisture contents. A possible explanation for this is found when the drying of the paperboard is included in the simulations. A parametric study of process and material parameters is also carried out by [51], and they find that the blank holder has limited effect on this hydro-forming process, and that the friction between the forming cavity and the paperboard has the largest influence on the formed volume. It is also observed that the relation between the forming pressure and extent of forming is non-linear, as expected (Figure 107). Regarding the influence of material parameters, their results indicate that there probably exists an optimal material stiffness for the particular experimental set-up utilised (Figure 108). Too low stiffness results in a material that does not hold it shape during spring-back, and too high stiffness makes the material too stiff to fill the forming cavity.

Thorough investigations of hydro-forming of paperboard are presented by [15], [72], [73] taking the starting point in general production engineering and material forming. In order to demonstrate the applicability of the paperboard bulge test for characterisation of the stress-strain properties of paperboard, an axisymmetric testing geometry according to Figure 110 was investigated in a hydroforming process and the results are compared to a simulation using the finite element method (FEM). Figures 110 and 111 show the shape of the measured and predicted shape of the formed structure compared with the shape of the forming cavity. The results in Figure 110 and for higher moisture content in Figure 111 indicate that the spring-back is under-predicted. Possible reasons for this, as discussed by the authors are that neither viscoelasticity nor deformations during the drying are considered. They also argue that different friction

Table 12. Hydro-forming parameter combinations used to evaluate the accuracy of the finite element model, [51].

Specimen	*Forming cavity temperature*	*Initial moisture content*
I	23 °C	6.9%
II	23 °C	10.6%
III	110 °C	6.9%
IV	110 °C	10.6%

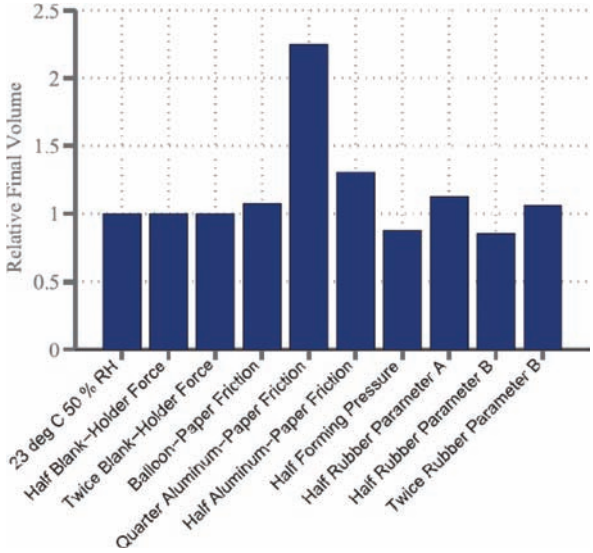

Figure 107. Parametric study of hydro-forming process parameters on the final volume of the formed structure, [51].

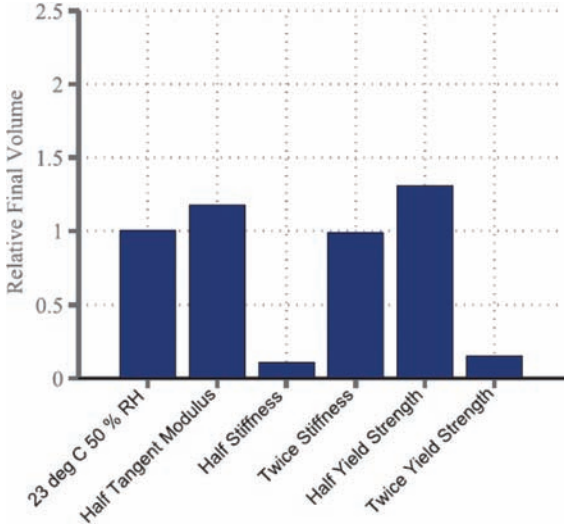

Figure 108. Parametric study of hydro-forming material parameters on the final volume of the formed structure, [51].

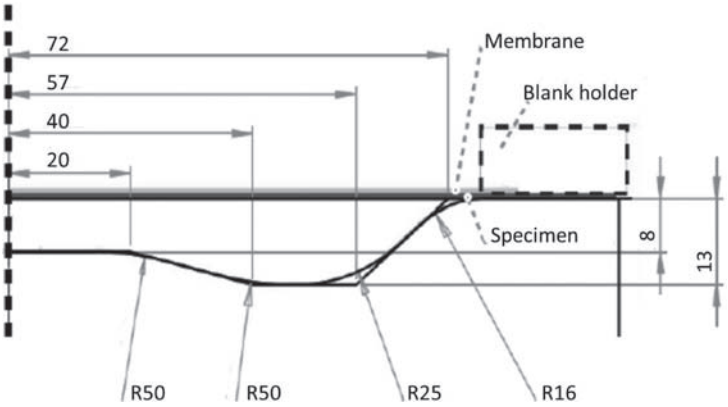

Figure 109. Hydroforming tool used in the hydroforming experiments, redrawn from [73].

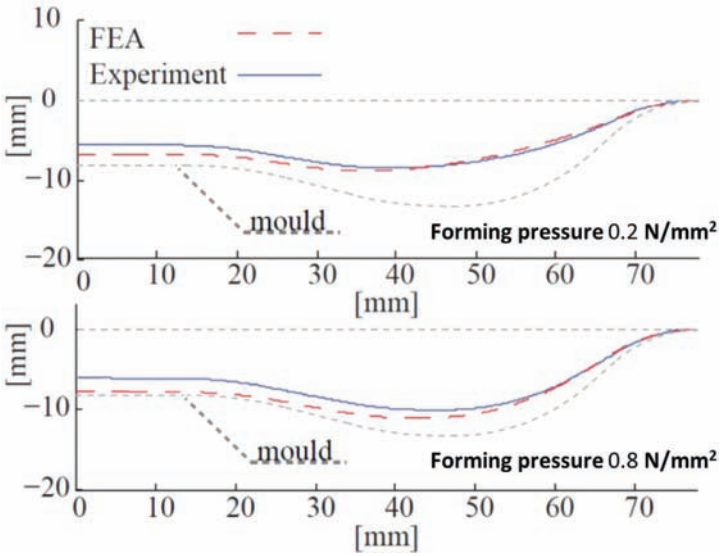

Figure 110. Shape of predicted (FEA) and measured (Experiment) paperboard structure compared to the shape of the mould at two different forming pressures, [73].

coefficients lead to different strain histories, and, thus, can lead to different spring back. Furthermore, they claim that the measurement of the frictional properties at higher normal stresses requires special equipment as was earlier discussed in section 4.2.

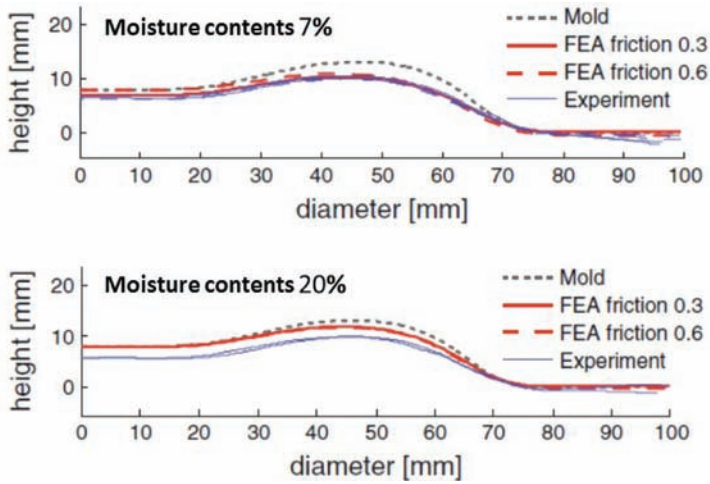

Figure 111. Shape of predicted (FEA) and measured (Experiment) paperboard structure compared to the shape of the mould at two different moisture contents for isotropic kraft handsheets at two different moisture contents, [15].

7 CONCLUSIONS

In the last decade, major advancements have been accomplished in the development of geometrically advanced 3D paperboard structures. This includes progress in the technology of various forming processes, enriched understanding of the importance and influence of process parameters, and new paperboard materials with significantly improved formability. A key concept in this development is the understanding of the deformation and damage mechanisms that paper and board are exposed to in the forming processes. While major improvements have been made also in this area, there are still many unresolved questions that need attention. The reason for this is often difficulties to experimentally identify the influence of individual material and process parameters. It is more or less impossible to experimentally isolate the influence of individual parameters, and they are in general related by complex non-linear relations. This is unmistakeably exemplified by the analysis of the immediate compression experienced by the blank when being fed into the drawing gap during deep-drawing. This state of deformation is dependent on the stiffness and wrinkling behaviour of the fibre network material that in turn is dependent on the drawing gap as well as moisture content and temperature. The drawing gap will be dependent upon the temperatures of the forming cavity and the punch. Finally, frictional properties between paperboard and forming tools will also influence the deformation and motion of the paperboard blank.

These frictional properties are themselves a major source of concern. Besides being functions of moisture content and temperature, they are also dependent upon the normal force and perhaps other parameters. The frictional properties of paper materials also contain a major contribution from chemistry requiring great care when handling the blanks prior to 3D forming. While improvements have been made recently regarding both methods for characterisation of paper-to-metal friction and understanding of friction in forming processes, knowledge on how to measure friction, include friction in conceptual and mathematical models and control friction in practise are of utmost importance for the future advancement of 3D forming of paperboard structures.

Mathematical modelling tools and numerical simulations should also play a key role in the analysis of such complex systems since they could contribute to physical understanding and would enable parametric studies of individual parameters without encountering many of the practical problems that are difficult or even impossible to tackle experimentally. This, of course, relies on the development of relevant models of both the forming processes and for the material behaviour. There are today continuum based models for paperboard taking into consideration local deformation mechanisms such as delaminations and wrinkling. While the influence of moisture content and temperatures on the material behaviour and friction have been considered, this is still based on models of limited applicability. For further improvements in process analysis and materials design, the constitutive models need to consider even more detailed analyses of deformation and damage mechanisms, particularly regarding models for the deformation mechanisms of compacted fibre networks subjected to multiaxial in-plane deformations. This also asks for multiscale models, founded in network analysis considering individual fibres and variations in the network structure. Furthermore, development of simulation tools is not only of importance for building knowledge on material and process parameters, but also an essential part in an efficient product development similarly to many other industrial branches. Therefore, this is one of the critical research areas in 3D paperboard forming.

Another important area is the development of tools for efficient quality analysis. This is needed both for objective quantitative analysis of large experimental series and for control of trouble-free large-scale manufacturing of e.g. packages. There has been some progress in this field, particularly with respect to paperboard deep-drawing, [53].

The potential success of 3D forming of paperboard is of course not restricted by the development of modelling and quality analysis tools. Both optimisation of existing forming processes and development of new processes should play an important role, as well as the development of tailored paper and paperboard materials with properties customised to the demands of such processes. There is today a large interest for development of new materials from cellulose, including paper

and board, and it is important that this development is also driven by the particular requirements of the 3D paperboard forming processes, and not limited to mimicking the properties of traditional plastics used in processes developed for such. Similarly, it is critical that the future development of manufacturing methods for 3D structures also take the particular properties of fibre network materials into account, because in many applications they require new methods. This development is only in its beginning and major progress is expected in the near future.

ACKNOWLEDGEMENTS

The author would like to acknowledge BiMaC Innovation and its member companies for the financial support and their highly motivating interest in this research area, Dr Eric Linvill and Dr Marek Hauptmann for many interesting and valuable discussions on different aspects of the mechanics of 3D forming of advanced paper structures, Prof. Peter Gudmundson and Prof. Nicolas Tiesler for valuable comments on the manuscript, and the many important contributions from scientists interested in this fascinating topic, particularly at Technische Universität Dresden, Germany, VTT, Finland and Lappeenranta University of Technology, Finland, but of course also elsewhere.

REFERENCES

1. A. Vishtal and E. Retulainen. Deep-drawing of paper and paperboard: The role of material properties. *BioResources* **7**(3):4424–4450, 2012.
2. M. Hauptmann and J.-P. Majschak. New quality level of packaging components from paperboard through technology improvements in 3D forming. *Packaging Technology and Science* **24**(7):419–432, 2011.
3. A. Vishtal and E. Retulainen. An approach for improved 3d formability of paper. *Das Papier* **12**:46–50, 2014.
4. F. Bös, M. Wardetzky, E. Vouga and O. Gottesman. On the incompressibility of cylindrical origami patterns. *Journal of Mechanical Design* **139**(2):021404–1–021404–9, 2017.
5. C. Schreck, D. Rohmer, S. Hahmann, M.-P. Cani, S. Jin, C. C. L. Wang and J.-F. Bloch. Nonsmooth developable geometry for interactively animating paper crumpling. *ACM Transactions on Graphics* **35**(1):Article 10, 2015.
6. Wikimedia Commons. 2006. [Online]. Available: commons.wikimedia.org/wiki/File:Origami-crane.jpg [acessed 11 June 2017].
7. SMRLab Harvard University, School of Engineering and Applied Sciences. Paper Crumpling Dynamics. 2017. [Online]. Available: http://projects.iq.harvard.edu/smrlab/paper_crumpling [accessed 20 April 2017].

8. M. Hauptmann, A. Schult, R. Zelm, T. Gailat, A. Lenske and J.-P. Majschak. Gastight paperboard package. *Professional Papermaking* **1**:48–51, 2013.
9. P. Tanninen, H. Lindell, E. Saukkonen and K. Backfolk. Thermal and mechanical durability of starch-based dual polymer coatings in the press forming of paperboard. *Packaging Technology and Science* **27**(5):353–363, 2014.
10. V. Leminen, P. Tanninen, S.-S. Ovaska and J. Varis. Convertability and oil resistance of paperboard with hydroxypropyl-cellulose-based dispersion barrier coatings. *Journal of Applied Packaging Research* **7**(3):91–100, 2015.
11. P. Tanninen, E. Saukkonen, V. Leminen, H. Lindell and K. Backfolk. Adjusting the die cutting process and tools for biopolymer dispersion coated paperboards. *Nordic Pulp and Paper Research Journal* **30**(2):336–343, 2015.
12. M. K. Ramasubramanian and M. D. Swecker. Mechanics of brim forming in paperboard containers – An experimental investigation. *Journal of Pulp and Paper Science* **27**(4):113–117, 2001.
13. M. Didone and G. Tosello. Green fiber bottle: the fully biodegradable packaging. Abstract from Sustain-ATV Conference 2016. Kgs. Lyngby, Denmark, 2016.
14. M. Didone, P. Saxena, E. Brilhuis-Meijer, G. Tosello, G. Bissacco, T. C. Mcaloone, D. C. Antelmi Pigosso and T. J. Howard. Moulded pulp manufacturing: overview and prospects for the process technology. *Packaging Technology and Science*, DOI: 10.1002/pts.2289, 2017.
15. P. Groche, D. Huttel, P.-P. Post and S. Schabel. Experimental and numerical investigation of the hydroforming behavior of paperboard. *Production Engineering – Research and Development* **6**:229–236, 2012.
16. B. Künne and D. Dumke. Vulcanized fiber as a high-strength construction material for highly loaded construction units. *International Paper Physics Conference*, Stockholm, 2012, June 10–14, pp. 50–55, 2012.
17. H. Huang and M. Nygårds. Numerical investigation of paperboard forming. *Nordic Pulp and Paper Research Journal* **27**(2):211–225, 2012.
18. D. W.Coffin and R. B. Pipes. Flange wrinkling in the forming of thermoplastic composite sheets. In *Materials Processing and Design: Modeling, Simulation and Applications NUMIFORM 2004*. Proceedings of the 8th International Conference on Numerical Methods in Industrial Forming Processes, 13–17 June, 2004, Columbus, OH, USA. Ed. by Somnath Ghosh, Jose C. Castro and Juni K. Lee. AIP Conference Proceedings, Vol. 712. New York: American Institute of Physics, 294–299, 2004.
19. BillerudKorsnäs. Reshape your approach to packaging. 2014. [Online]. Available: http://billerudkorsnas.com/Our-Offer/Materials/3D-Paper/ [accessed 25 March 2017].
20. FreeFormPack®. The Formable Paper Packaging. 2017. [Online]. Available: http://freeformpack.com/ [accessed 25 March 2017].
21. F. Burgstaller and R. A. Krauss. Grossversuche über die Eignungsbeurteilung von Sackpapier. *Das Papier* **9**(11/12):237–247, 1955.
22. C. B. Ihrman and J. Jacobsen. Untersuchungen zur Frage der Beurteilung von Kraftsackpapier. *Das Papier* **19**(11)**:**778–787, 1965.
23. R. C. McKee and W. J. Whitsitt, *Tappi Journal* **47**(4):215–233, 1964.
24. Arcwise. 2016. [Online]. Available: www.arcwise.se [accessed 1 March 2017].

25. M. Hauptmann, S. Ehlert and J.-P. Majschak. The effect of concave base shape elements in the three-dimensional forming process of advanced paperboard structures. *Packaging Technology and Science* **27**(12):975–986, 2014.
26. M. Hauptmann, S. Kaulfürst and J.-P. Majschak. Advances on geometrial limits in the deep drawing process of paperboard. *BioResources* **11**(4):100042–10056, 2016.
27. M. Hauptmann, M. Wallmeier, K. Erhard, R. Zelm and J.-P. Majschak. The role of material composition, fiber properties and deformation mechanisms in the deep drawing of paperboard. *Cellulose* **22**(5):3377–3395, 2015.
28. A. Vishtal, M. Hauptmann, R. Zelm, J.-P. Majschak and E. Retulainen. 3D forming of paperboard: The influence of paperboard properties on formability. *Packaging Technology and Science* **27**(9):677–691, 2014.
29. K. Scherer. Untersuchungen über Ziehfähigkeit und den Ziehvorgang von Pappe. Doctoral thesis. Technische Hochschule Dresden, Dresden, 1932.
30. M. Wallmeier, K. Noack, M. Hauptmann and J.-P. Majschak. Shape accuracy analysis of deep drawn packaging components made of paperboard. *Nordic Pulp and Paper Research Journal* **31**(2):323–332, 2016.
31. M. Hauptmann, J. Weyhe and J.-P. Majschak. Optimisation of deep drawn paperboard structures by adaption of the blank holder force trajectory. *Journal of Materials Processing Technology* **232**:142–152, 2016.
32. M. Hauptmann. Die gezielte Prozessführung und Möglichkeiten zur Prozessüberwachung beim mehrdimensionalen Umformen von Karton durch Ziehen. Doctoral thesis. Technische Universität Dresden, Dresden, 2010.
33. P. Määttä, R. Vesanto, P. Tanninen, P. Laakso and J. Hovikorpi. Method for manufacturing a board tray, a blank for the tray, and a tray obtained by the method. United States of America Patent 8011568, 2011.
34. G. H. Cross and R. T. Bernier. Method and apparatus for forming rigid paper products from wet paperboard stock. United States of America Patent 3305434, 1967.
35. P. Tanninen, S. Matthews, S.-S. Ovaska, J. Varis and K. Backfolk. A novel technique for the evaluation of paperboard performance in press-forming. *Journal of Materials Processing Technology* **240**: 284–292, 2017.
36. V. Leminen, P. Tanninen, H. Lindell and J. Varis. Effect of blank holding force on the gas tightness of paperboard trays manufactured by the press forming process. *BioResources* **10**(2):2235–2243, 2015.
37. V. Leminen, P. Tanninen, P. Mäkelä and J. Varis. Combined effects of paperboard thickness and mould clearance in the press forming process. *BioResources* **8**(4):5701–5714, 2013.
38. V. Leminen, P. Mäkelä, P. Tanninen and J. Varis. Methods for analyzing the structure of creases in heat sealed paperboard packages. *Journal of Applied Packaging Research* **7**(1):49–60, 2015.
39. M. Östlund, S. Borodulina and S. Östlund. Influence of paperboard structure and processing conditions on forming of complex paperboard structures. *Packaging Technology and Science* **24**(6):331–341, 2011.
40. M. Östlund, S. Östlund, L. A. Carlsson and C. Fellers. Experimental Determination of Residual Stresses in Paperboard. *Experimental Mechanics* **45**:493–497, 2005.

41. M. Golzar and A. Ghaderi. Effect of temperature on the spring back of cellulose-based sheet in hot pressing. *International Journal of Advanced Manufacturing Technology* **42**:633–642, 2009.
42. M. Wallmeier, M. Hauptmann and J.-P. Majschak. The occurrence of rupture in deep-drawing of paperboard. *BioResources* **11**(2):4688–4704, 2016.
43. E. Linvill, P. Larsson and S. Östlund. Advanced three-dimensional paper structures: Mechanical characterization and forming of sheets made from modified cellulose fibers. *Materials & Design* **128**:231–240, 2017.
44. P. Tanninen, V. Leminen, M. Kainusalmi and J. Varis. Effect of process parameter variation on the dimensions of press-formed paperboard trays. *BioResources* **11**(1):140–158, 2016.
45. M. Hauptmann and J.-P. Majschak. Characterization of influences on the wall stability of deep drawn paperboard structures. *BioResoureces* **11**(1):2640–2654, 2016.
46. P. Tanninen, V. Leminen, H. Eskelinen, H. Lindell and J. Varis. Controlling the folding of the blank in paperboard tray press forming. *BioResources* **10**(3):5191–5202, 2015.
47. A. Vishtal. Formability of paper and its improvement. Doctoral thesis. Tampere University of Technology, VTT Technical Research Centre of Finland Ltd, Espoo, Finland, 2015.
48. L. Salmén and E. L. Back. Glass transition of wood components hold implications for molding and pulping processes. *Tappi Journal* **65**:107–109, 1982.
49. L. Salmén and E. L. Back. Moisture-dependant thermal softening of paper evaluated by its elastic modulus. *Tappi Journal* **63**:117–120, 1980.
50. E. Linvill and S. Östlund. The combined effects of moisture and temperature on the mechanical response of paper. *Experimental Mechanics* **54**:1329–1341, 2014.
51. E. Linvill and S. Östlund. Parametric study of hydroforming of paper materials using the explicit finite element method with a moisture-dependent and temperature-dependent constitutive model. *Packaging Technology and Science* **29**(3):145–160, 2016.
52. V. Kunnari, P. Jetsu and E. Retulainen. Formable paper for new packaging applications. *Proceedings of the 23rd IAPRI Symposium on Packaging*, Windsor, UK, 3–5 September 2007.
53. M. Wallmeier, M. Hauptmann and J.-P. Majschak. New methods for quality analysis of deep-drawn packaging components from paperboard. *Packaging Technology and Science* **28**(2):91–100, 2015.
54. D. Huttel, P. Groche, A. May and M. Euler. Friction measurement device for fiber material forming processes. *Advanced Materials Research,* Vols. 966–967, pp. 65–79, 2014.
55. J. Kuusipalo, *Paper and board converting*, 2nd edn. Helsinki: Finnish Paper Engineers Association, 2008.
56. M. Nygårds, C. Fellers and S. Östlund. Development of the Notched Shear Test. In **Advances in Pulp and Paper Research**, *Trans. 14th Fund. Res. Symp.,* pp. 877–897, Cambridge, U.K., 2009.
57. M. Nygårds, M. Just and J. Tryding. Experimental and numerical studies of creasing of paperboard. *International Journal of Solids and Structures* **46**:2493–2505, 2009.

58. L. A. A. Beex and R. H. J. Peerlings. An experimental and computational study of laminated paperboard creasing and folding. *International Journal of Solids and Structures* **46**:4192–4207, 2009.
59. H. Huang and M. Nygårds. A simplified material model for finite element analysis of paperboard creasing. *Nordic Pulp and Paper Research Journal* **25**(4):505–512, 2010.
60. E. Borgqvist, M. Wallin, M. Ristinmaa and J. Tryding. An anisotropic in-plane and out-of-plane elasto-plastic continuum model for paperboard. *Composite Structures* **126**:184–195, 2015.
61. H. Huang and M. Nygårds. Numerical and experimental investigation of paperboard folding. *Nordic Pulp and Paper Research Journal* **26**(4):452–467, 2011.
62. V. Leminen, S.-S. Ovaska, M. Wallmeier, M. Hauptmann, K. Backfolk and J. Varis. Effect of material properties and drawing parameters on the quality of deep-drawn paperboard products. *Proceedings of Flexible Automation and Intelligent Manufacturing,* pp. 459–466, 2016.
63. M. Wallmeier, E. Linvill, M. Hauptmann, J.-P. Majschak and S. Östlund. Explicit FEM analysis of the deep drawing of paperboard. *Mechanics of Materials* **89**: 202–215, 2015.
64. E. Linvill, M. Wallmeier and S. Östlund. A constitutive model for paperboard including wrinkle prediction and post-wrinkle behavior applied to deep drawing. *International Journal of Solids and Structures* **117**:143–158, 2017.
65. E. J. Obermeyer and S. A. Majlessi. A review of recent advances in the application of blank-holder force towards improving the forming limits of sheet metal parts. *Journal of Materials Processing Technology* **75**: 222–234, 1998.
66. M. Hauptmann, T. Kustermann, M. Schmalholz, H. Haug and J.-P. Majschak. Examination of the transferability of technological key features of paperboard deep-drawing towards the application in fast-running packaging machines. *Packaging Technology and Science* **30**(1–2):21–31, 2017.
67. A. Löwe, A. Hofmann and M. Hauptmann. The use and application of ultrasonic vibrations in 3D deformation of paper and cardboard. *Journal of Material Processing Technology* **240**:23–32, 2017.
68. V. Leminen, *Leak-proof heat sealing of press-formed paperboard trays*, Lappeenranta, Finland: Doctoral thesis, Lappeenranta University of Technology, 2016.
69. P. Tanninen, M. Kasurinen, H. Eskelinen, J. Varis, H. Lindell, V. Leminen, S. Matthews and M. Kainusalmi. The effect of tool heating arrangement on fibre material forming. *Journal of Materials Processing Technology* **214**(8):1576–1582, 2014.
70. L. Mozetic. *Design and development of a laboratory equipment for forming of double-curved paperboard surfaces*. Master thesis, Department of Solid Mechanics, KTH Royal Institute of Technology, Stockholm, Sweden, 2008.
71. A. Svensson, T. Lindström, M. Ankerfors and S. Östlund. 3D-shapeable thermoplastic paper materials. *Nordic Pulp and Paper Research Journal* **28**(4):602–610, 2013.
72. P. Groche and D. Huttel. Paperboard forming – Specifics compared to metal forming. *BioResources* **11**(1):1855–1867, 2016.

73. D. Huttel, P.-P. Post, S. Schabel and P. Groche. The stress strain behaviour of paperboard in tensile and bulge tests. *Proceedings of the 10th International Conference on Technology of Plasticity, ICTP 2011,* Aachen, Germany, pp. 811–816, 2011.
74. G. Bolzon and M. Talassi. A combined experimental and numerical study of the behaviour of paperboard composites up to failure. *Composites: Part B* **66**:258–367, 2014.
75. R. Seth. Understanding sheet extensibility. *Pulp & Paper Canada* **106**(2):T33–38, 2005.
76. A. Vishtal and E. Retulainen. Boosting extensibility potential of fibre networks: A review. *BioResources* **9**(4):7933–7983, 2014.
77. A. Hagman and M. Nygårds. Thermographical analysis of paper during tensile testing and comparison to digital image correlation. *Experimental Mechanics* **57**:325–339, 2017.
78. A. Hagman and M. Nygårds. Investigation of sample-size effects on in-plane tensile testing of paperboard. *Nordic Pulp and Paper Research Journal* **27**(2):2295–304, 2012.
79. S. Bruschi, T. Altan, D. Banabic, P. F. Bariani, A. Brosius and J. Cao. Testing and modelling of material behaviour and formability in sheet metal forming. *CIRP Annals – Manufacturing Technology* **63**(2):727–749, 2014.
80. K. Nakazima, K. Kikuma and K. Hasuka. *Study on the formability of steel sheets*. Yawata Technical Report Nr. 284, 1968.
81. D. Banabic, L. Lazarescu, L. Paraianu, I. Coibanu, I. Nicodim and D. S. Comsa. Development of a new procedure for the experimental determination of the forming limit curves. *CIRP Annals – Manufacturing Technology* **62**(1):255–258, 2013.
82. E. Linvill and S. Östlund. Biaxial in-plane yield and failure of paperboard. *Nordic Pulp and Paper Reserach Journal* **31**(4):659–667, 2016.
83. X. Zeng, A. Vishtal, E. Retulainen, E. Sivonen and S. Fu. The elongation potential of paper – How should fibre be deformed to make paper extensible?. *BioResources* **8**(1):472–486, 2013.
84. S. L. Cluett. Modified paper and method for its manufacture. United States of America Patent 2624245, 1953.
85. F. H. Freuler. Increasing cross machine direction extensibility of paper webs. United States of America Patent 3220116, 1965.
86. F. H. Freuler and J. M. Futch. Angle bar compactor for producing isotropic extensibility in a web. United States of America Patent 3359156, 1967.
87. F. H. Freuler. Compacting apparatus for fibrous webs. United States of America Patent 3630837, 1971.
88. I. Bentov. Method and apparaturs for treating paper. United States of America Patent 2979131, 1961.
89. S. Back and R. E. Linde. Extensible paperand the process of producing the same. United States of America Patent 3104197, 1963.
90. W. C. Dabroski and B. F. Herr. Apparatus for treating paper webs. United States of America Patent 3131118, 1964.
91. J. R. Wagner and C. A. Lee. Method and apparaturs for making paper by contracting the forming carrier to compact the web. United States of America Patent 3207657, 1965.

92. C. H. Hilton. Compressive shrinkage of textile and paper webs. Great Britain Patent 2043727, 1980.
93. C. B. A. Ihrman. Apparatus for compacting a paper web. United States of America Patent 3290209, 1966.
94. C. B. A. Ihrman. Method for producing extensible paper. United States of America Patent 3523865, 1970.
95. E. J. Groome. Nip rolls for treating web materials. United States of America Patent 4092917, 1978.
96. G. Trani, M. Sterner and G. Manfré. Method for obtaining dimensionally and structurally stable objects, in particular disposable containers, starting from flexible film, and object obtained by the method. United States of America Patent 6378273, 2002.
97. G. Trani and M. Sterner. Method for forming of continuous paper web extensible in the longitudinal direction and in the transverse direction. Europe Patent 2295634 A2, 2010.
98. E. M. Burrow. Extensible paper-its development, production and use. *Paper Technology* **6**(5):423–434, 1965.
99. H. S. Welsh. Fundamental properties of high stretch papers. In **Consolidation of the Paper Web**. *Trans. 3rd Fund. Res. Symp.* (ed. F. Bolam), pp. 397–409, Cambridge, U.K., 1965.
100. C. B. Ihrman and O. E. Öhrn. Extensible paper by the double-roll compacting process. In **Consolidation of the Paper Web**. *Trans. 3rd Fund. Res. Symp.* (ed. F. Bolam), pp. 410–434, Cambridge, U.K., 1965.
101. J. Lahti, F. Schmied and W. Bauer. A method for preparing extensible paper on the laboratory scale. *Nordic Pulp and Paper Research Journal* **29**(2):317–321, 2014.
102. F. B. Cramer and E. G. Parrish. Process for producing an extensible paper. United States of America Patent 3266972, 1966.
103. A. Marais, S. Utsel, E. Gustafsson and L. Wågberg. Towards a super-strainable paper using the Layer-by-Layer technique. *Carbohydrate Polymers* **100:** 218–224, 2014.
104. A. Khakalo, I. Filpponen, L.-S. Johansson, A. Vishtal, A. R. Lokanathan, O. J. Rojas and J. Laine. Using gelatin protein to facilitate paper thermoformability. *Reactive & Functional Polymers* **85**: 175–184, 2014.
105. A. Vishtal and E. Retulainen. Improving the extensibility, wet web and dry strength of paper by addition of agar. *Nordic Pulp and Paper Research Journal* **29**(3): 434–443, 2014.
106. A. Vishtal, A. Khakalo, O. J. Rojas and E. Retulainen. Improvning the extensibility of paper: Sequential spray addition of gelatine and agar. *Nordic Pulp and Paper Research Journal* **30**(3):452–460, 2015.
107. P. A. Larsson and L. Wågberg. Towards natural-fibre-based thermoplastic films produced by conventional papermaking. *Green Chemistry* **18**:3324–3333, 2016.
108. R. Uggla, J. Laamanen, J. Paako, J. Jantunen, M. Torio and E. Partio. *Undersökning av faktorer som påverkar djup-dragningen och präglingen av kartong och papper*. KCL Rapport 1611, Esbo, 1988.
109. H. Huang, A. Hagman and M. Nygårds. Quasi static analysis of creasing and folding for three paperboards. *Mechanics of Materials* **69**:11–34, 2014.

110. E. Borgqvist, M. Wallin, J. Tryding, M. Ristinmaa and E. Tudesco. Localized deformation in compression and folding of paperboard. *Packaging Technology and Science* **29**(7):397–414, 2016.
111. R. Hill. A theory of the yielding and plastic flow of anisotropic metals. *Proceedings of the Royal Society of London. Series A* **193**:281–297, 1948.
112. Q. S. Xia, M. C. Boyce and D. M. Parks. A constitutive model for the anisotropic elastic-plastic deformation of paper and paperboard. *International Journal of Soilds and Structures* **39:**4053–4071, 2002.
113. D. D. Tjahjanto, O. Girlanda and S. Östlund. Anistropic viscoelastic-viscoplastic continuum model for high-density cellulose-based materials. *Journal of the Mechanics and Physics of Solids* **84**:1–20, 2015.
114. J. Suhling, R. Rowlands, M. Johnson and D. Gunderson. Tensorial strength analysis of paperboard. *Experimental Mechanics* **25**(1):75–84, 1985.
115. M. Awais. *Enhancing the 3-dimensional forming of paperboard with modelling and simulation*. Master thesis, Lappeenranta Univeristy of Technology, Finland, 2016.

Transcription of Discussion

THREE-DIMENSIONAL DEFORMATION AND DAMAGE MECHANISMS IN FORMING OF ADVANCED STRUCTURES IN PAPER

Sören Östlund

BiMaC Innovation, KTH Royal Institute of Technology, Department of Solid Mechanics, SE-100 44 Stockholm, Sweden

Sebastiaan Akerboom NALCO

I was wondering, we have seen in the past couple of days some presentations about the 3D forming of paper structures starting from a flat sheet of paper, and we have seen a lot of difficulties there as well, so I am wondering what is the major advantage of this technique over techniques that already existed?

Sören Östlund KTH Royal Institute of Technology

That's very good question. We have at this conference seen some very interesting results for the molding of bottles. Two things, one is of course that there is a huge infrastructure for producing paperboard, and secondly there are still issues related to the surface properties that could be of importance. There are other issues as well, but these two are probably the most important. If companies are producing a lot of paperboard and it should be used and this is an efficient way of doing it, and, typically, if you look at an egg box the surface quality is still not comparable to paperboard. However, the bottle that Mattia Didone showed at this conference certainly has an improved surface, although there is still a lot of work to do to improve it, but the existing infrastructure is not the least an important issue for 3D forming of paperboard.

Discussion

Peter de Clerck PaperTec Solutions Pte Inc

Just an observation, your hydroforming process is very similar to the stresses applied on the paper during the Müllen burst test. You mentioned that friction is a very important factor in hydroforming. Would this also be an important factor when measuring burst? I haven't seen any papers referring to the influence of friction on burst measurements. Do you have any such information?

Sören Östlund

We are well aware of the burst strength test and the different models that have been proposed for analysis of this test, and the frictional properties are in general not an issue in these models. The reason for this is that the burst strength is a measure of the load at failure, while the analyses indicating the importance of the frictional properties in 3-D forming are typically related to shape accuracy. The target parameter for the parametric FEM hydroforming analysis was the final volume of the formed structure and not the failure load. This is also a matter of how the sheet is filling the mold. The frictional properties will have different impact if the paperboard is sliding along the mold or if it is filling the mold by approaching the mold surface in the normal direction. In our hydroforming device we can, as an alternative, first push the paperboard blank downwards in the middle so that it reaches the bottom of the mold and then fills the mold outwards. However, we haven't seen any notably differences between the two ways of filling the mold. Also the shape of the formed structure will have an impact on the influence of friction. The more advanced the shape is such as the donut shape, the more important friction will be.